Mining Machines

QUARTERLY OF SCIENCE AND TECHNOLOGY

(2024) VOLUME 42
ISSUE 4

e-ISSN 2719-3306

Mining Machines

(2024) Vol. 42 Issue 4

KOMAG Research Institute

Quarterly of Science and Technology

December, 2024

Pages 240-248

Jozef MASCENIK, Tibor KRENICKY, Juraj RUZBARSKY, Tomas CORANIC

Monitoring of selected parameters of the belt transmission on a specific design solution

Pages 249-263

Przemysław DEJA, Marcin SKÓRA, Piotr HYLLA

ZZB battery supply unit for the self-propelled SWS-1700ENB blast truck

Pages 264-276

Wojciech KURPIEL, Bogdan MIEDZIŃSKI

Safety of operation of lithium batteries with active-passive BMS Systems in mining machinery systems

Pages 277-287

Andrii KOSENKO, Oleh KHOMENKO, Maksym KONONENKO, Rostyslav YEGORCHENKO, Grygorii STARIKOV, Roman DYCHKOVSKYI

Management of Scraper-Self-Propelled Ore Delivery Parameters in Caving Operations

Pages 288-300

Jacek KORSKI, Wojciech KORSKI

Automated longwall in Polish hard coal mines – conditions and limitations

Pages 301-311

Volodymyr ANTONCHIK, Valentin HANKEVICH, Oleksandr PASHCHENKO, Artem PAZYNICH, Olena VORON, Nataliia PEREDERII, Stanislav SHUBNIKOV

Efficiency coefficient of wind installations

KOMAG Institute of Mining Technology
Pszczyńska 37, 44-101 Gliwice, POLAND

miningmachines@komag.eu

OPEN ACCESS

CC BY NC

e-ISSN 2719-3306

https://doi.org/10.32056/KOMAG2024.4.1.

Monitoring of selected parameters of the belt transmission on a specific design solution

Received: date 12.08.2024

Accepted: 27.11.2024

Published online: 17.12.2024

Jozef MASCENIK [1*], **Tibor KRENICKY** [1], **Juraj RUZBARSKY** [1], **Tomas CORANIC** [1]

Author's affiliations and addresses:

[1] Technical University of Kosice
Faculty of Manufacturing Technologies
Bayerova 1, 08001 Presov,
Slovak Republic

*** Correspondence:**

e-mail: jozef.mascenik@tuke.sk

Abstract:

Belt drives have been used for decades to transmit power from a drive unit to an end device in a variety of applications. There is constant scientific, technical and technological progress in the production and use of belts, which has led to a variety of types and types of belts. Belt drives have several advantages over other methods of power transmission, including light weight, affordability, and the ability to be used as a slip clutch. As the requirements for V-belts increase, so does the required quality of the offered belts. When analyzing belt transmissions, it is also possible to examine their influence on other components of the machine or equipment on which they are installed. If the belt drive transmits large forces, this can have consequences on the bearings and other parts of the transmission. It is therefore essential to ensure that belt drives are optimally designed and installed to minimize potential damage to other components. On the designed specific design solution for testing belt transmissions, the actual revolutions of the input and output pulleys were monitored, the belt float was measured using high-precision distance measurement sensors, and the vibrations were measured using a magnetically fixed sensor. During the experimental measurements, parameters such as belt tension, input speed and output load were changed. The experimental measurements themselves were carried out on three A1450Lw 13x1420Li belts of the same dimensions, but manufactured by other manufacturers (Optibelt, Rubena and Gufero).

Keywords: construction, monitoring, belt transmission, load, belt tension, vibration, belt slip

Publisher: **KOMAG Institute of Mining Technology, Poland**
© 2024 Author(s). This is an open access article licensed under the Creative Commons BY-NC 4.0 (https://creativecommons.org/licenses/by-nc/4.0/)

1. Introduction

Designing even specific design solutions is an active and repetitive process of innovation, while at the same time it represents a decision-making procedure. This process often requires decisions that are based on limited information and sometimes conflicting data. Like a person who has two clocks and knows what time it is but is uncertain about the two clocks, a designer often has to make decisions based on limited information [1]. Nevertheless, problem solving and decision making should be satisfying and welcome activities for the designer. Designing is an equally demanding communication process that involves the use of words and images and involves both written and oral communication. Designers must be able to communicate and collaborate effectively with professionals from different fields who have different levels of knowledge about their work. The ability to communicate effectively and collaborate with colleagues from different industries is also a key factor for a designer's success.

During the construction of new design solutions, it is important to divide the processes and phases of the life cycle of technical systems, which allow to gain an overview of their creation, functioning, maintenance and termination (Fig. 1). During the design phase, it is crucial that the designer takes into account the requirements that arise from the stages and processes that the technical system will go through during its life cycle [2]. The extent to which these requirements are included depends significantly on the awareness and knowledge of the constructor, as well as on the availability of the information system.

Due to the non-negligible position of belt transmissions in a wide range of industries, there is a need to devote attention to this type of transmissions, which is why the idea of designing a new test device arose. To contribute to this issue, a proposal for testing belt transmissions under controlled load was developed. Based on the initial designs, a 3D model was created, which was subsequently physically produced and integrated into a complex measuring system. This device is composed of three main parts: measuring, controlling and monitoring.

This newly developed test stand was built within the Center for Testing and Monitoring of Technical Systems at the Department of Design and Monitoring of Technical Systems at the Faculty of Manufacturing Technologies of TU Kosice, located in Presov. The measuring station has two uses: it serves for research in the field of testing existing and new types of belts and pulleys, and at the same time it serves as an educational aid for students to improve the quality of education in the field of technically oriented subjects.

An important aspect in the analysis of belt transmissions is their correct installation and maintenance. Belt drives can become worn or damaged due to improper tension, excessive load, and other factors. Regular inspection of the condition of belt transmissions and their necessary maintenance are therefore essential. When evaluating belt drives, it is equally important to consider their use in a particular application. There are many different types of belt drives that are designed for different purposes and applications. Therefore, it is crucial to choose the belt transmission that best suits the specific requirements of the given machine or equipment [3].

For efficient operation and durability, the correct fit and tension of the belt of belt drives is of key importance. Belt tension and tension force are key factors affecting the operation of a belt drive. Correct belt tension is essential to ensure reliable operation and minimize the risk of breakdowns. The calculation of the tensioning force of the belt depends on its size, material and application. A higher tension force can improve transmission efficiency because power transmission also depends on higher belt tension. However, excessive tensioning force can cause belt overload and premature wear. There are several methods for determining proper belt tension, including measuring its elasticity within a certain range. Tension gauges and other tools are available to check belt tension. When setting belt tension, it is important to follow the manufacturer's specifications, which determine the optimal tension for a particular belt type and application.

When using belt transmissions, it is also important to define terms such as belt slippage and slippage. Belt slippage occurs when the belt is loose or under-tensioned, and this can be eliminated by proper tensioning [4]. Belt slip, also known as measured slip, exists even with proper belt tension, increasing as belt tension increases. Slippage itself cannot be excluded from the operating conditions of belt drives, and that is why belt slippage was also the subject of my measurements.

© 2024 Author(s). This is an open access article licensed under the Creative Commons BY-NC 4.0 (https://creativecommons.org/licenses/by-nc/4.0/)

2. Specific technical solution of the measuring device

The measuring system as a device for testing belt transmissions is designed as universal and easily modifiable, allowing the addition or replacement of individual components. With this device, it is possible to change the drive and driven pulley, exchange belts, change input and output parameters, and the like. For example, the replacement of pulleys is often performed in order to modify the transmission ratio between input and output, which corresponds to the objectives of testing belt transmissions as part of innovative research in this field [5].

Autodesk Inventor 3D modeling and simulation software was used during the development and design phase. This program makes it possible to create and examine the entire product before its physical production. Inventor makes it possible to combine the advantages of digital prototyping and integrate 2D drawings from AutoCAD software and merge 3D model data into one model [6].

The newly designed system includes a basic frame on which the driving electric motor and the driven electric motor are placed, which serves as part of the braking system. The shafts of the driving electric motor and the driven electric motor are fitted with pulleys and connected by a V-belt, creating a belt transmission. Siemens asynchronous electric motors (type 1LA7090-2AA10ZA11, 1.5 kW, 2900 min^{-1}, 400 V, Y, 50 Hz, IMB3, PTC thermistor) are slidably located on the frame, while the V-belt tension can be adjusted. The driven electric motor, which is controlled by a frequency converter, serves as a brake, and its braking effect can be adjusted as needed. This braking effect creates corresponding forces in the belt in the loaded and unloaded branches, which leads to a pulley slip that is measurable [7]. The tension of the belt and the displacement of the drive electric motor are controlled through a tensometric sensor of the pressure force by means of a threaded rod and a pressure bracket. The quantities needed to calculate the slip are sensed and analyzed by a computer through sensors of the actual revolutions of the driving and driven electric motors. Belt tension values are evaluated via PC. Figure 1 shows a 3D model and a real manufactured system for monitoring belt transmissions and testing different types of belts.

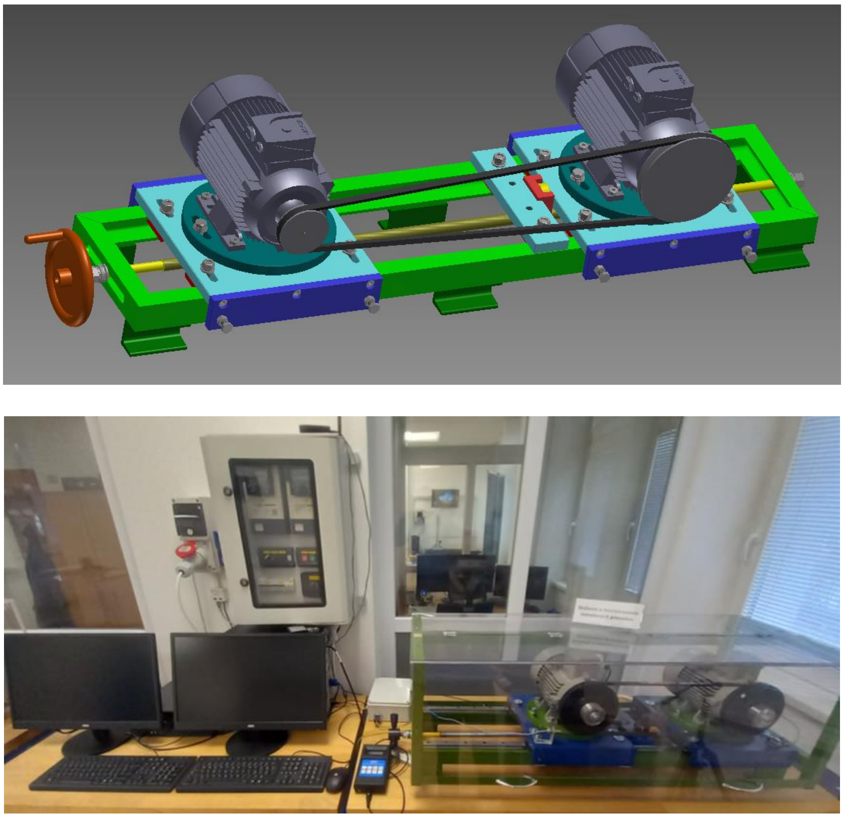

Fig. 1. 3D model and real measuring and monitoring equipment

Publisher: **KOMAG Institute of Mining Technology, Poland**
© 2024 Author(s). This is an open access article licensed under the Creative Commons BY-NC 4.0 (https://creativecommons.org/licenses/by-nc/4.0/)

3. Measurements and results

3.1. Measurement of belt transmission slip

When monitoring the slippage of the belt transmission, the speed of the electric motor, the theoretical transmission ratio indicated on the label, together with the values of the belt tension and the torque are considered as input parameters [8]. These values are obtained directly from the sensors located on the device. The measured parameters, which are obtained from the device and then transferred to the computer using an analog-digital converter, represent the real revolutions of the drive pulley of the electric motor n1s and the real revolutions of the driven pulley (brake) n_{2s}. These data are subsequently processed by the "*Motor*" software to calculate the necessary values, the result of which is the determination of the final slip of the belt transmission.

The belt slip measurement parameters are:

n_{1t} – table revolutions of the electric motor - driving machine,

n_{1s} – the actual revolutions of the motor under the load of the driven part under the given conditions of the tension force F,

n_2 – revolutions without slippage on the driving machine,

$$n_2 = \frac{n_{1s}}{i_t} \tag{1}$$

i_t – theoretical gear ratio

$$i_t = \frac{D_p}{d_p} \tag{2}$$

n_{2s} – measured (actual) revolutions of the driven machine with slip,

Δn_2 – slip revolutions

$$\Delta n_2 = n_2 - n_{2s} \tag{3}$$

T – measured (actual) time of slip revolution [s],

ξ - relative slip

$$\xi = \frac{60}{T.n_{1s}}.i_t \tag{4}$$

ψ - coefficient of elastic slip

$$\psi = 1 - \xi \tag{5}$$

i - gear ratio in a belt drive

$$i = \frac{D_p}{d_p.\psi} \quad \text{so} \quad i = \frac{i_t}{\psi} \tag{6}$$

The "Motor" software is designed directly for the monitoring system, while it is necessary to enter the set input and output revolutions and gear ratio at the beginning. The measurement can be carried out in two different ways:

- at constant speed of the electric motor and brake load (same torque), it is necessary to obtain the values of ψ and ξ for at least five different values of tensioning force, both during loading and unloading of the transmission. Based on these obtained values, it is possible to process graphs of the dependence of the coefficient of elastic slip on the value of the tension force and include these values in the data table [9].
- when maintaining constant values of the input speed of the electric motor and tension force, it is necessary to measure the elastic slip coefficient ψ at least five different values of the torque

© 2024 Author(s). This is an open access article licensed under the Creative Commons BY-NC 4.0 (https://creativecommons.org/licenses/by-nc/4.0/)

on the electric motor. The value of the torque is obtained from the measured input power of the electric motor according to the following procedure:

Power of the electric motor P_e:

$$P_e = P_{ke}.\eta_e \tag{7}$$

where: P_{ke} – measured power with a wattmeter,

η_e – the efficiency of the electric motor specified in the technical specifications.

Subsequently, the torque on the pulley can be calculated:

$$M_{ke} = \frac{P_e}{\omega_{1s}} \quad \text{whilst} \quad \omega_{1s} = \frac{2\pi n_{1s}}{60} \tag{8}$$

where: n_{1s} – real (actual) revolutions of the driven pulley obtained from the "*Motor*" program.

Measurements were made with the gear under load and unloaded. The results of the measurements were displayed in the form of the dependence of the quantity ψ on the torque with the given additional parameters. All these dependencies were recorded and tabulated. Instead of measuring power, we can use the measurement of electrical quantities such as voltage and current or measure the electrical power directly on the driving (driven) devices. The purpose of this measurement was to demonstrate how slip affects the efficiency of the belt transmission, while the efficiency of this transmission is defined by the well-known relationship [10].

$$\eta = \frac{P_2}{P_1} \cdot 100\% \tag{9}$$

Subsequently, the efficiency with slip acceptance is expressed by the following mathematical relationship:

$$\eta_s = \frac{P_2}{P_1 \psi} \cdot 100\% \tag{10}$$

Laboratory determination of power with the help of electrical quantities must be completed by physically connecting and expanding the monitoring software with power quantities and determining the accuracy of the power measurement with the gradual determination of the observed efficiency of the belt transmission according to the given relationships [11]. Experimental monitoring of selected type A belts was carried out by changing the tensioning force of the belt, which was selected and set based on the tabular value of the optimal tension of this type of belt to a value of 254 N.

Table 1. Table of specific weights and values of belt tension

	mm		rpm		N	N	kg/m	
Z	40	60	1 000	2 500	104	69	0,051	n/a
			2 501	4 000	121	81		
	61 over		1 000	2 500	174	116		
			2 501	4 000	174	116		
A	75	90	1 000	2 500	332	222	0,115	0,150
			2 501	4 000	254	169		
	91	120	1 000	2 500	391	261		
			2 501	4 000	332	222		
	121	175	1 000	2 500	469	313		
			2 501	4 000	411	274		

Publisher: **KOMAG Institute of Mining Technology, Poland**
© 2024 Author(s). This is an open access article licensed under the Creative Commons BY-NC 4.0 (https://creativecommons.org/licenses/by-nc/4.0/)

Due to the optimal value of the belt tension (see Table 1) given by the manufacturer, the belt tension values of 50 N, 250 N and 450 N were proposed for the experiment. The following Figure 2 shows the dependence of the resulting values of the elastic slip coefficient on the changed values of the revolutions on the input drive pulley and the output load on the driven pulley by changing the torque when the belt is tensioned to 50 N. The adjustment of the output load change is possible by connecting the output electric motor via the FM2 frequency converter. The values of the elastic slip coefficient were read from the "*Motor*" program, which simultaneously monitored the actual revolutions on the driving and driven pulleys [12]. The optimal belt tension is at 254 N, which is taken into account in the measurements and the results are shown in Figure 3, and the overload above the table value is shown in Figure 4 when the belt is tensioned at 450 N.

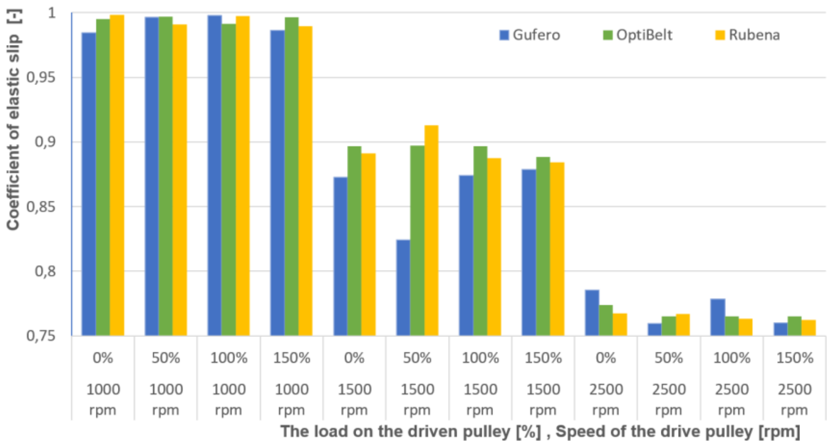

Fig. 2. Graph showing the dependence of the coefficient of elastic slip on the input speed and the load at the output of the belt transmission with a belt tension of 50 N

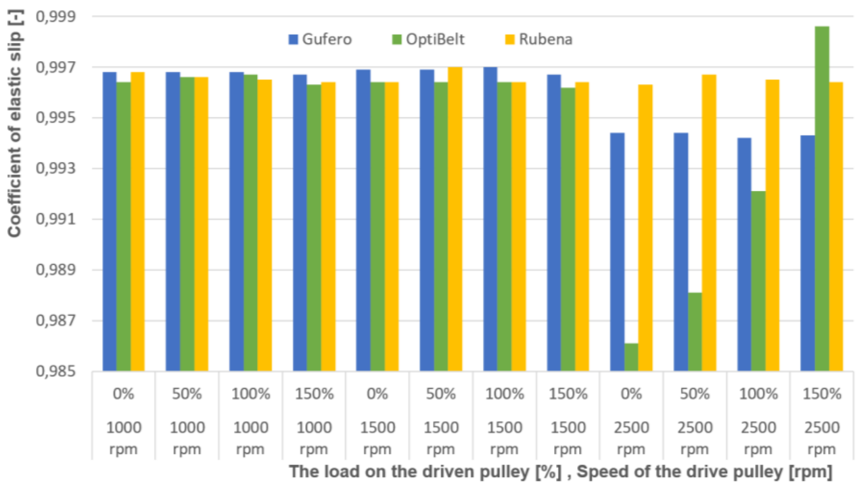

Fig. 3. Graph showing the dependence of the coefficient of elastic slip on the input speed and the load at the output of the belt transmission with a belt tension of 250 N

Publisher: **KOMAG Institute of Mining Technology, Poland**
© 2024 Author(s). This is an open access article licensed under the Creative Commons BY-NC 4.0 (https://creativecommons.org/licenses/by-nc/4.0/)

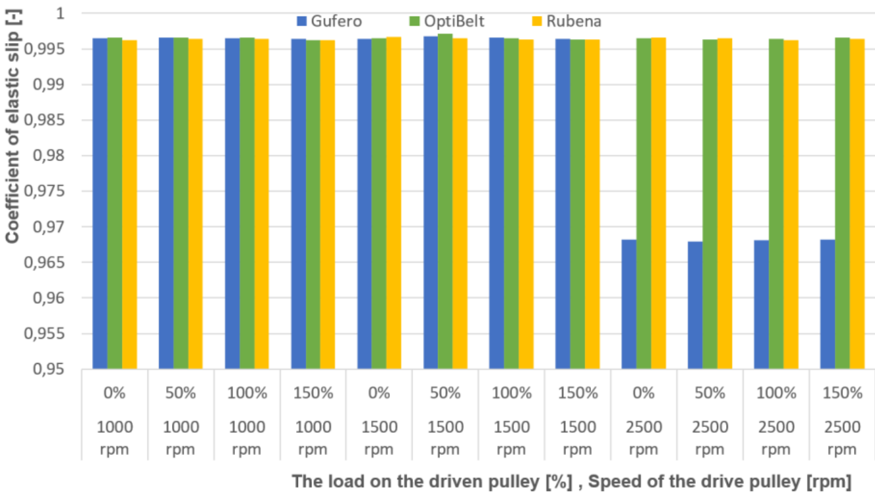

Fig. 4. Graph showing the dependence of the coefficient of elastic slip on the input speed and the load at the output of the belt transmission with a belt tension of 450 N

3.2. Measuring vibration velocity from a belt transmission

Due to the emerging vibrations on devices with a belt transmission, and thus the connection with belt floating, it is important to address this issue. Since it is possible to controllably change the belt tension of the belt transmission on the newly designed test device by changing the axial distance of the pulleys, it also allows us to monitor the change of vibrations in selected places [13, 14]. From practical experience, due to the resulting vibrations, there is a high possibility of shortening the service life and at the same time damaging the storage of the pulley shafts in the bearings. Therefore, it is appropriate to point out the influence of the vibration value depending on the change in the input speed of the drive pulley and at the same time the change in the load on the output drive pulley.

Due to the possibilities within the experiment, vibration measurement was performed by the contact method using a handheld device for measuring and diagnosing machines CMMS Checker (Figure 5a). This measuring system allows for the display of faults also on color machine diagrams generated on the display. A vibration sensor was connected to the measuring unit, which was attached to a predetermined location with a magnet (Figure 5b).

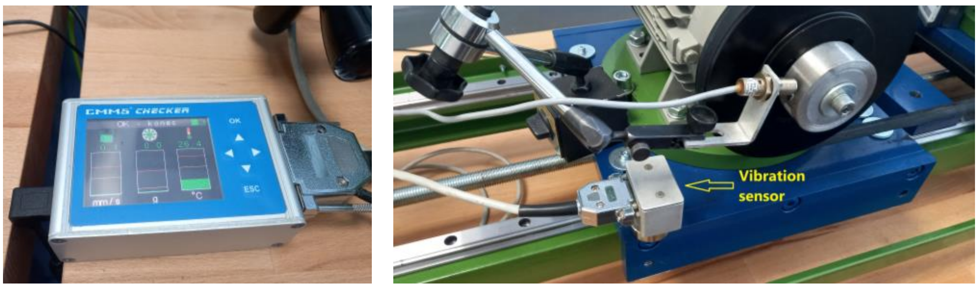

a) b)

Fig. 5. Measuring unit CMMS and sensor for vibration velocity monitoring

The following Fig. 6 shows only minor changes in vibration velocity values when changing a belt of the same type "A" but from different manufacturers. More pronounced changes in vibrations can be observed at higher revolutions, which in our case of the experiment were set to a value of 2500 rpm. At lower speeds of 1000 and 1500 rpm, there were not so many differences. From the results of experimental vibration measurements, it is possible to state and, based on this, to present further recommendations for the general public and users of this type of belts [15, 16]. Fig. 6 shows the

Publisher: **KOMAG Institute of Mining Technology, Poland**
© 2024 Author(s). This is an open access article licensed under the Creative Commons BY-NC 4.0 (https://creativecommons.org/licenses/by-nc/4.0/)

change in vibration velocity at the optimal belt tension of 250 N, while experiments were also carried out at 50 N and 450 N tension.

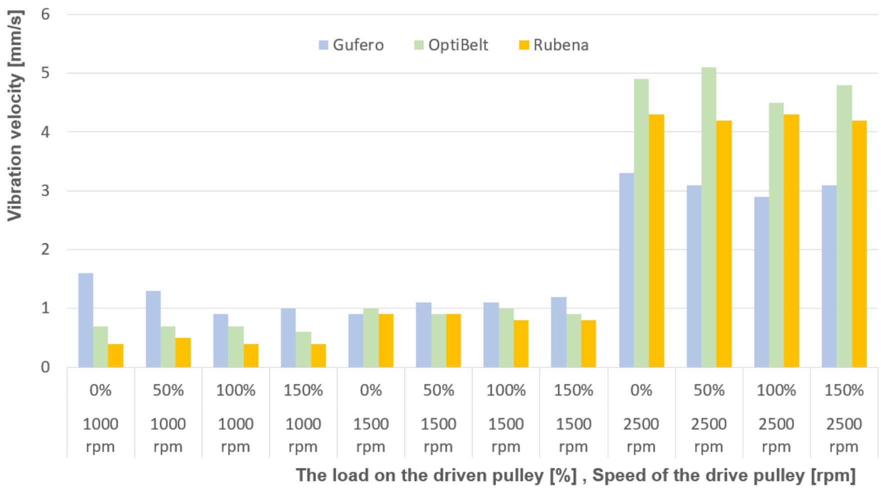

Fig. 6. Graph showing the dependence of vibration velocity on the input speed and the load at the output of the belt transmission at a belt tension of 250 N

After processing the measured values of vibrations at the selected place of the stand, we can evaluate that with different types of belts and at input speeds of 1000 and 1500 rpm, the values are not as large as at increased speeds to a value of 2500 rpm.

4. Conclusion

This article presents a specific design solution as an alternative for monitoring, determining and verifying key parameters affecting the operation and lifetime of various devices and systems using belt transmission. When designing new structural solutions, the economic costs have the greatest impact on the design and development stage and not the production itself, while the construction itself has a great impact on the functionality and reliability of the product.

The presented design solution is modular and at the same time implemented within the framework of the development of laboratories, the professional training of students within the educational process and the creation of final theses, or the solution of tasks in the field of design, control and testing of belt transmissions. If the results of the presented article inspired the expansion of the investigation of the given issue, then it can be concluded that the newly designed system and the results of its measurements are also important in practice.

Acknowledgements

This work was supported by the Ministry of Education, Research, Development and Youth of the Slovak Republic within projects VEGA 1/0509/23 and KEGA 052TUKE-4/2024.

References

[1] Novak-Marcincin, J.: *New trends in computer aided manufacturing engineering*. In: New trends in mechanical design and technologies. Cluj-Napoca: Risoprint, 2005, p. 125-172, ISBN 9737510844.

[2] Mischke Ch. R., Shigley J. E., Budynas R. G.: *Construction of machine parts, Academic publishing house*, VUTIUM, p. 1159, r. 2010, ISBN 9788021426290.

[3] Pavlenko, S., Halko, J., Mascenik, J., Novakova, M.: *Machine parts 2*, 1. vyd - Presov: FVT TU - 2008. 185 p. ISBN 978-80-553-0103-7.

Publisher: **KOMAG Institute of Mining Technology, Poland**
© 2024 Author(s). This is an open access article licensed under the Creative Commons BY-NC 4.0 (https://creativecommons.org/licenses/by-nc/4.0/)

[4] Rerabek, A.: *Construction and operation of machines for school and practice 2*, SCIENTIA, 2009, 256p, ISBN 978-80-86960-21-0.

[5] Pavlenko, S., Halko, J., Mascenik, J.: *Parts and mechanisms of machines*, Kosice TU - 2017. 249 p. ISBN 978-80-553-2844-7.

[6] Cepon, G., Manin, L., Miha, B.: *Introduction of damping into the flexible multibody belt-drive model,* A numerical and experimental investigation." Journal of Sound and Vibration 324, (2009) 283-296.

[7] Pollak, A., Temich, S., Ptasiński, W., Kucharczyk, J., & Gąsiorek, D. (2021). Prediction of belt drive faults in case of predictive maintenance in industry 4.0 platform. Applied Sciences, 11(21), 10307.

[8] Romaniuk, V., Mascenik, J., Krenicky, T., Panda, A., Zaborowski, T. E.: *Design of a concept for online monitoring of beam deflection under controlled loading*, 2023. In: Mechanical and physical properties of materials in different constellations Monograph. - Poznan (Poland): Polish Academy of Sciences, Institute of Research and Scientific Expertise s. 86-92. ISBN 978-83-66246-66-9.

[9] Halko, J., Pavlenko, S., Mascenik, J.: *Designing power stations with gear, belt and chain transmissions,* 1. Presov: TU - 2013. - 220 s. ISBN 978-80-553-1504-1.

[10] Ryba, T., Bzinkowski, D., Siemiątkowski, Z., Rucki, M., Stawarz, S., Caban, J., & Samociuk, W. (2024). Monitoring of Rubber Belt Material Performance and Damage. Materials, 17(3), 765.

[11] Kozłowski, T., Wodecki, J., Zimroz, R., Błażej, R., & Hardygóra, M. (2020). A diagnostics of conveyor belt splices. Applied Sciences, 10(18), 6259.

[12] Mascenik, J.: *Monitoring of parameters directly influencing performance transfer by belt gear*, 2017. In: MM Science Journal. Vol. 2017, no. December (2017), p. 1959-1962. - ISSN 1803-1269.

[13] Raad, H. A., Mohsen K. A.: *Dignosis of pulley-belt system faults using vibration analysis technique*. Journal of University of Babylon for Eng. Sciences (2018).

[14] Algule, S. R., Hujare, D. P.: *Experimental study of unbalance in shaft rotor system using vibration signature analysis*. International Journal 124. Prashant Athnekar, 2015.

[15] Valencik, S., Stejskal, T.: Machine maintenance, diagnostics and repairs, 2015, 230 p TU, Kosice, EAN: 9788055322490, ISBN: 978-80-553-2249-0.

[16] Jamrichova, Z., et Al.: Machine and equipment diagnostics, EDIS, 2011, 280 p, ISBN 9788055403854.

© 2024 Author(s). This is an open access article licensed under the Creative Commons BY-NC 4.0 (https://creativecommons.org/licenses/by-nc/4.0/)

https://doi.org/10.32056/KOMAG2024.4.2.

ZZB battery supply unit for the self-propelled SWS-1700ENB blast truck

Received: 29.09.2024

Accepted: 12.12.2024

Published online 17.12.2024

Author's affiliations and addresses:

[1] KOMAG Institute of Mining Technology, Pszczyńska 37
44-101 Gliwice, Poland

*** Correspondence:**

e-mail: pdeja@komag.eu

Przemysław DEJA [1*], Marcin SKÓRA [1], Piotr HYLLA [1]

Abstract:

The article presents the latest solution of the ZZB battery power unit for the working system of SWS-1700ENB self-propelled blast truck, developed at the KOMAG Institute of Mining Technology in Gliwice. Use of an internal electric charger allows charging the ZZB batteries assembly from the power grid with a rated voltage of 500V and 1000 V without the need for the blast truck to travel to the charging place with the possibility of charging the batteries from the electric generator while the vehicle is driving. SWS-1700ENB self-propelled blast truck, manufactured by Lena Wilków Sp. z o. o. with the ZZB assembly is intended for use in underground, non-methane mining plants extracting metal ores and underground, non-methane mining plants extracting minerals other than hard coal and metal ores.

Keywords: mining industry, electric machines, battery supply, battery supply assembly, blast truck.

Publisher: **KOMAG Institute of Mining Technology, Poland**
© 2024 Author(s). This is an open access article licensed under the Creative Commons BY-NC 4.0 (https://creativecommons.org/licenses/by-nc/4.0/)

1. Introduction

In mining plants extracting the minerals from hard or very hard rocks with high uniaxial compressive strength (over 150 MPa), drilling and blasting processes are used [1]. After drilling the blast holes in the face, they are filled with explosives. After blasting, the mined material is transported with wheel loaders and transportation cars, and the roof is secured by bolting machines [2]. The diagram of the copper ore extraction process is shown in Fig. 1.

Fig. 1. Copper ore extraction process

Face machines (i.e. drilling jumbos, blast trucks cars, bolting machines) have two power sources: a diesel engine is used for run, while in the face machines (due to ventilation conditions and the emission of toxic exhaust gases into the surrounding mine atmosphere) electricity is used. This requires to unwind the electric cable each time when the machine arrives at the work place and roll it up after the technological operations are completed.

2. Current solution

Self-propelled blast trucks use a diesel engine to drive the system. However, an electric motor is used to drive the technological devices installed in these trucks, which drive a hydraulic pump, which in turn drives a modular pumping device used to produce and load explosives [3, 4]. The vehicle is staffed by three people: an operator and two blast miners. In the existing solutions, the electric motor is supplied by 500 V from the mine network via a retractable electric cable. Each time unwinding and rewinding the cable is burdensome, it takes about 2/3 of the time required for placing explosives in blast holes and poses a high risk of rockfall for the working crew of the truck in the face area F. Experience gained in development of battery suspended drive trains for coal mining industry, KOMAG Institute specialists used in development of power supplying of machines with batteries (32 kWh) composed of lithium-iron-phosphate cells (instead of the previously used wire power supply) for the electric motor driving the pump of the MUP-4 module, which prepares and loads explosive emulsion into the blast holes. KGHM-ZANAM implemented this solution in the WS-172, WS-153 (WS1.5L), (WS1.7) and WS-173/S (WS1.7B) blast trucks - 42 machines (Fig. 2). The battery of the first machine (WS-172) is charged from an external, free-standing, dedicated charging module. For the next machines, the electric charger was installed inside the battery unit, as a result of the modernization of the ZB-1 power supply unit, what enabled charging the batteries directly from the mine's power grid with a rated voltage of 500 V, without the need to run the blast truck to the dedicated charging module. The above solutions use an electric motor with a power of 15 kW and a rated voltage of 150 VAC [3, 4].

Fig. 2. WS-173 blast truck [5]

Publisher: **KOMAG Institute of Mining Technology, Poland**
© 2024 Author(s). This is an open access article licensed under the Creative Commons BY-NC 4.0 (https://creativecommons.org/licenses/by-nc/4.0/)

All previous solutions of blast trucks are powered by an electric cable or a diesel engine. Unwinding an electric cable at a mine face is difficult and time-consuming, and poses a risk of rockfalls, so operators sometimes prefer power supply from a diesel engine despite the nuisance associated with exhaust gases and the deterioration of the microclimate and work comfort.

Using the sodium-nickel batteries in the SWS-1700ENB self-propelled blast trucks, manufactured by Lena Wilków Sp. z o. o., Poland is another stage of the battery drive development.

As part of the project co-financed by NCBR from the European Regional Development Fund: "A new generation of modular drilling and bolting machines with battery drives, intended for operation in underground mines of copper ore and mineral raw materials", implemented by Mine Master in cooperation with AGH University of Science and Technology, Wrocław University of Science and Technology and the Łukasiewicz Research Network - EMAG Institute of Innovative Technologies, the prototypes of Roof Master RM 1.8KE self-propelled bolting machine and the Face Master FM 1.7KE drilling jumbo were developed and manufactured for testing (Fig. 3).

Fig. 3. Face Master 1.7KE (BEV) [6]

These are the first machines in Poland designed for conditions in the mines belonging to KGHM SA, in which a battery drive consisting of five sodium-nickel batteries with a capacity of 190 Ah and an energy of 123.5 kWh is used (instead of a diesel engine), with nominal voltage of 650 V driving a permanent magnet motor with a power of 133 kW. However, bolting/drilling uses power supply from the mine network and (in an emergency) from the traction battery. Both machines have built-in chargers that allow charging the batteries from the mine power grid (in the voltage range of 500 - 1000 V), as well as during braking and descending on slopes [7]. After surface tests, the machines were subjected to underground tests at KGHM, ZG Lubin Branch [8, 9]. A comparison of selected battery-powered heavy machinery used in underground workings of mineral extraction plants is presented in Table 1.

Table 1. Comparison of Selected Battery-Powered Heavy Machinery Solutions

Manufacturer	**KGHM ZANAM**		**MINEMaster**	
Model	WS-173	WS-153	FM 1.7KE	FM 1.8KE
Type of machine	Blast truck	Blast truck	Drilling vehicle	Bolting vehicle
Length	9 950 mm	8 900 mm	14 400 mm	13 600 mm
Width	2 750 mm	3 150 mm	2 400 mm	2 450 mm
Height	1 700 mm	1 500 mm	2 200 mm	1 800 mm
Total weight	21 000 kg	19 200 kg	18 500 kg	20 500 kg

Publisher: **KOMAG Institute of Mining Technology, Poland**
© 2024 Author(s). This is an open access article licensed under the Creative Commons BY-NC 4.0 (https://creativecommons.org/licenses/by-nc/4.0/)

Engine power	115 kW	115 kW	133 kW	133 KW
Drive engine type	Diesel	Diesel	Electric	Electric
Battery module	ZB2 (LiFePO4)		Sodium-nickel battery	
Nominal battery voltage	264 V; DC		650V DC	
Battery energy	32 kWh		123,5 kWh	
Nominal charging voltage	500 V; 50 Hz		500-1000 V; 50 Hz	
Communication interface	CAN bus		CAN bus	
Enclosure protection rating	IP 67		IP67	
Weight	850 kg		1080 kg	

3. SWS-1700ENB self-propelled blast truck

The SWS-1700ENB self-propelled blast truck (Fig. 4) is an articulated machine on a tire chassis consisting of two main units: driving one and working one. Both are connected to each other by a joint with a vertical axis of rotation on roller bearings. One hydraulic cylinder is installed between the parts to turn the machine. The hydraulic cylinder is controlled by a steering wheel (controller) from the operator's cabin through a hydraulic turn distributor. The drive unit makes a frame with the driving system. Additionally, the drive unit is equipped with operator's cabin, electrical installation, hydraulic installation, fire extinguishing installation, and hydraulic unit of the working system. The working part is a platform with a self-supporting structure welded from steel sheets with a built-in operating system - a modular pumping unit.

Fig. 4. SWS-1700ENB self-propelled blast truck

Characteristics of the SWS-1700 ENB self-propelled blast truck:

- the machine is equipped with a raised work platform with an opened shield which can be used as additional platform, dismantled in the areas with low seam height,
- battery power supply of the working system drive with a possibility of charging the battery from the 500 V or 1000 V mine network,
- sodium-nickel batteries of increased fire safety, adapted to work in a high-temperature environment,

Publisher: **KOMAG Institute of Mining Technology, Poland**
© 2024 Author(s). This is an open access article licensed under the Creative Commons BY-NC 4.0 (https://creativecommons.org/licenses/by-nc/4.0/)

- high battery power guaranteeing the operation of the battery system in optimal parameters with enough energy for reliable blasting operation with a double-filled emulsion tank (750 liters),
- charging the battery while driving from an electric generator installed on a diesel engine,
- possibility of operating the pump device module also using a diesel engine,
- air-conditioned, closed operator's cabin,
- air-conditioned, open service compartment,
- supporting structure resistant to the conditions prevailing in KGHM mines (i.e. bumpy and water-logged transport roads, temperature, dust, high humidity, aggressiveness of mine water),
- the machine is equipped with the required auxiliary systems, such as:
  - permanent, automatic fire extinguishing installation,
  - central lubrication system,
  - operator system prevention against collision,
  - optional DOTRA radio communication system.

The basic mechanical and electrical parameters of the SWS-1700ENB vehicle are presented in Table 2.

Table 2. Basic parameters of the SWS-1700ENB truck

Parameter	SWS-1700ENB
Weight	19,500 kg
Length	9,250 mm
Width	2,610 mm
Height	1,700 mm
Payload	1,400 kg
Wheelbase	3,700 mm
Track width	2,340 mm
Ground clearance	325 mm
Turning radius	±41°
Engine type	CUMMINS QSB4.5C160
Max engine output	119 kW at 2,200 RPM
Payload material weight	100 kg
Fire suppression system	Lena IP-4M
Electrical installation	24V DC (2x12 V)
Battery capacity (24V)	180 Ah or 185 Ah
Battery pack type	ZZB

Publisher: **KOMAG Institute of Mining Technology, Poland**
© 2024 Author(s). This is an open access article licensed under the Creative Commons BY-NC 4.0 (https://creativecommons.org/licenses/by-nc/4.0/)

4. ZZB battery power supply unit

The ZZB battery power supply unit developed at the KOMAG Institute of Mining Technology in Gliwice was installed in the SWS-1700ENB blast truck (Fig. 5) manufactured by Lena Wilków Sp. z o. o.

Fig. 5. ZZB battery power supply unit installed in the SWS-1700ENB blast truck

Using the ZZB unit is very simple. After turning on the main switch on the ZZB unit, it is controlled from the control panel installed in the truck operator's cabin. All information about the battery, charge status, voltage, current, temperatures and more is available on the panel. There are also diagnostic connectors in the operator's cabin for servicing.

The ZZB battery power supply unit enables powering an electric motor with a power of 22 kW and voltage of 400 V, as well as an auxiliary 24V DC circuit of the truck.

Charging takes place from the 500V or 1000 V mine network. Selecting the charging voltage does not require any electrical switching. Two electrical cables are used, one for 500 V and 1000 V, and by coding the cables, the control system detects which network the device is connected to.

While the blast car is moving, it is possible to recharge the battery from a 6 kW electric generator.

A graphic control panel (Fig. 6 and Fig. 7) is installed in the truck operator's cabin, which provides text and graphic alarm signalling and the ability to monitor the process (operation of the electric motor, charging from the network and charging from the generator) in the form of a synoptic screen and parameter lists. A program managing the unit’s operation is implemented in the control panel. In turn, the ZZB unit has an installed programmable controller, dedicated to use in mobile applications. This controller is an input/output module and enables control of the ZZB unit devices. The panel communicates with the controller, the MBS system supervising the battery pack, the inverter and the charger via the CAN bus. Information is also sent via the CAN bus to a display screen installed in the ZZB unit. Functionality of the display screen is similar to the functionality of the operator panel and its location in the ZZB unit facilitates servicing.

Publisher: **KOMAG Institute of Mining Technology, Poland**
© 2024 Author(s). This is an open access article licensed under the Creative Commons BY-NC 4.0 (https://creativecommons.org/licenses/by-nc/4.0/)

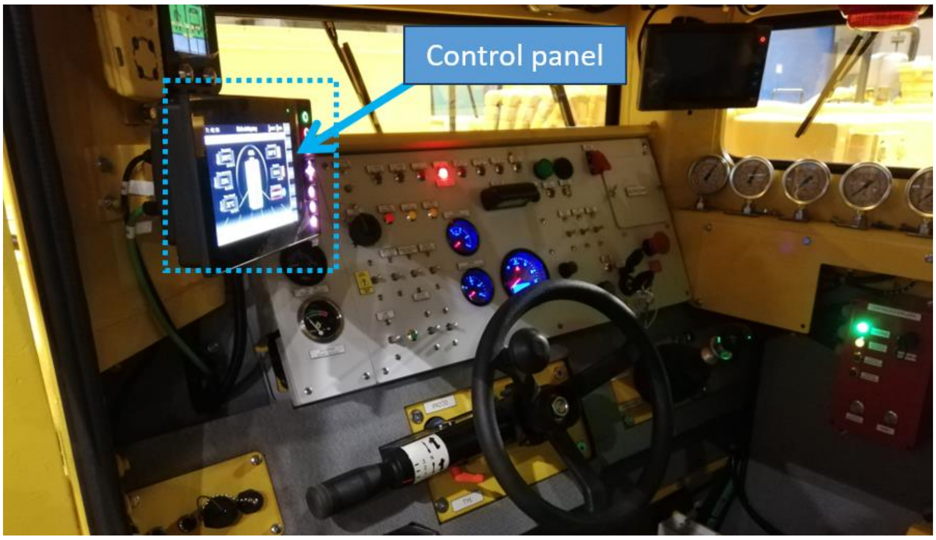

Fig. 6. Operator's cabin with a panel controlling the ZZB unit

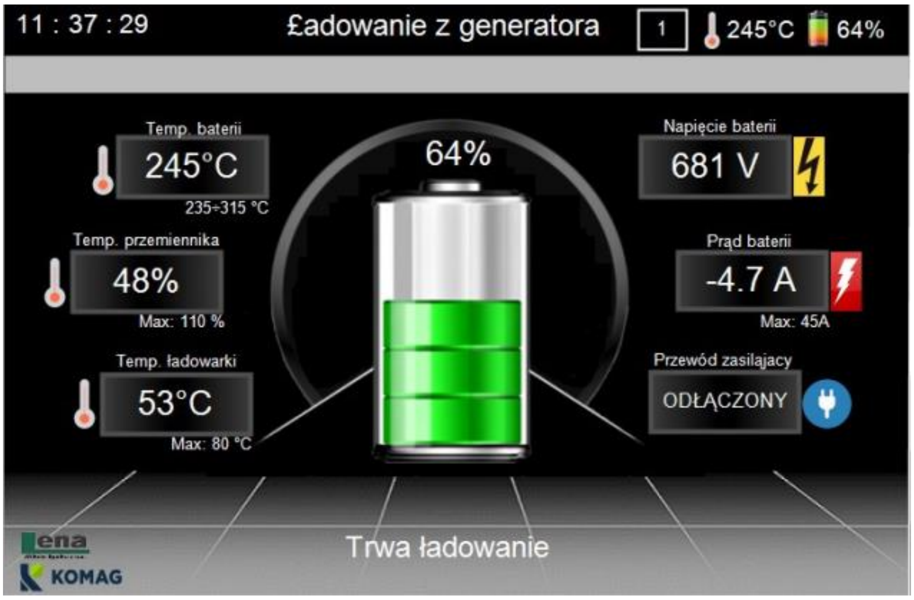

Fig. 7. Screenshot of the control panel of the ZZB-1 module

Publisher: **KOMAG Institute of Mining Technology, Poland**
© 2024 Author(s). This is an open access article licensed under the Creative Commons BY-NC 4.0 (https://creativecommons.org/licenses/by-nc/4.0/)

Structure of the control system is presented in Fig. 8.

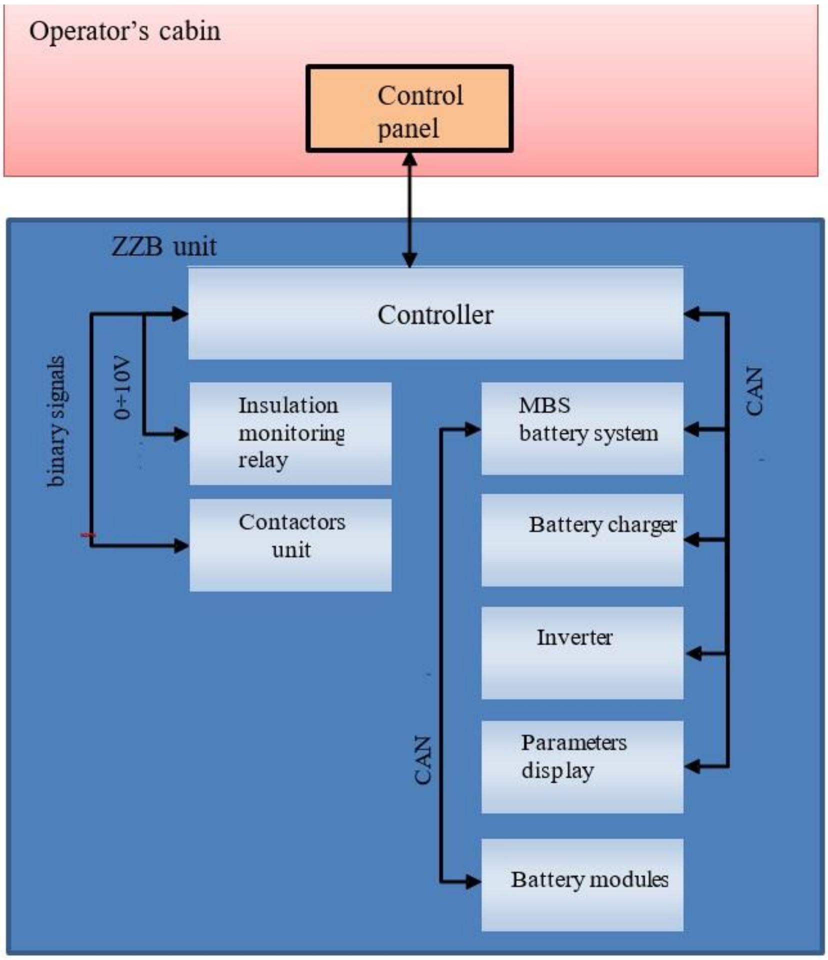

Fig. 8. Structure of the control system

Main technical parameters of the ZZB battery power supply unit is presented in Table 3.

Table 3. Technical parameters of the ZZB battery power supply unit

Type of battery cells	Sodium-nickel
Rated battery voltage	650 V; DC
Battery energy	2 x 24.7 kWh
Rated output voltage	3 x 400 V; 50 Hz
Maximum output power	22 kW
Battery charging	3 x 500 V or 3 x 1000 V
Charging the battery from a diesel engine	generator 3 x 500 V, 6 kW
Cooling	water
Communication interface	CAN bus
Degree of enclosure protection	IP 67
Dimensions	1126 x 885 x 1270 mm
Mass	1250 kg

Publisher: **KOMAG Institute of Mining Technology, Poland**
© 2024 Author(s). This is an open access article licensed under the Creative Commons BY-NC 4.0 (https://creativecommons.org/licenses/by-nc/4.0/)

5. Functionality of sodium-nickel battery

The main innovative feature of the SWS-1700ENB blast truck is the powering of the hydraulic power unit motor from the ZZB unit with sodium-nickel batteries.

Compared to batteries constructed from lithium-iron-phosphate cells, the use of sodium-nickel cells is characterized by [9, 10]:

- increased resistance to high ambient temperatures,
- a higher degree of safety in production and use, the battery composition is free of harmful substances, eliminating potential health hazards for users,
- can be fully recycled, supporting sustainable environmental practices,
- the lack of use of lithium,
- the use of cheap and readily available materials - such as sodium, iron, nickel and aluminium,
- the need to keep the internal operating temperature high, which reduces overall energy efficiency.

Z60 series batteries with a voltage of 650 V and a capacity of 38 Ah (Z60-650-38) were used in the ZZB unit solution used These are high temperature batteries. The enclosure contains cells, thermally insulated from the enclosure with an internal negative pressure. Outside each battery there is a BMI electronic module, which plays a control role.

This series of batteries is intended for mobile applications, therefore tight and shock-resistant connectors are used, the battery electronics communicates using the CAN bus, insulation resistance (electrical) is measured, and in the case of a threat, the battery terminals are disconnected (after a power supply failure of EMERGENCY line). The battery is equipped with an optional air cooling system, which allows excess heat to be removed from the interior of the battery after intensive use. The cooling system was neglected in the case of ZZB modules due to the low load compared to the battery capacity and the intermittent nature of operation. functionality of the BMI module includes control of built-in contactors, control of battery warm-up circuits, measurement of insulation resistance, communication and measurement functions (including voltage, current, battery temperature, SOC calculation). Additionally, BMI has a built-in soft start system ("precharge") that limits the battery's starting current and numerous self-diagnostic functions. If necessary, it reports information (errors) at four levels of significance and impact on the operation of the battery - from the information level to the level of immediate disconnection of the battery from the firing vehicle installation.

The battery has two installed heaters. The first one (power approx. 750 W) is supplied by 230 V AC, 50/60 Hz and also used to keep the battery temperature while charging. Warming up the battery from a cold state to a state allowing charging/operation takes up to 24 hours, usually slightly less. The second heater, with lower power (approx. 200 W), is supplied by DC voltage from the battery and is used to independently maintain the battery temperature. An example of the temperature curve of the sensors and the average battery temperature during warm-up is shown in Fig. 9a - in this case, the operating temperature (235°C) was reached after less than 20 hours of warm-up. 9b shows an example of the process of maintaining the temperature of the internal battery heaters - the average battery temperature is maintained at 245°C±3°C. In the utilized batteries, the temperature sensors are located near the front panel [12].

Publisher: **KOMAG Institute of Mining Technology, Poland**
© 2024 Author(s). This is an open access article licensed under the Creative Commons BY-NC 4.0 (https://creativecommons.org/licenses/by-nc/4.0/)

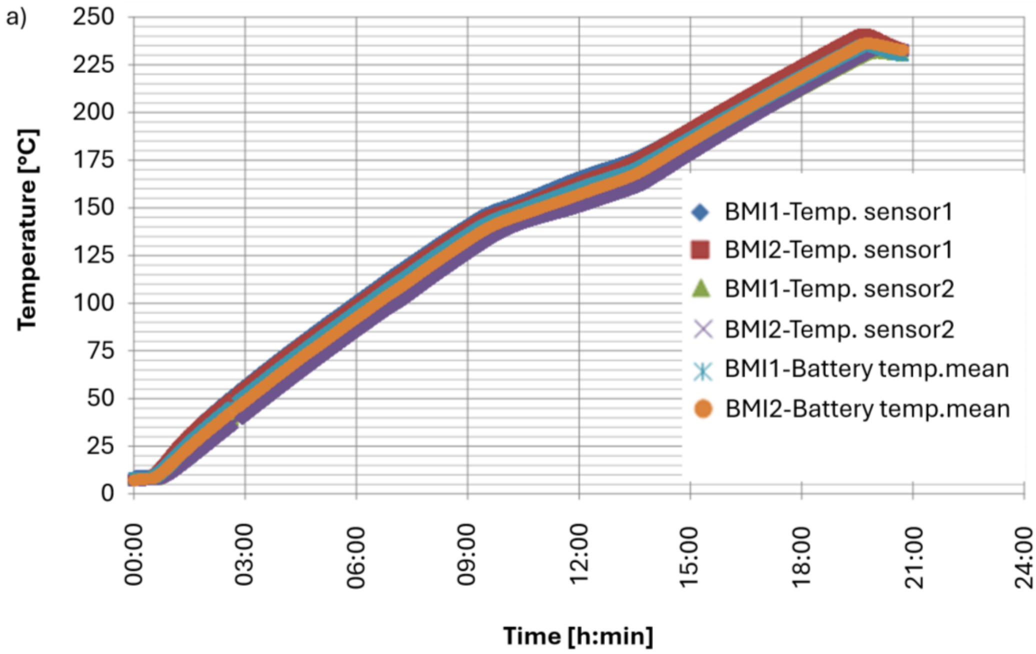

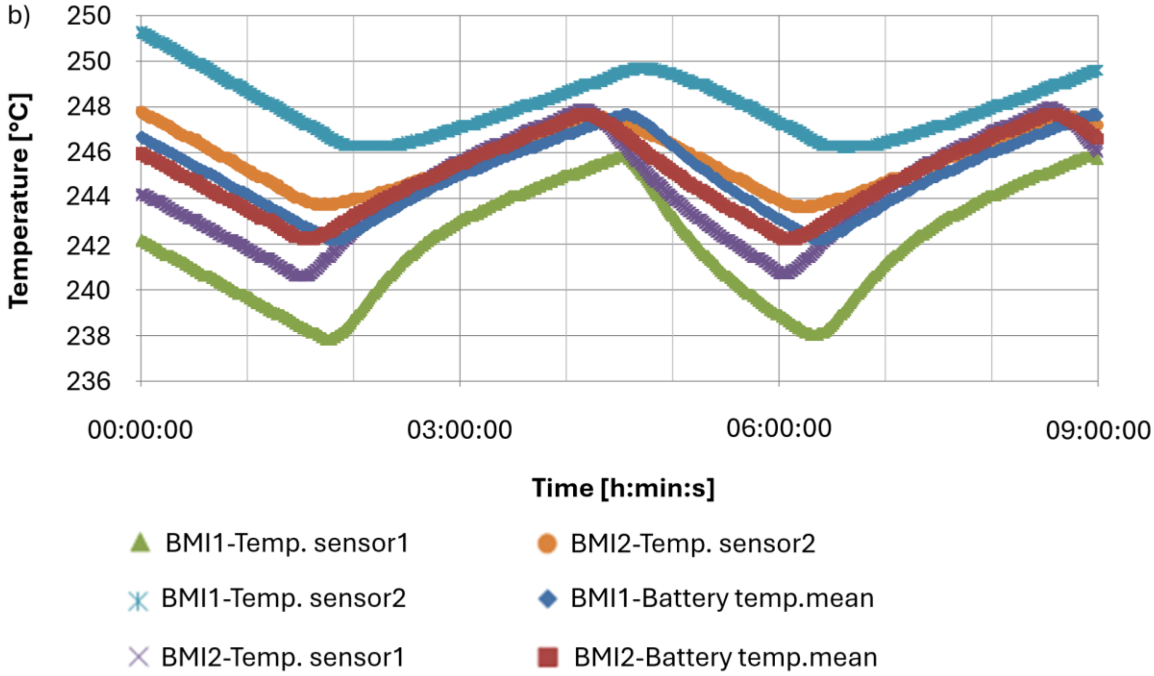

Fig. 9. Examples of sensor temperature and average battery temperatures recorded during: a) warming up the battery, b) while maintaining the battery temperature

In the case of the trucks operating in mines underground, this requires installing a transformer on the truck supplying 230 V voltage (when powered from 500 V or 1000 V). This, in turn, requires additional space for the transformer and its accessories (contactor, fuse, etc.). Not every charging place has a 230 V power supply that can be used. In addition, it would require connecting the additional cable, presence of an additional socket, etc.

Publisher: **KOMAG Institute of Mining Technology, Poland**
© 2024 Author(s). This is an open access article licensed under the Creative Commons BY-NC 4.0 (https://creativecommons.org/licenses/by-nc/4.0/)

Charging the battery is a long process. It consists of a charging phase with a constant current of 10 A (CC phase), which then turns into a charging phase with a constant voltage of 672.8 V + 1 V (CV phase). The charger should regulate the voltage with an accuracy of 0.1%. Charging is completed when the charging current drops below 0.5 A for a set time. The charging process time is up to 12 hours (first charging from SOC=0%), typically less than 8-9 hours (charging from SOC>20%). An example of the charging current and state of battery charge (SOC) during the first and subsequent charging is shown in Fig.10.

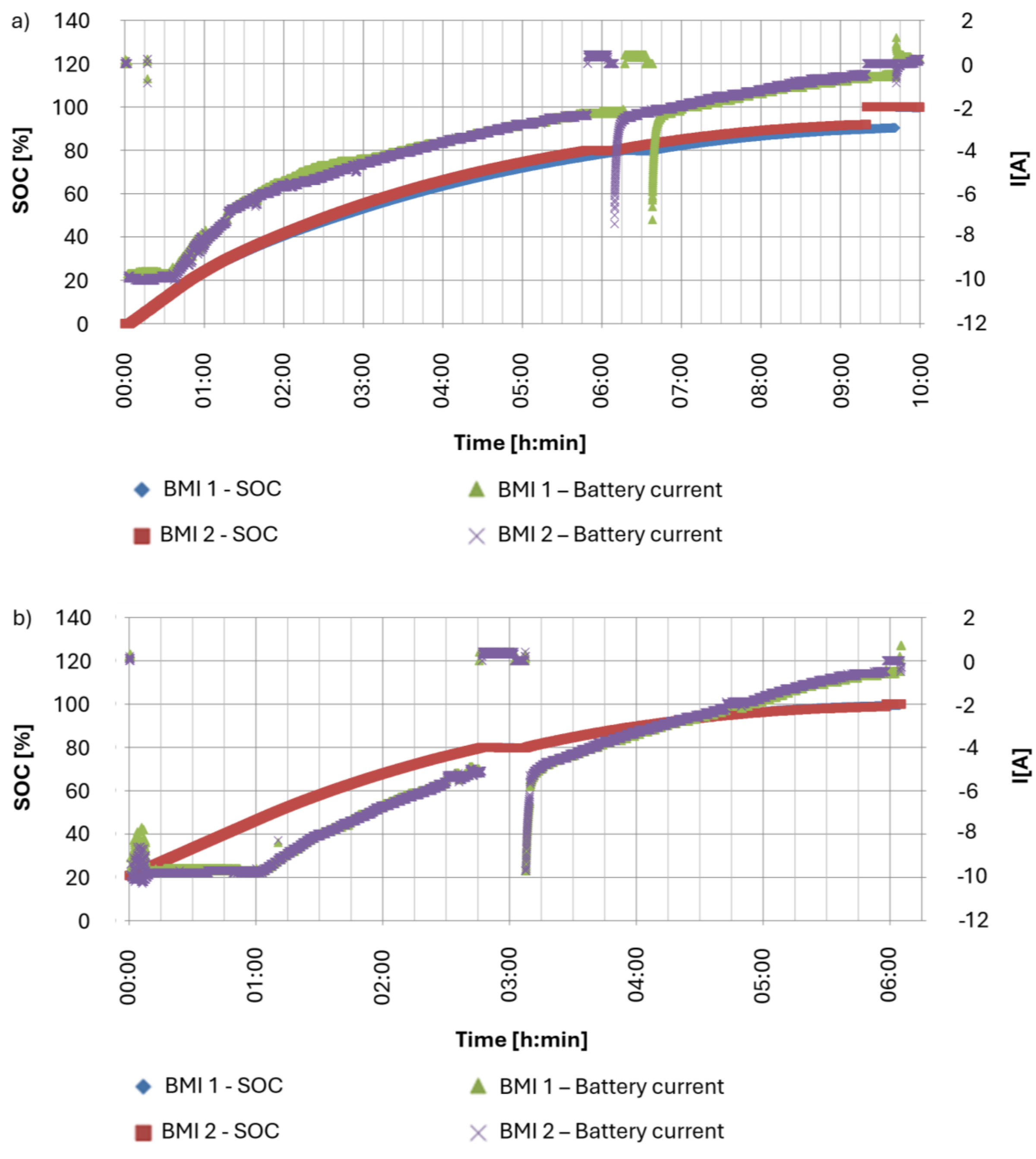

Fig. 10. Examples of curves of states of charge (SOC) and battery charging currents, recorded during: a) the first charging, b) subsequent charging of one of the ZZB sets being started

Publisher: **KOMAG Institute of Mining Technology, Poland**
© 2024 Author(s). This is an open access article licensed under the Creative Commons BY-NC 4.0 (https://creativecommons.org/licenses/by-nc/4.0/)

During charging, there is a break managed by the BMI module (typically at SOC = 80%), approx. 25-30 minutes, needed for the battery internal OCV test. During this time, voltage of the battery open circuit is determined, as well as the heating efficiency of the internal DC heater.

In addition, it is necessary to fully charge (reach the EOC state), preferably in each charging cycle or every 24 hours of using the battery. Using the battery for 36 hours after reaching the last EOC will generate a warning, and after another 24 hours warning to complete the charging process. Then, discharge current is limited, up to the discharge lock, which is removed when full charging is completed (up to the EOC state).

Recommended battery discharge time is minimum 2 hours. Temporary discharges with higher power are allowed, so that the total discharge time is a minimum of 2 hours. In these cases, increase in internal temperature and the possible use of a cooling system should be taken into account. In the case of a single 38 Ah battery, the permissible instantaneous current is 85 A. That is, the permissible momentary power is over 50 kW, and the continuous power, guaranteeing discharge within 2 hours, is approximately 12 kW (depending on the battery voltage).

The BMI battery module can communicate at a speed of 250 kbps using the CAN bus. This bus is connected to an additional controller called MBS (Multiple Battery Server). It acts as an intermediary between batteries connected to its B-CAN (Battery CAN) line and the V-CAN (Vehicle-CAN) bus with the PLC controller in the blast truck. It is also possible to connect a diagnostic computer with ZEBRA Monitor software to the B-CAN bus, which is used to monitor the battery, read current diagnostic information, read historical battery data and reset errors. It also allows data to be recorded over time, which is useful for analysing the anomalies. The program supports up to 16 batteries (limitation in the MBS module). The data exchange protocol on the B-CAN bus is secret and is not available to the user.

6. Implementation and initial operation

After the positive certification tests, the SWS-1700ENB self-propelled blast truck with a ZZB battery power unit was approved for operation in mine undergrounds by the decision of the President of the State Mining Authority. At the beginning of 2023, it was implemented in the underground mines of KGHM Polska Miedź S.A. "Rudna" Mining Plant, 11 items. The next two items are planned for implementation in 2025.

The truck operates in very difficult environmental conditions, where the ambient temperature reaches +45°C, air humidity up to 98% and dust content in the surrounding environment up to 20 mg/m^3. The electrical system of the ZZB battery power unit is exposed to shocks, impacts and mechanical impacts while the blast truck is moving.

The vehicle's initial operation allowed for drawing the following conclusions:

- the charged battery is enough for the truck operation for up to 3 work shifts, i.e. to pump out over 2 tons of explosives,
- using the internal battery charger enables charging the batteries directly from the mine network with a rated voltage of 500 V or 1000 V without the need for the operator to make additional switches in the electrical system,
- full battery charging cycle is up to 10 hours,
- using the electric generator enables recharge the battery while the truck is moving,
- shortening the time spent by the crew at the face by eliminating the need to unwind and rewind the power cable, thus protecting the crew against rockfalls,
- reducing the emission of exhaust gases and noise at the mine face,
- using the high-temperature sodium-nickel batteries requires the battery to be maintained at the proper operating temperature and to be regularly fully charged.

Publisher: **KOMAG Institute of Mining Technology, Poland**
© 2024 Author(s). This is an open access article licensed under the Creative Commons BY-NC 4.0 (https://creativecommons.org/licenses/by-nc/4.0/)

7. Conclusions

The main innovation of the SWS-1700ENB blast truck is the power supply of the hydraulic motor from the ZZB with sodium-nickel batteries.

Compared to batteries made of lithium-iron-phosphate cells, the sodium-nickel cells have the following features:

- increased resistance to high ambient temperatures,
- a greater degree of safety in manufacture and use, in composition of the batteries there are no harmful substances, eliminating a potential threat to users' health,
- operation at ambient temperatures from -40°C to +50°C, enabling using them in various climatic conditions,
- possibility of their recycling, supporting sustainable ecological practices,
- competitive price,
- no need to use a BMS system,
- no need to use lithium (a rare earth element).

Table 4 summarizes the key differences between LFP (LiFePO4) and nickel-sodium cells.

Table 4. The comparison of the parameters of LFP and nickel-sodium cell technologies

Parameter	**LFP (LiFePO4)**	**Nickel-Sodium (NaNiCl2)**
Nominal Voltage (per cell) [13]	3.2V	2.58V
Charge/Discharge Efficiency [14]	90-98%	85-90%
Self-Discharge (per month) [13]	<3%	Very low (<0.1%) with high temperature maintenance
Energy Density (volumetric)	Medium (220-350 Wh/l)	Low (100-150 Wh/l)
Energy Density	90-160 Wh/kg	10-120 Wh/kg
Cathode Active Material [15]	Lithium iron phosphate	Nickel chloride (NiCl)
Anode Active Material [15]	Graphite	Metallic sodium
Electrolyte Conductivity [15]	Liquid electrolyte based on lithium salt	Molten salt (depends on high temperature)
Resistance to Deep Discharge	High	Very high (no degradation)
Capacity Degradation over Time [13]	Low (10-20% loss after approx. 2000 cycles)	Minimal degradation under stable operating conditions
Cycle Life [14]	2000-7000 cycles	3000-4500 cycles
Charging Time	Fast	Medium
Cold Start	Problem-free even at low temperatures	Requires pre-heating to operating temperature
Heat Dissipation	Minimal	Significant, requires thermal insulation
Production Cost ($/kWh) [14]	100-150	200-400
Operating Temperature Range [13]	-20°C to 60°C	250°C to 350°C

Publisher: **KOMAG Institute of Mining Technology, Poland**
© 2024 Author(s). This is an open access article licensed under the Creative Commons BY-NC 4.0 (https://creativecommons.org/licenses/by-nc/4.0/)

Typical Applications	- Electric vehicles, - Portable devices, - Home energy storage	- Stationary energy storage, - Emergency power systems, - Grid energy storage
Advantages [16]	- High stability, - Low cost, - No toxic materials	- Resistance to extreme conditions, - Low capacity degradation
Disadvantages [16]	- Medium energy density, - Sensitive to temperatures below -20°C	- High production cost, - Requires maintenance of high temperature

The solutions presented in the article give pro-ecological effects as well as improving safety i.e.:

- increased efficiency of the truck operation compared to the existing solutions with cable power supply by shortening the time of loading the explosive material into the blast holes,
- ensuring the continuous operation of the truck for up to 3 work shifts on one battery charge, (applying over 2 tons of explosives into blast holes),
- increased mobility of the truck in loading the explosives into blast holes - in the case of a sudden threat, the truck can be immediately withdrawn from the face,
- increased work safety by eliminating the operation of the operator outside the cabin related to unwinding and rewinding the power cable,
- reduced emissions of exhaust gases and noise at mine faces,
- possibility of charging batteries from the mine's electrical network with a rated voltage of 500 V or 1000 V (at different places of the mine),
- functional interface for the truck operator with full monitoring of battery operating parameters in every state of its operation.

The following two inventions submitted to the Polish Patent Office were used in developing the described solution:

- P.443134 - Three-source system for charging mining machine batteries with electricity (authorized KOMAG).
- W.131551 - Self-propelled blast truck (authorized Lena Wilków Sp. z o.o.).

The SWS-1700ENB self-propelled blast truck with the ZZB battery power unit was awarded a platinum medal during the 17th International Fair of Inventions and Innovations INTARG 2024, which took place on May 21-23, 2024 at the International Congress Centre in Katowice.

References

[1] Wu H., & Jia Y. (2024). Strength, deformation, and fracture properties of hard rocks embedded with tunnel-shaped openings suffering from dynamic loads. Applied Sciences, 14(8), 3175. https://doi.org/10.3390/app14083175

[2] Marcinowicz I., Górniak J.: Rozwój wozów strzelniczych – pracować bezpieczniej i szybciej. Napędy Sterow. 2019 nr 7/8 s. 64-67.

[3] Deja P., Okrent K., Polnik B.: Zastosowanie ogniw litowych do zasilania urządzeń technologicznych w górniczych wozach strzelniczych. Masz. Gór. 2019 nr 3 s. 42-49.

[4] Deja P., Okrent K., Polnik B.: Akumulatorowy zespół zasilający samojezdnego wozu strzelniczego. Masz. Elektr., Zesz. Probl. 2019 nr 122 s. 9-13.

Publisher: **KOMAG Institute of Mining Technology, Poland**
© 2024 Author(s). This is an open access article licensed under the Creative Commons BY-NC 4.0 (https://creativecommons.org/licenses/by-nc/4.0/)

[5] https://www.kghmzanam.com/produkty/maszyny-gornicze/wozy-strzelnicze/ws17/(Access 11.2024)

[6] https://www.minemaster.eu/pl/produkt/battery-electric-face-master-1-7ke//(Access 11.2024)

[7] Kozłowski A.; Bołoz Ł. Design and Research on Power Systems and Algorithms for Controlling Electric Underground Mining Machines Powered by Batteries. Energies 2021, 14, 4060. https://doi.org/10.3390/en14134060

[8] Bołoz Ł., Sarecki Ł., Ostapów L.: Samojezdny wóz kotwiący zasilany bateryjnie, przeznaczony do warunków kopalni miedzi KGHM Polska Miedź SA. Napędy i Sterowanie. 2022 nr 7/8 s. 58-62.

[9] Kozłowski A.; Bołoz Ł. Battery Electric Roof Bolter versus Diesel Roof Bolter—Results of Field Trials at a Polish Copper Mine. Energies 2024, 17, 3033. https://doi.org/10.3390/en17123033

[10] Armand M.; Ortiz-Vitoriano N.; Olarte J.; Salazar A.; Ferret R. Salt Batteries: Opportunities and applications of storage systems based on sodium nickel chloride batteries. Available online: https://www.europarl.europa.eu/RegData/etudes/IDAN/2023/740064/IPOL_IDA(2023)740064_EN.pdf, accessed 01.10.2024

[11] Nikolic M.; Schelte N.; Velenderic M.; Adjei F.; Severengiz S. Life Cycle Assessment of Sodium-Nickel-Chloride Batteries. Proceedings of the International Renewable Energy Storage Conference (IRES 2022), AHE 16, pp. 336–362, 2023. https://doi.org/10.2991/978-94-6463-156-2_234

[12] FZSONICK SA. (2023). 202302_UM-Zebra Battery Handbook EN FZS_Rev2.3. FZSONICK SA. Available at: http://www.FZSONICK.com.

[13] Leonardi S.G. et al. (2023) 'A review of sodium-metal chloride batteries: Materials and cell design, Batteries, 9(11), p. 524. doi:10.3390/batteries9110524.

[14] Nekahi A. *et al.* (2024) 'Comparative issues of metal-ion batteries toward sustainable energy storage: Lithium vs. sodium', *Batteries*, 10(8), p. 279. doi:10.3390/batteries10080279.

[15] Jekal S. et al. (2024) 'Enhanced electrochemical performance of lithium iron phosphate cathodes using plasma-assisted reduced graphene oxide additives for lithium-ion batteries', Batteries, 10(10), p. 345. doi:10.3390/batteries10100345.

[16] https://goenergylink.com/blog/what-types-of-commercial-batteries-are-used-in-energy-projects/(Access 11.2024)

Publisher: **KOMAG Institute of Mining Technology, Poland**
© 2024 Author(s). This is an open access article licensed under the Creative Commons BY-NC 4.0 (https://creativecommons.org/licenses/by-nc/4.0/)

e-ISSN 2719-3306 **Mining Machines, 2024, Vol. 42 Issue 4, pp. 264-276**

https://doi.org/10.32056/KOMAG2024.4.3.

Safety of operation of lithium batteries with active-passive BMS Systems in mining machinery systems

Received: 19.08.2024

Accepted: date 28.11.2024

Published online: 17.12.2024

Author's affiliations and addresses:

[1] KOMAG Institute of Mining Technology, Pszczyńska 37

44-101 Gliwice, Poland

[2] Wroclaw University of Science and Technology Department of Power Engineering, Faculty of Electrical Engineering

ul. Wybrzeże Wyspiańskiego 27
50-370 Wroclaw

*** Correspondence:**

e-mail: wkurpiel@komag.eu

Wojciech KURPIEL[1*], **Bogdan MIEDZIŃSKI**[2]

Abstract:

The use of lithium batteries in power supply systems for devices and/or machines in mines requires ensuring an appropriate level of work safety. This applies in particular to hard coal mines, and especially methane mines and mines at risk of fire or explosion. For this reason, the lithium cells used must, together with the BMS battery management system, be isolated from the influence of the environment by placing them in special explosion-proof housings. In connection with the above, the operation of cells without the so-called BMS is, as the authors' preliminary research shows, practically prohibited. In practice, various BMSs are used, most often with the so-called passive balancing. However, their use means that the lithium battery is balanced only during charging, which means that the weakest cells in the battery determine its operating time. As for active BMSs, they are used less often due to their rather complicated structure and costs, but their use extends the operation of the lithium battery.

The article presents a new version of the special structure of the BMS system, which will balance the battery cells using the passive and active method. This will extend the battery life and ensure a safe charging process. The BMS system can be used in mining machines and devices and energy storage devices powered by a battery consisting of lithium cells.

Keywords: lithium battery, passive and active cell balancing, battery

Publisher: **KOMAG Institute of Mining Technology, Poland**
© 2024 Author(s). This is an open access article licensed under the Creative Commons BY-NC 4.0 (https://creativecommons.org/licenses/by-nc/4.0/)

1. Introduction

Safe use of lithium batteries as an effective source of battery power for electric drives in mines, especially those at risk of fire or explosion, requires both appropriate selection of the battery's electrical parameters and on-line control of changes in these parameters during operation. From the point of view of the requirements for reducing mine operating costs and ensuring the shortest possible downtimes, it is also important for the battery used to work as long as possible on a single charge/recharge. The development of technology allows the use of commercially available lithium batteries with much better electrical properties and lower weight, which allows for the gradual elimination of difficult to operate and heavy lead-acid batteries. It should be emphasized that underground mining in the world takes place at increasingly greater depths at temperatures exceeding 40°C. Increased temperature usually reduces the safety of mine operation, increasing the failure rate of working machines and devices, also contributing to the damage of lithium batteries. This is caused by the process of electrolyte decomposition at elevated temperature, which increases the internal pressure of the cells and as a result promotes cell ignition and its explosion. In this situation, it is necessary to equip lithium batteries with appropriate electronic monitoring modules designated as Battery Management Systems (BMS) [1]. Their task is both to control the operating state and, above all, to balance (balance) the cells, so as to prevent their damage as a result of overcharging, excessive discharge and/or overheating [2, 3]. Lithium batteries are, above all, very sensitive to complete and/or so-called deep discharge. Left in such a state for a long time, they may be irreversibly damaged. The task of the BMS system is therefore to control the cell parameters online and, in the event of exceeding their limit values (voltage, current, temperature), to alarm or disconnect the battery [4]. The need for energy balancing results from differences in the nominal values of the charge, capacity and/or resistance of individual battery cells. These differences result from manufacturing tolerances and operating conditions of cells of the same type and tend to increase during operation [5].

The article presents and discusses the results of research on the operation of a lithium battery consisting of lithium-iron-phosphate ($LiFePO_4$) cells equipped with a passive and active battery management system (BMS). Due to its intended use in underground mines, the research was conducted with particular attention paid to the efficiency of the cell balancing system when there is a mismatch of one to three cells in the battery. Due to its intended use in underground mines, the tests were conducted both at room temperature (20°C) and with free cooling and with degraded cooling at various mine ambient temperatures (from +5°C to +60°C) at a constant humidity of 75%. The tests were conducted for an example battery consisting of 8 cells connected in series. Such conditions are inevitable in mining applications [6]. Based on conclusions from the conducted research, a new version of the special structure of the BMS system was presented, which will balance the battery cells using the passive and active method. This will allow for extending the battery life and ensuring a safe charging process. The BMS system can be used in mining machines and devices and energy storage devices, the power source of which is a battery consisting of lithium cells.

2. Cell balancing methods

Monitoring and controlling the energy storage process in cell sets should serve to ensure that the cells can function, as the longest, as reliable and stable sources of electrical energy, while being characterized by high efficiency and a high level of safety.

Proper and safe operation of lithium cell batteries requires a BMS (Battery Management System) system that supervises their operating parameters to prevent damage, and balances them to increase efficiency and service life. Balancing methods can be divided into two basic groups (Fig. 1):

- passive - consists in dissipating excess energy into heat using appropriately selected resistors or transistors (less frequently used),

Publisher: **KOMAG Institute of Mining Technology, Poland**
© 2024 Author(s). This is an open access article licensed under the Creative Commons BY-NC 4.0 (https://creativecommons.org/licenses/by-nc/4.0/)

- active balancing the charges stored in the cells by transferring energy between them. Consists in balancing the energy stored in the cells by using an external system designed to actively transfer energy between them.

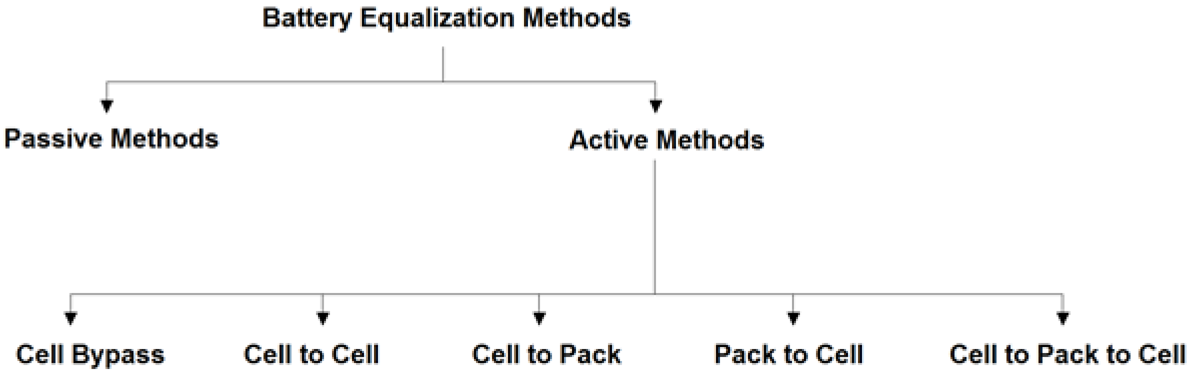

Fig. 1. Battery Cell Balancing Methods

There are several methods of active cell balancing and they are divided in different ways. Due to the energy flow, these methods are grouped into four basic subcategories: cell to cell, cell to battery, battery to cell and combined method cell to battery and from battery to cell [7].

The most commonly used battery management systems built from lithium cells are currently BMS systems using the passive method, based on the principle of dissipating excess electrical energy by converting it into heat. This is an unfavorable method, especially in machines and devices intended for use in mining, which should meet the requirements of the ATEX directive, including temperature limits of elements in contact with the mine atmosphere.

An alternative to the passive method is active cell balancing. The basic idea is to use an external system designed to actively transfer energy between cells. This significantly reduces the unfavorable phenomenon associated with energy dissipation, provides energy savings and creates optimal operating conditions for cells, resulting in extended battery life.

As part of the work carried out earlier [8], research was carried out which showed that regardless of the use of active balancing of the lithium battery during operation, the process of charging the lithium battery when the load is disconnected is also important. In such cases, the best solution is a BMS system with passive balancing, which protects against overcharging of the cells. Considering the functioning of both the BMS system with active and passive balancing and the expectations of hard coal mines in the scope of implementing technical solutions that allow for meeting quality, efficiency and economic requirements, it seems important to develop and build a comprehensive BMS system that functionally combines both types of balancing, i.e. active and passive. Both have their advantages and disadvantages. The active BMS system, which is more technologically complex and more expensive to produce, but ensures better energy management, which causes the battery cells to wear out more slowly, and the passive system, which is cheap and easy to implement, but due to the way it works, it can lead to faster wear of the cells, especially during discharge, because it converts excess electrical energy into thermal energy, equalizing the charge level of individual cells to the level of the weakest cell.

The use of a BMS system that combines both types of balancing can significantly improve the functioning of a device powered by a lithium battery. This is because the battery protection will be ensured at every moment of its use, i.e. during operation, standstill and charging.

Publisher: **KOMAG Institute of Mining Technology, Poland**
© 2024 Author(s). This is an open access article licensed under the Creative Commons BY-NC 4.0 (https://creativecommons.org/licenses/by-nc/4.0/)

3. Research on BMS systems

Research conducted by the authors shows that there is a real [9] chance for the safe and effective use of selected lithium-iron-phosphate batteries to power various mining devices and drives. However, this requires the use of a BMS system to increase both durability, safety and high operational reliability in mining conditions. It is obvious that the use of wireless and zero-emission drives can significantly improve environmental conditions in mines with reduced ventilation requirements.

Since it is extremely difficult to obtain any active BMS system on the market, especially one for specific requirements, the authors developed models of two different active BMS designs. Generally, the active BMS systems offered are quite complex and relatively expensive. Their complexity and price increases as the number of cells increases. Therefore, the authors limited their considerations to a battery set consisting of only eight cells connected in series (Fig. 2). However, the approach to a much larger number of cells and the conclusions drawn from the research are not limited to the size of the battery pack and its voltage level.

Fig. 2. The battery consists of eight lithium-iron-phosphorus cells ($LiFePO_4$)

The first of the two active BMS developed at ITG KOMAG uses the cell-to-battery method and was described in detail in the article [10]. Cell balancing in this BMS system is performed by transferring energy from the most charged cells to the entire battery pack. Thanks to this, the electric charges of individual battery cells are equalized. This means that excess energy from a single, specific overcharged cell is then delivered to the load to keep the battery in a state of top-up. However, when the battery is in a state of charge, this energy is returned to the entire pack. The view of the BMS system installed on the cell pack (battery) and the block diagram of the measurement system are shown in Fig. 3.

Fig. 3. BMS system installed on the cell pack

The second solution of the active BMS system, developed by ITG KOMAG, uses the battery-to-cell method [11]. This balancing method is based on transferring energy from the entire battery to the "weakest" cell. In this way, the charge of individual battery cells is equalized. The developed BMS system consists of a measurement and control module (Fig. 4) and a balancing module (Fig. 5).

Publisher: **KOMAG Institute of Mining Technology, Poland**
© 2024 Author(s). This is an open access article licensed under the Creative Commons BY-NC 4.0 (https://creativecommons.org/licenses/by-nc/4.0/)

Fig. 4. Measurement and control module

Fig. 5. Balancer module

Assessment of the operational efficiency of the newly developed active BMS system also required reference to passive systems available on the market. For this purpose, a technically suitable passive BMS system was selected and adapted for comparative testing. Its operation, as already mentioned, is to dissipate excess energy into heat using appropriately selected resistors. The block diagram of the measurement system is similar to a BMS system with active cell-to-battery balancing. In this case, the voltage values of individual cells are monitored online by a microcontroller using an analog-to-digital converter to which the cell inputs are connected. If the voltage of one of the cells significantly exceeds the value of the others, it is immediately shunted in parallel by a resistor. Discharging continues until the voltage of all cells used in the pack equalizes.

Scope of research

The tests were carried out for batteries (consisting of eight LiFePO4, 10 Ah lithium cells, Headway LFP38120 (S) [12] type) operating both at room temperature (approx. +20°C, humidity approx. 40%), with free heat transfer from the battery to the surroundings. The station was equipped with a temperature and voltage measurement system (DT8873-24 VOLTpoint) and a computer with specialized software (Fig. 6).

Publisher: **KOMAG Institute of Mining Technology, Poland**
© 2024 Author(s). This is an open access article licensed under the Creative Commons BY-NC 4.0 (https://creativecommons.org/licenses/by-nc/4.0/)

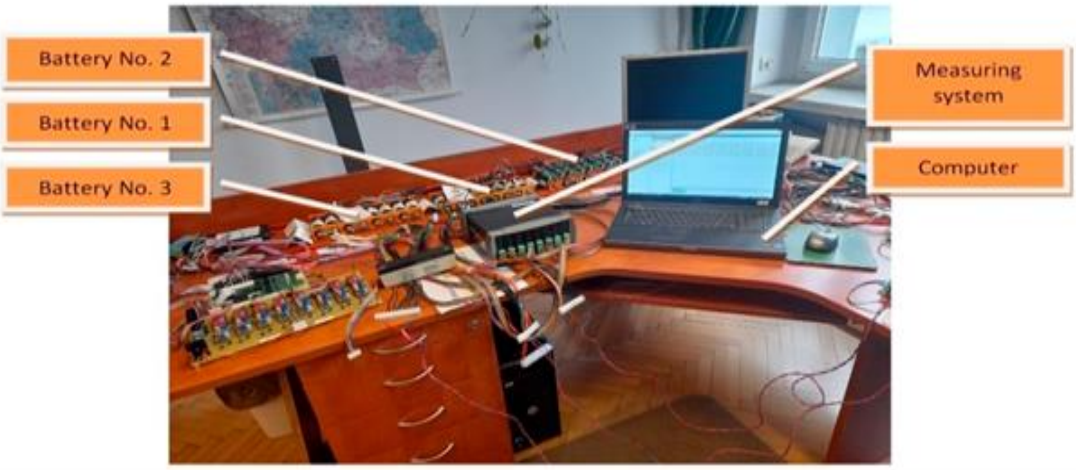

Fig. 6. Station for measuring and recording data (Battery 1 - with a battery for the active BMS battery, Battery 2 - with a battery for the active BMS battery, Battery 3 - with a passive BMS)

The finished battery packs (unloaded) were then connected to the appropriate active/passive BMS system under study. However, the load asymmetry of selected cells (from 1 to 3 tested, respectively) was performed for a discharge current equal to approximately 25% of the standard discharge value (2.5 A) as shown in Fig. 7. Each test began with a fully charged battery (voltage of all cells equal to the rated Un = 3.2 V). The load with a current of 2.5 A lasted until the voltage at the terminals of any of the cells reached the minimum value Umin (equal to 2.5 V).

The research has shown that both the voltage value of individual cells and their temperature may differ from each other even when loaded (discharged) with the same current value. For selected two cells in a battery without a BMS system, it is shown, for example, in Fig. 8. This justifies the need to control the voltage and temperature of all cells, and therefore the need to use a BMS.

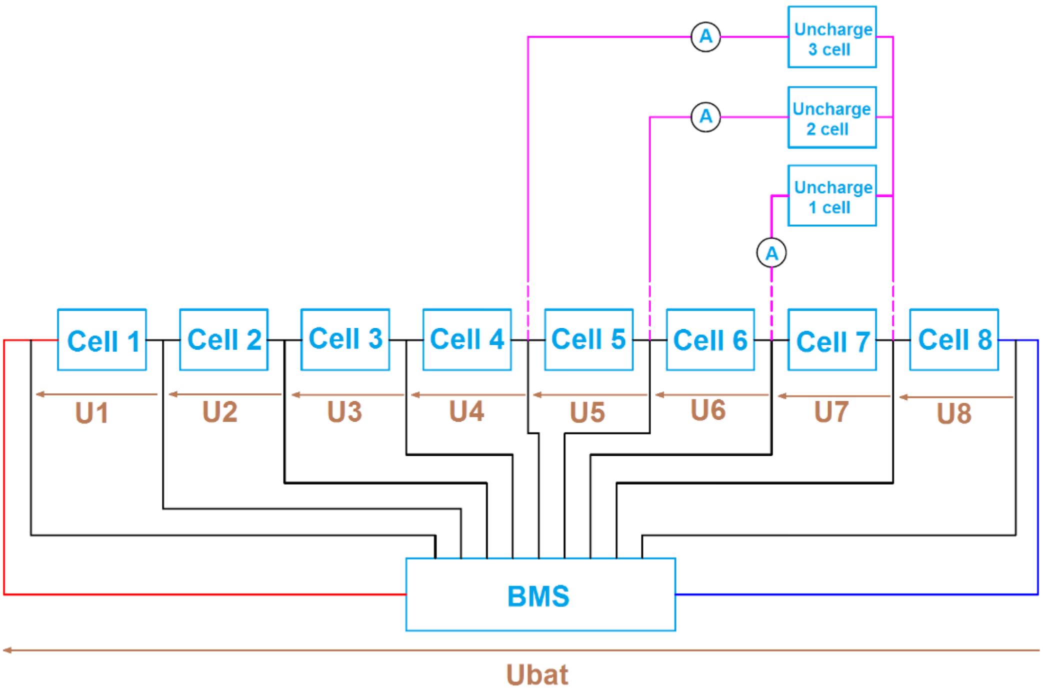

Fig. 7. Block diagram of the BMS system testing system during battery load simulation

Publisher: **KOMAG Institute of Mining Technology, Poland**
© 2024 Author(s). This is an open access article licensed under the Creative Commons BY-NC 4.0 (https://creativecommons.org/licenses/by-nc/4.0/)

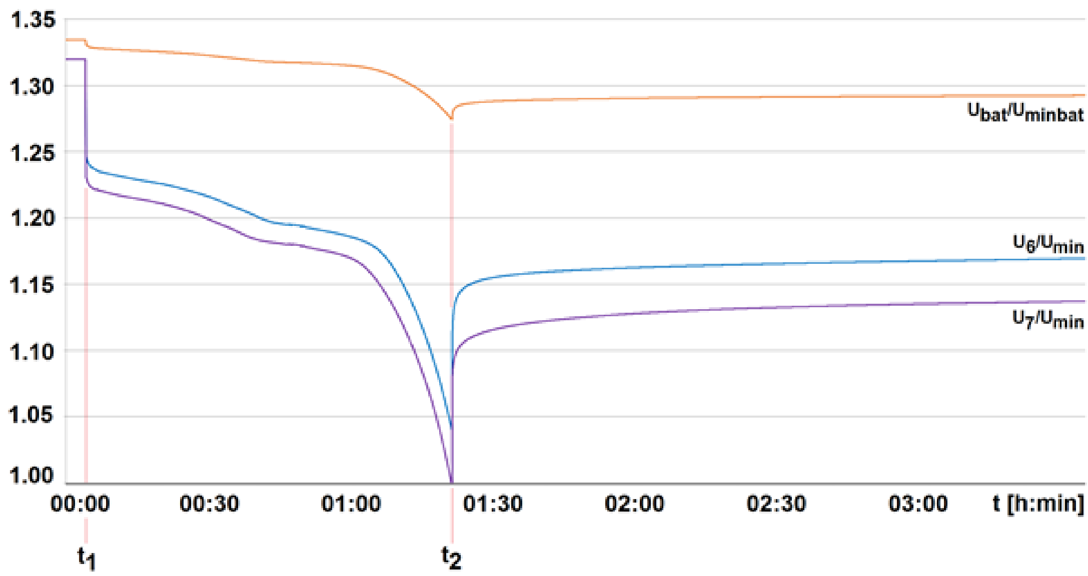

Fig. 8. Graph of the voltage value on two loaded cells without a BMS system connected

In order to compare the performance of the developed active BMS systems, their technical parameters were configured accordingly. Therefore, for both active systems, balancing is activated when the cell voltage drops below 3.05 V (U/U_n = 0.95). Balancing is interrupted when the voltage on the terminals of any of the cells used is lower than U_{min} = 2.5 V or higher than 3.65 V (U/U_n = 1.14) (Fig. 9 and Fig. 10). The balancing current value was set at 2 A (approximately 40% of the standard charging current). However, for a commercial BMS system with passive balancing, the value of the balancing current was set arbitrarily by the manufacturer and is 350 mA. However, other technical parameters could be determined by configuration using computer software. As a result of the configuration, passive cell balancing starts during charging, when the cell voltage value is between U_n = 3.2 V and 3.65 V (1.14 U_n). However, it turns off when the voltage at the terminals of any of the cells is lower than U_{min} = 2.5 V and/or above 1.14 U_n (3.65 V) (Fig. 11).

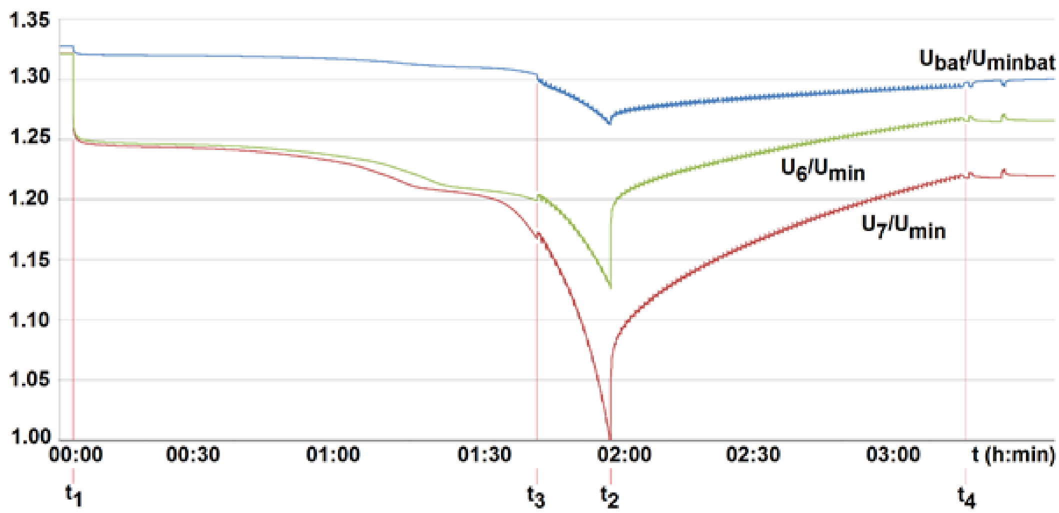

Fig. 9. Graph of the voltage value on two loaded cells for a BMS system with active balancing (cell-to-battery method). Voltages U_6/U_{min} and U_7/U_{min} over time for two cells loaded in series in an unloaded battery without a BMS system (room temperature T_o = 20°C, free cooling, t_1, t_2 - moment of switching on and off the load current, t_3, t_4 - moment of turning on and off the balancer, U_{min} - minimum cell voltage equal to 2.5 V)

Publisher: **KOMAG Institute of Mining Technology, Poland**
© 2024 Author(s). This is an open access article licensed under the Creative Commons BY-NC 4.0 (https://creativecommons.org/licenses/by-nc/4.0/)

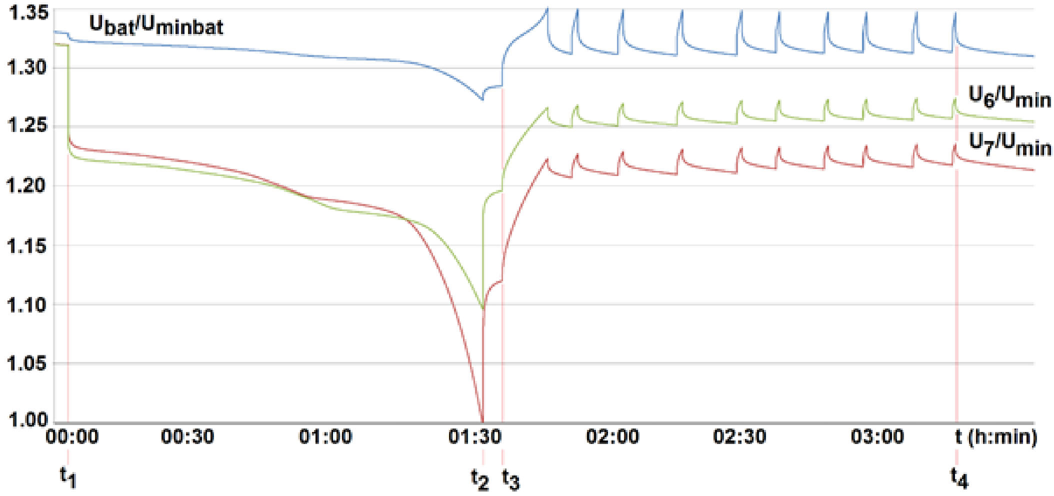

Fig. 10. Graph of the voltage value on two loaded cells for a BMS system with active balancing (battery-to-cell method). Voltages U_6/U_{min} and U_7/U_{min} over time for two cells loaded in series in an unloaded battery without a BMS system (room temperature T_o = 20°C, free cooling, t_1, t_2 - moment of switching on and off the load current, t_3, t_4 - moment of turning on and off the balancer, U_{min} - minimum cell voltage equal to 2.5 V)

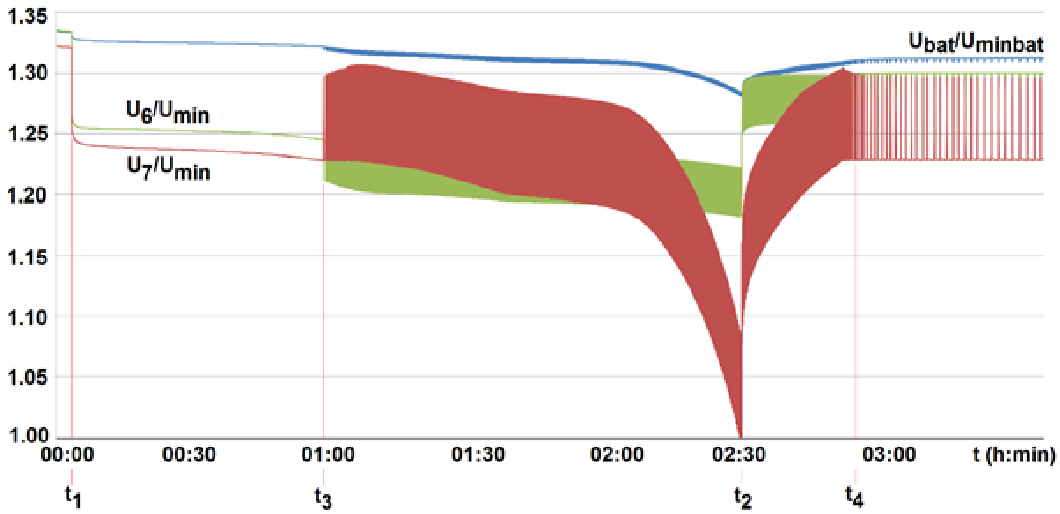

Fig. 11. Graph of the voltage value on two loaded cells for a BMS system with passive balancing. Voltages U_6/U_{min} and U_7/U_{min} over time for two cells loaded in series in an unloaded battery without a BMS system (room temperature T_o = 20°C, free cooling, t_1, t_2 - moment of switching on and off the load current, t_3, t_4 - moment of turning on and off the balancer, U_{min} - minimum cell voltage equal to 2.5 V)

Findings

The research shows that active balancing systems (BMS) contribute to extending battery life, especially when cells are discharged to the minimum voltage (Umin = 2.5 V). The improvement in battery life is particularly noticeable as the number of cells in the system increases, but these effects remain effective only until the number of cells exceeds 50%. The increase in lifespan results from better management of cell discharge, which improves their efficiency. However, in the case of passive balancing systems, the charging process of cells occurs only after the load is disconnected, allowing

Publisher: **KOMAG Institute of Mining Technology, Poland**
© 2024 Author(s). This is an open access article licensed under the Creative Commons BY-NC 4.0 (https://creativecommons.org/licenses/by-nc/4.0/)

for the equalization of energy differences between cells, preventing overcharging, and protecting the battery from damage. The passive method ensures safety but does not result in the same significant improvements in lifespan and efficiency as active systems. Therefore, based on the research findings, it can be concluded that active balancing systems offer a clear advantage in terms of battery lifespan and efficiency, especially as the number of cells increases. While passive balancing is effective in terms of safety, it does not provide the same benefits in performance and system durability.

4. Description of the concept of the new solution

Previous research has shown that regardless of the use of active balancing of the lithium battery during operation, the process of charging the lithium battery when the load is disconnected is also important. In this case, a BMS with passive balancing works best, protecting against overcharging the cells, because they dissipate excess energy in the form of heat. On the other hand, a BMS with active balancing is more effective in energy management, because it does not dissipate excess energy in the form of heat, but transforms it and balances it between the cells. This is especially important in a situation where the battery cells being charged are already fully charged and the charging process is not fully completed. In such conditions, a BMS with active balancing allows for more precise energy management by transferring excess energy from overcharged cells to less charged ones. This type of balancing ensures evenly distributed voltage in the cells, which allows for their longer durability and also reduces the risk of damage caused by uneven charging. On the other hand, a passive BMS system works less efficiently in such cases, because excess energy from overcharged cells is dissipated in the form of heat. Although it is a protective mechanism against overcharging, the generation of excess heat can lead to unnecessary energy loss and an increase in temperature, which in turn can reduce the life of the battery. In the context of charging lithium batteries, when the cells are almost fully charged, active balancing offers a clear advantage, as it ensures an even distribution of energy between the cells, which increases the efficiency of the charging process. This reduces the risk of overheating and damage to the cells, and the battery itself is able to withstand more charge and discharge cycles. However, it is worth noting that in the actual use of lithium batteries, the use of a BMS system in which both types of balancing, i.e. active and passive, are used, is beneficial, as it will be possible to achieve both safety and high energy efficiency. Active balancing can be used in more demanding conditions, while passive balancing can play a protective role during charging, especially in the absence of load.

The concept of a passive-active BMS system

In the developed concept of a mixed BMS system, two balancing methods will be used: active and passive. The system will consist of three modules (Fig. 12):

- measurement and control module - a control system used to measure the voltages of connected cells and control the operation of the entire BMS system and supervise battery operating parameters,
- passive balancing module - assigned to each cell, they allow for the physical implementation of the balancing process, i.e. dissipation of excess energy into heat using resistors connected in parallel to the cells,
- active balancing system module - assigned to each cell, they allow for the physical implementation of the balancing process, i.e. transfer of energy to other cells using the battery-to-cell method.

Publisher: **KOMAG Institute of Mining Technology, Poland**
© 2024 Author(s). This is an open access article licensed under the Creative Commons BY-NC 4.0 (https://creativecommons.org/licenses/by-nc/4.0/)

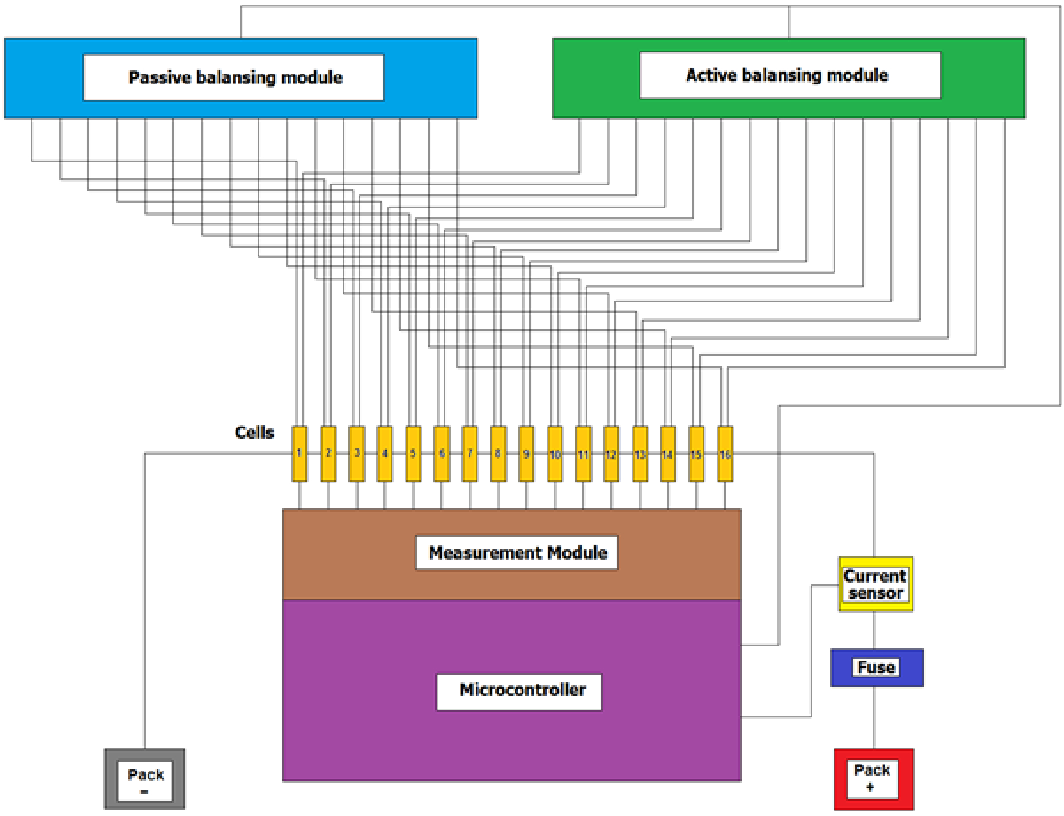

Fig. 12. An example of a mixed BMS system designed to manage battery operation

Measurement module

In the measurement module, the voltage values of individual cells will be monitored in the microcontroller via analog-to-digital converters to whose input individual cells will be connected. Additionally, temperature measurements of individual cells will be performed via the microcontroller's analog-to-digital converter.

If overload, overvoltage, undervoltage or overheating and/or any other dangerous situation occurs, the battery will be disabled. Maintaining an unsafe situation is both undesirable and dangerous. It shortens the battery life and may affect the safety of its use.

The measuring module also performs the function of checking the battery charge level. This value will be calculated on the basis of data from measuring the voltage value on individual battery cells.

Active balancing module

Balancing in the battery-to-cell method involves transferring energy from the entire battery to the weakest cell. The balancing process equalizes the state of charge of individual cells in the battery and aims to maximize the use of its capacity and extend its service life. Typically, the cells that make up the battery do not differ much in capacity, but after several charging-discharging cycles without balancing, this difference becomes significant and may lead to a situation in which the voltage on one of the cells drops below the safe operating limit recommended by the manufacturer. Continued use may be dangerous and may damage the battery. This situation means that the maximum energy obtained from the battery is limited by the cell with the smallest capacity.

The discrepancy in the amount of energy stored in the cells in the battery system is very important in relation to the life expectancy of the battery. Without a BMS system, the voltage values on

© 2024 Author(s). This is an open access article licensed under the Creative Commons BY-NC 4.0 (https://creativecommons.org/licenses/by-nc/4.0/)

individual cells may differ significantly from each other after some time. The capacity of the entire battery may also decrease rapidly during operation, resulting in the battery system becoming completely unusable.

Passive balancing module

The operation of this system is based on the dissipation of excess energy into heat using resistors. If the voltage of any cell significantly exceeds the voltage of the others, it is short-circuited by an appropriate switch. This results in the discharge of a given cell through an element of the passive balancing circuit - a resistor, connected in parallel with each cell and continues until the voltage of the overcharged cell equals the voltage of the remaining cells. The package loading then continues.

Operation of the passive-active BMS system

The passive-active BMS system will measure the voltage and temperature on each battery cell and, depending on the measured value and type of operation, activates one of the two balancing modules or both at the same time. There are two types of work: discharging and charging.

In the event of discharge during operation or standstill of a device or machine powered by a lithium battery, when the voltage drops below a set threshold (e.g. 3 V), the active balancing system will be activated, while the passive balancing system will be inactive. Cell balancing will continue until the voltage levels on all battery cells are equal or if the voltage on any cell drops below the minimum value set by the manufacturer.

When charging battery cells, both balancing systems are activated. In this situation, the active balancing system adds additional energy to the weakest link. However, when the voltage on any cell approaches the maximum limit set by the manufacturer, the passive balancing system is activated to prevent the cell from overcharging by dissipating excess heat using resistors. If there is a situation in which there is more energy in the charging process than can be dissipated into heat, the controller turns off the charger and switches to the state of measuring cell voltages. As soon as the cell voltages drop below the maximum value, the controller turns on the charger and both balancing systems again. If the voltages on the cells are already close to the maximum voltage, then only the passive balancing system will be turned on, while the active balancing system will be turned off. The operation of the mixed BMS system will be completed when the voltages on all cells have the same value (close to the maximum voltage consistent with the voltage specified by the manufacturer).

This operation of the passive-active BMS system should shorten the time needed to charge a lithium battery, because downtime caused by turning off the charger due to energy saturation of the strongest cells will occur less often. An example simulation of the operation of a passive-active BMS system is presented in Fig. 13.

Publisher: **KOMAG Institute of Mining Technology, Poland**
© 2024 Author(s). This is an open access article licensed under the Creative Commons BY-NC 4.0 (https://creativecommons.org/licenses/by-nc/4.0/)

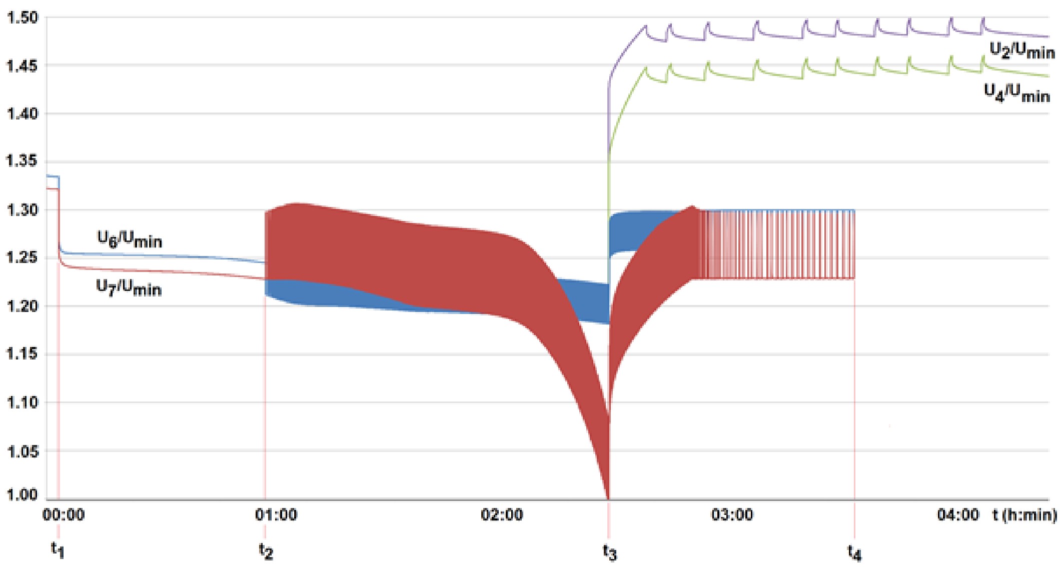

Fig. 13. Example of theoretical simulation of the voltage waveform on two loaded cells for a passive-active BMS system

5. Conclusions

An analysis of BMS systems with active and passive balancing of lithium cells was carried out. On this basis, the concept of a passive-active BMS system was proposed, which by combining active and passive balancing in one system will increase the possibility of effective and safe operation of batteries made of lithium cells.

The proposed solution will extend the operating time of a machine or device powered by a lithium battery because balancing battery cells is a key issue in managing the batteries of electrically powered vehicles, increasing the efficiency of the battery pack while extending its life cycle and ensuring safe operation at all times.

The benefit of a BMS system constructed in this way is that the active part of the balancing system will equalize the voltages on all cells and extend the battery life, while the passive part will ensure a safe charging process by leveling the differences between cells with lower and higher energy levels, protecting the battery against overcharging the cells.

The operation of the passive-active BMS system will shorten the time needed to charge a lithium battery, because downtime caused by turning off the charger due to energy saturation of the strongest cells will occur less often.

The use of such a solution can significantly improve the functioning of a device powered by a lithium battery. The battery will be protected at every moment of its use, i.e. during operation, parking and charging. The efficiency of the battery results from the efficiency of individual cells, especially the weakest ones.

Currently, energy storage is a dynamically developing industry, especially in connection with photovoltaic installations. The use of active balancing allows you to extend the battery life, as well as the use of recycled batteries that were no longer suitable for cooperation with passive balancers due to their insufficient performance. An active balancing system, the use of which will be economically justified, will constitute a market innovation.

Publisher: **KOMAG Institute of Mining Technology, Poland**
© 2024 Author(s). This is an open access article licensed under the Creative Commons BY-NC 4.0 (https://creativecommons.org/licenses/by-nc/4.0/)

References

[1] Carkhuff, Bliss G., Plamen A. Demirev, and Rengaswamy Srinivasan. Impedance-based battery management system for safety monitoring of lithium-ion batteries. *IEEE Transactions on Industrial Electronics* 2018, Vol. 65.8, pp. 6497-6504.

[2] Cao J., Schofield N., Emadi A. Battery Balancing Methods: A Comprehensive Review. *IEEE Vehicle Power and Propulsion Conference, VPPC,* September 3-5, 2008, Harbin, China.

[3] Lisbona, D., Snee, T. A review of hazards associated with primary lithium and lithium-ion batteries. *Process safety and environmental protection* 2011, Vol. 89(6), pp. 434-442.

[4] Sihua Wen. *Cell Balancing Buys Extra Run Time and Battery Life*, Texas Instruments, Inc., 2009.

[5] Ziegler A., Oeser D., Arndt B., and Ackva A. Comparison of Active and Passive Balancing by a Long Term Test Including a Post-Mortem Analysis of all Single Battery Cells. *in 2018 International IEEE Conference and Workshop in Óbuda on Electrical and Power Engineering (CANDO-EPE)* Budapest, 2018, pp. 000015–000020.

[6] Kurpiel W., Deja P., Polnik B., Skóra M., Miedziński B., Habrych M., Debita G., Zamłyńska M., Falkowski-Gilski P. Performance of Passive and Active Balancing Systems of Lithium Batteries in Onerous Mine Environment Bibliografia 33 poz. - // Energies. - 2021, nr 14(22), 7624, s.1-15.

[7] Kurpiel W., Polnik B. Miedziński B. System nadzorujący pracę baterii akumulatorów (BMS) w celu zwiększenia bezpieczeństwa ich funkcjonowania i żywotności stosowanych ogniw. *Mechanizacja i Automatyzacja Górnictwa* 2014, Vol. 5, pp. 47-49.

[8] Kurpiel W., Polnik B. Miedziński B. Właściwości eksploatacyjne ogniw litowych. *elektro.info* 2018, Vol. 10, pp. 44-48.

[9] Kurpiel W.: Research on balancing BMS systems in a climatic chamber. Bibliogr. 19 pozycji. - Min. Mach. - 2020, 3, 53-63.

[10] Bartoszek S., Jura J.: Układ aktywnego balansowania baterii ogniw litowych przeznaczony do górniczych maszyn mobilnych. Masz. Gór. 2019 nr 1 s. 52-65, ISSN 2450-9442.

[11] Kurpiel W.: Badania i analiza pracy baterii litowych z aktywnym systemem balansowania ogniw w układach zasilania maszyn górniczych w skali laboratoryjnej i na obiekcie rzeczywistym w kopalni. Praca własna ITG KOMAG. EG/E56-25147

[12] Dokumentacja baterii LiFePO4 3,2 V. Dostępna online: https://www.bto.pl/produkt/31801/headway-lfp38120(s)-10000mah-lifepo4 (dostęp 10 sierpnia 2021 r.).

Publisher: **KOMAG Institute of Mining Technology, Poland**
© 2024 Author(s). This is an open access article licensed under the Creative Commons BY-NC 4.0 (https://creativecommons.org/licenses/by-nc/4.0/)

e-ISSN 2719-3306 Mining Machines, 2024, Vol. 42 Issue 1, pp. 277-287

https://doi.org/10.32056/KOMAG2024.4.4.

Management of Scraper-Self-Propelled ore delivery parameters in caving operations

Received: 18.10.2024

Accepted: 13.11.2024

Published online: 17.12.2024

Author's affiliations and addresses:

[1] Dnipro University of Technology, 19 Yavornytskoho Ave., 49005, Dnipro, Ukraine

[2] AGH University of Krakow, Al. Mickiewicza 30, 30059, Krakow, Poland

***Correspondence:**

e-mail: kmn211179@gmail.com

Andrii KOSENKO [1], Oleh KHOMENKO [1], Maksym KONONENKO [1*], Rostyslav YEGORCHENKO [1], Grygorii STARIKOV [1], Roman DYCHKOVSKYI [1, 2]

Abstract:

This paper analyzes ore delivery methods suitable for the deep-level mining environments of the Kryvbas region. The study focuses on the feasibility and economic advantages of utilizing a combined scraper-self-propelled ore delivery system within sublevel caving operations. Through comprehensive analysis, it is found that the integration of self-propelled equipment significantly enhances the efficiency and cost-effectiveness of ore transport. The proposed delivery method involves using multi-bucket scraper winches for primary ore movement and deploying a self-propelled load-haul-dump (LHD) machine for secondary transport. Economic and mathematical modeling results demonstrate that this combined approach enables optimization of operational parameters, identifying the most effective application ranges for different types of self-propelled LHDs in secondary ore transport. Specifically, the study highlights that the ST7 model of self-propelled LHD is the most cost-effective solution for secondary transport, minimizing specific delivery costs while maintaining productivity. Additionally, the findings provide practical guidance on the optimal usage limits for various self-propelled LHD types, helping to inform equipment selection for enhanced operational efficiency in caving systems. These insights contribute to improved decision-making in mining operations, promoting both economic and technical benefits in high-depth mining scenarios.

Keywords: ore drawing and delivery, actual mining, ore drawing intensity, ore delivery methods, self-propelled loading and hauling machine, capital ore pass

© 2024 Author(s). This is an open access article licensed under the Creative Commons BY-NC 4.0 (https://creativecommons.org/licenses/by-nc/4.0/)

1. Introduction

The effectiveness of extraction operations and the comprehensive quantitative and qualitative recovery of ore reserves are critical issues in the development of high-grade iron ore through sublevel caving systems in Kryvbas mines [1]. A primary technological process in this system is ore release through horizontal bottom drifts of the receiving levels [2]. Ore transportation is a crucial component of the extraction process, determining the efficiency of ore release and overall mining productivity [3]. The selection of transportation equipment significantly impacts the organization of work and the productivity of the entire block [4].

In modern underground ore deposit extraction systems, ore release and transportation are among the most labor-intensive and inefficient processes [5]. The release of fragmented ore from the extraction area is typically carried out from under caved surrounding rock or through a network of specialized drifts uniformly distributed beneath the extraction face [6]. The ore moves through the extraction area and release drifts under the influence of gravity [7]. However, only about 50% of pure ore is recovered due to horizontal limitations in the release figure dimensions [8]. To reduce ore dilution, sequential releases from adjacent drifts are made in equal or varied doses, as per established release plans [9]. However, current release methods cannot fulfill these plans due to frequent blockages in the release drift necks and the avalanching flow of ore when these blockages are cleared [10]. Consequently, the release process is prolonged and marked by high ore losses and dilution, reaching up to 25% and 18%, respectively [11].

The inefficiency of gravity-based ore release and the use of low-capacity transportation equipment create a "bottleneck" in the technological work complex of modern extraction systems, especially when using advanced mass caving systems for ore and surrounding rock [12]. For example, the use of scraper installations in the extraction of high-grade iron ore deposits in Kryvbas with mass caving systems allows for an ore release intensity of 1.2–1.8 tons/m² per day, which is relatively low [13]. This low release intensity also negatively impacts the formation of compensation chambers, where volume accounts for only 8–12% (instead of the required 20–25%) of the primary reserve volumes needed for stable extraction units throughout their operational life [14]. Therefore, ore extraction is conducted under highly confined conditions, which at greater depths leads to the compaction of loose material [15]. Increasing rock pressure with depth further consolidates the ore within the extraction panels due to gravity [16], adversely affecting the physical and mechanical properties of the already fragmented ore [17]. Its cohesion increases to a point where it practically loses flow properties [18], leading to higher ore losses and dilution [19]. Additionally, working conditions deteriorate in the extraction area, with early failures of release and transport drifts [20].

The intensity of rock pressure is significantly influenced by the intensity of ore release; as ore release increases, the pressure from caved rock decreases toward a stable level that depends on the extraction unit parameters and the ore's physical and mechanical properties [21]. Due to the uneven ore release, characteristic of all Kryvbas mines, the pressure on the receiving level bottom is distributed unevenly [22].

To optimize extraction, it is essential to achieve a high-intensity, evenly dosed ore release across the entire receiving level bottom area. However, traditional scraper transport methods fall short in maintaining such uniformity and intensity due to their limitations in handling large volumes consistently. As a result, alternative transport solutions must be considered to enhance ore release efficiency and minimize ore loss and dilution during extraction operations.

2. Literature and patterns background

Currently, both Ukrainian and international mining operations utilize various ore transport methods, including scraper winches with a capacity of 150–250 tons per shift [23], self-propelled load-haul-dump machines (LHDs) with a capacity of 800–1200 tons per shift [24], conveyors with a capacity of 800–1500 tons per shift [25], and vibrating feeders with a capacity of 700–900 tons per shift [26]. Additionally, there are combinations of multi-bucket scraper winches and self-propelled LHDs, with the capacity ranging from 400 to 2200 tons per shift, depending on the type of LHD used.

Publisher: KOMAG Institute of Mining Technology, Poland
© 2024 Author(s). This is an open access article licensed under the Creative Commons BY-NC 4.0 (https://creativecommons.org/licenses/by-nc/4.0/)

Another method involves blast-assisted ore transport, where productivity depends on the cleaning space parameters, the ore body's dip angle, and the transport distance, and can vary significantly [5, 27, 28].

Scraper transport is the most widely used method in Kryvbas mines due to its simplicity and low cost, but it has low productivity [29]. Conveyors are the most productive, yet they are rarely used due to rapid wear, frequent ore blockages, and resulting downtime for maintenance [30]. Vibrating feeders have proven efficient mainly in near-surface mining, as their installation underground is labor-intensive and costly [31]. Blast-assisted transport is feasible only with chamber mining systems and ore bodies with a dip angle of 15–45°, making it unsuitable for Kryvbas underground mines. Despite the high productivity of self-propelled LHDs with end-discharging ore techniques in foreign mining practices [32], these machines are not widely used in Kryvbas mines due to significant ore losses between discharge points, leading to increased ore dilution levels of 25–35% [33]. Furthermore, using high-capacity self-propelled LHDs in Kryvbas's complex geomechanical conditions requires large cross-section openings of 12–14 m², which increases maintenance costs due to high ground pressure, impacting labor intensity and ore transport costs [34, 35].

The combined scraper-self-propelled transport method (Fig. 1) is both rational and effective due to the complementary advantages of scraper winches and self-propelled load-haul-dump machines (LHDs) [5]. By employing multi-bucket scraper winches, it becomes possible to achieve an evenly dosed release from each discharge point along the transport axis, enhancing control and efficiency. Furthermore, utilizing larger discharge niches, measuring 2×2 m instead of the conventional 1.5 m diameter holes, significantly reduces equipment downtime, as it helps to localize blockages of oversized ore pieces at the discharge throat, thus minimizing interruptions. To ensure continuous high productivity of the self-propelled LHDs, larger diameter permanent ore passes are necessary, allowing for independent transport processes without bottlenecks [36, 37]. These larger passes contribute to a steady flow of material and reduce reliance on multiple transport points, increasing overall efficiency. Consequently, the productivity of the transport process is determined primarily by the average ore transport trajectory length for the LHDs, allowing for a more predictable and stable operation. This optimized combination of transport methods offers an adaptable solution that aligns with the operational demands and geomechanical constraints typical of deep-level mining operations.

This proposed combined ore transport scheme is well-suited to the complex geomechanical conditions of Kryvbas's deep mine levels and allows for:

- minimizing the impact of human factors on ore release management;
- ensuring evenly dosed ore release from all discharge points along the primary transport line;
- performing sequential ore release from discharge points, moving from the hanging to the footwall side of the ore body via multi-bucket scraper installations;
- reducing blockages in discharge points during ore release;
- improving the structural layout of the ore release and transport levels, reducing the specific length of preparatory development by 1.5–2.5 m per 1000 tons of ore reserve;
- enhancing the sanitary and hygienic working conditions for miners and increasing safety during ore release and transport operations; – enabling selective extraction of ore of varying quality.

The research on and optimization of the combined scraper-self-propelled transport parameters in caving systems is a relevant scientific and practical task with significant potential benefits. By optimizing these parameters, mining operations can enhance labor productivity within the ore transport process, making it more efficient and cost-effective. Improved transport efficiency can lead to faster material handling, reducing the overall operational time and minimizing delays. Additionally, fine-tuning these parameters can significantly reduce the specific costs associated with ore transport, allowing for better allocation of resources. Ultimately, this optimization supports more sustainable

Publisher: **KOMAG Institute of Mining Technology, Poland**
© 2024 Author(s). This is an open access article licensed under the Creative Commons BY-NC 4.0 (https://creativecommons.org/licenses/by-nc/4.0/)

mining practices by lowering operational expenses and improving the overall efficiency of resource extraction processes.

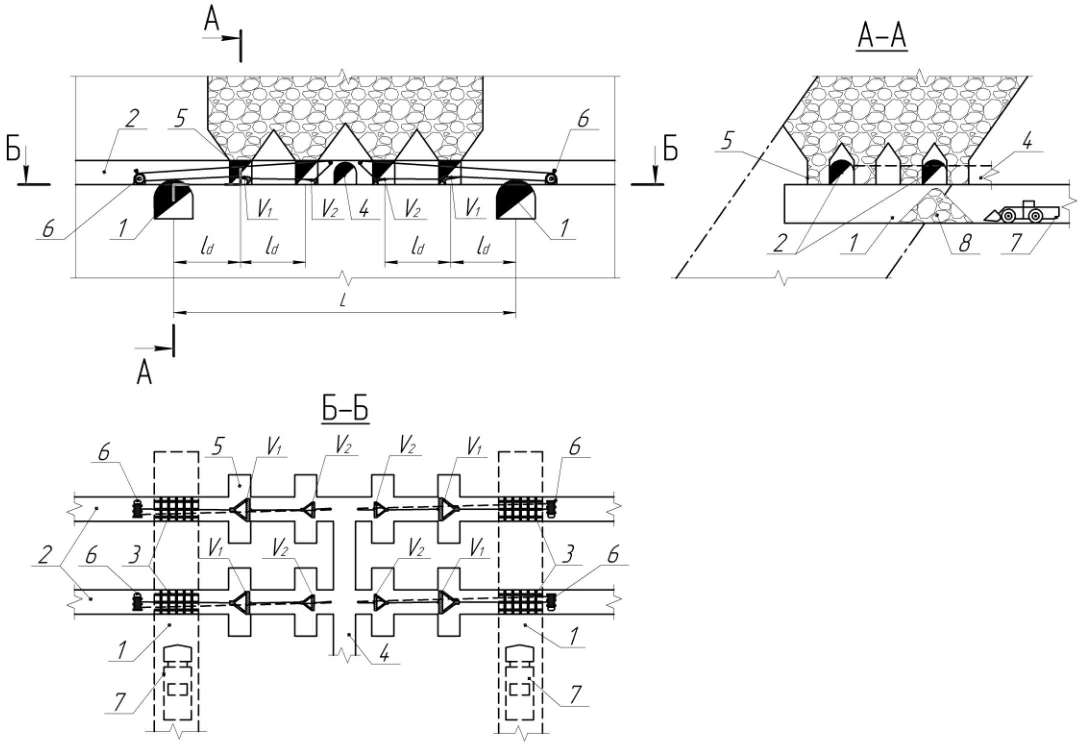

Fig. 1. Diagram of the Combined Scraper-Self-Propelled Ore Transport Method Using a Multi-Bucket Scraper Winch and Self-Propelled LHD Complex: 1 – Load-haul-dump drifts; 2 – Scraper drifts; 3 – Grizzly screen; 4 – Ventilation drift; 5 – Discharge niches; 6 – Multi-bucket scraper winches; 7 – Self-propelled LHD; 8 – Ore pile; $V_1 = 2V_2$ – Volume of the first scraper, m³; V_2 – Volume of the second scraper, m³; l_d – Distance between adjacent discharge niches and the center of the load-haul-dump drift; L – Distance between load-haul-dump drifts [own study]

3. Methods & methodology of research

To determine the optimal parameters and application boundaries for the scraper-self-propelled ore delivery method, an economic-mathematical modeling approach was employed. Based on the literature review, an economic-mathematical model was found to be the most suitable for the conditions of the Kryvbas region. This model uses the cost of transporting one ton of ore, factoring in the amortization of mine development and preparatory work, as its primary criterion and general functional.

The modeling involved assessing both technical and economic factors impacting the efficiency of ore transport, including equipment type, transport distances, and operational capacity. Various transport scenarios were simulated to analyze the effect of scraper winches and self-propelled load-haul-dump (LHD) machines in isolation, as well as in combination. This allowed for a comparative evaluation of the productivity and costs associated with each transport method under different mining conditions.

The model considered the physical limitations and wear factors of equipment, such as the maintenance frequency and expected lifespan of scraper winches and LHD machinery. The model was calibrated using data from actual ore delivery operations in Kryvbas mines, making it possible to reflect real-life constraints and optimize the system to local geological and operational conditions. To ensure accuracy, data collection involved detailed analysis of existing ore delivery systems, including factors such as loading capacity, fuel and energy consumption, and ore dilution rates. A cost analysis

Publisher: **KOMAG Institute of Mining Technology, Poland**
© 2024 Author(s). This is an open access article licensed under the Creative Commons BY-NC 4.0 (https://creativecommons.org/licenses/by-nc/4.0/)

was conducted for each component, allowing for a detailed breakdown of expenditures associated with different aspects of the scraper-self-propelled delivery method.

The methodology also included sensitivity analysis to examine how changes in various parameters- such as transport distance and ore density – would affect the overall efficiency of the ore delivery system. By adjusting these variables within the model, the research was able to identify the most cost-effective and operationally efficient configurations under varying conditions. The proposed model and resulting recommendations were validated through pilot implementation in select mining sites within Kryvbas. The outcomes of these trials were compared to the model's projections, allowing for further refinement of the system parameters. This validation phase ensured that the model's recommendations align with practical constraints and demonstrate improved productivity and reduced costs in real-world applications.

The following input data were selected for the modeling. The combined scraper-self-propelled ore delivery method involves using 55LS-2SMA scraper winches for primary delivery and various types of self-propelled LHD machines for secondary delivery, suitable for the geomechanical conditions found at the deep levels of the Kryvbas mines (models EST2D, ST2D, ST3.5, ST7, ST1030, LH409E, TORO400D). The ore deposit thickness was chosen to reflect the average conditions in Kryvbas, at 25 meters. In all cases, the sublevel height is fixed at 37.5 meters. Ore extraction was carried out into a compensation space with a volume equivalent to 23% of the total reserves of the mining unit.

4. Results of the research

Based on the calculations performed using the economic-mathematical model, graphical dependencies were constructed to illustrate the specific costs of ore delivery relative to the productivity of various types of Load-Haul-Dump (LHD) machines used in secondary ore transport. These relationships are presented in Fig. 2. The results provide insights into the cost-effectiveness of different LHD machine types under varying productivity conditions, allowing for an optimized approach to secondary ore transportation.

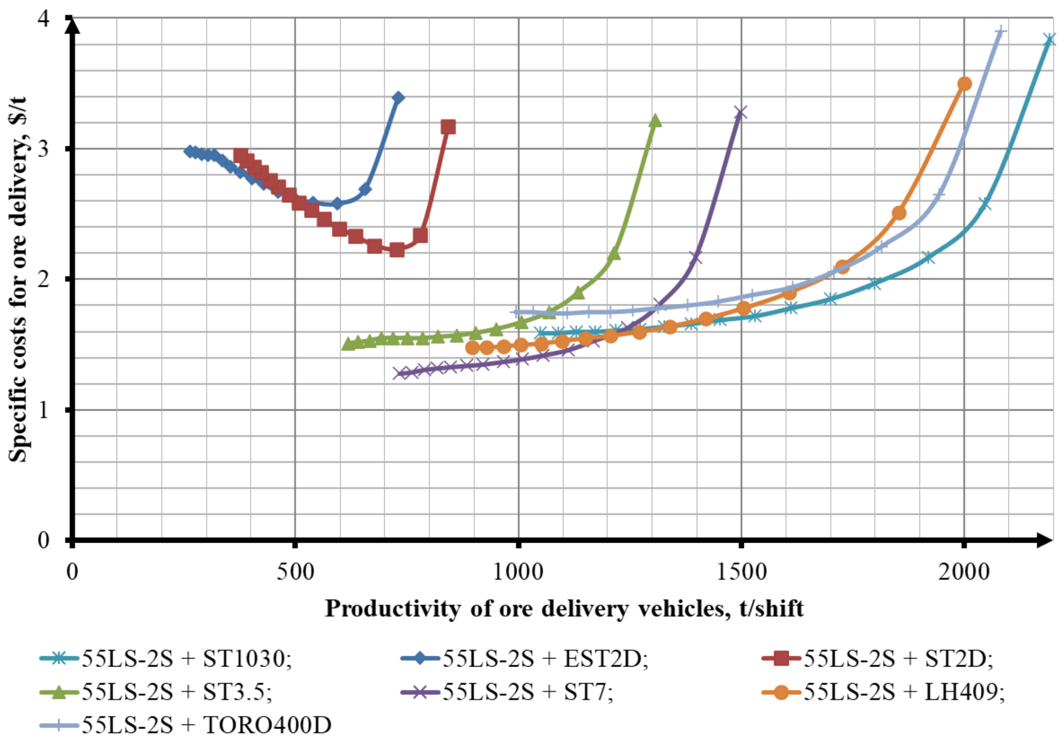

Fig. 2. The dependence of specific ore delivery costs on the productivity of various LHD machine types [own study]

Publisher: **KOMAG Institute of Mining Technology, Poland**
© 2024 Author(s). This is an open access article licensed under the Creative Commons BY-NC 4.0 (https://creativecommons.org/licenses/by-nc/4.0/)

Fig. 2 shows that the lowest specific ore delivery costs are achieved when using a combined scraper-self-propelled transport method, utilizing multi-bucket scraper winches of the 55LS-2SMA type for primary delivery, and the self-propelled LHD ST7 type for secondary delivery. This scheme has the lowest cost indicators when the average transport distance is within the range of 120–270 m. Under these conditions, the productivity of the system is between 720–1110 tons per shift, which is 1.4–3.3 times higher than when using only scraper winches for ore delivery.

A significant reduction in specific ore delivery costs is achieved by increasing the average transport distance from 120 m to 270 m, as seen in Fig. 3. This reduction is due to a notable decrease in specific capital expenditure for constructing the primary ore pass, dropping from $1.24 per ton to $0.21 per ton. However, there is a corresponding decline in the productivity of the self-propelled LHDs used in secondary ore delivery, with performance decreases as follows: EST2D from 460 tons per shift to 264 tons per shift, ST2D from 600 tons per shift to 375 tons per shift, ST3.5 from 950 tons per shift to 620 tons per shift, ST7 from 1110 tons per shift to 730 tons per shift, ST1030 from 1610 tons per shift to 1050 tons per shift, LH409E from 1500 tons per shift to 890 tons per shift, and TORO400D from 1520 tons per shift to 990 tons per shift.

By approximating the maximum values (Fig. 3), an empirical dependency was obtained to describe how specific capital costs for constructing the primary ore pass change with respect to the balance of ore reserves. This dependency highlights the relationship between the ore reserves allocated to a single ore pass and the associated capital investment required for its construction. As the balance of ore reserves increases, the model demonstrates how specific costs can be optimized, providing a clear framework for cost management. The empirical model also allows for adjustments based on varying reserve balances, making it adaptable to different mining conditions. Overall, understanding this dependency is crucial for making informed decisions on resource allocation and reducing construction expenses in ore pass development. The specific costs for constructing the primary ore pass, depending on the balance of ore reserves transported by one ore pass to the receiving level, can be determined by the formula:

$$P_{vytr.} = 200.27 B_{zap.}^{1.422}, \text{ \$/thousands tons with } R^2 = 0.9848,$$

where:

$B_{zap.}$ – ore reserves per primary ore pass, thousands of tons;
R^2 – approximation accuracy.

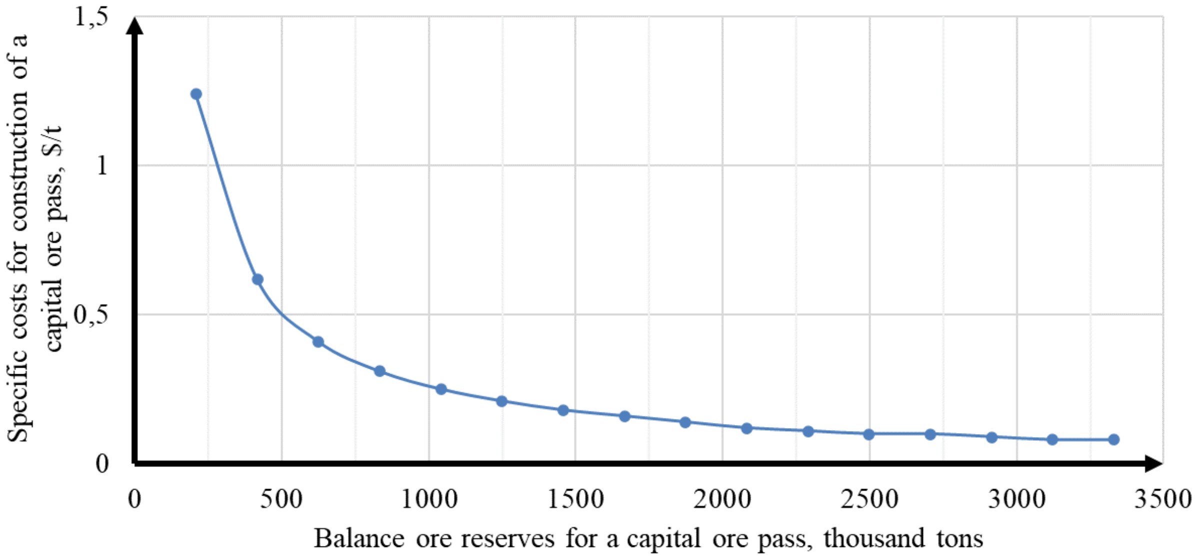

Fig. 3. The dependence of specific costs for constructing a primary ore pass on ore reserves delivered by a single pass to the receiving level [own study]

Publisher: **KOMAG Institute of Mining Technology, Poland**
© 2024 Author(s). This is an open access article licensed under the Creative Commons BY-NC 4.0 (https://creativecommons.org/licenses/by-nc/4.0/)

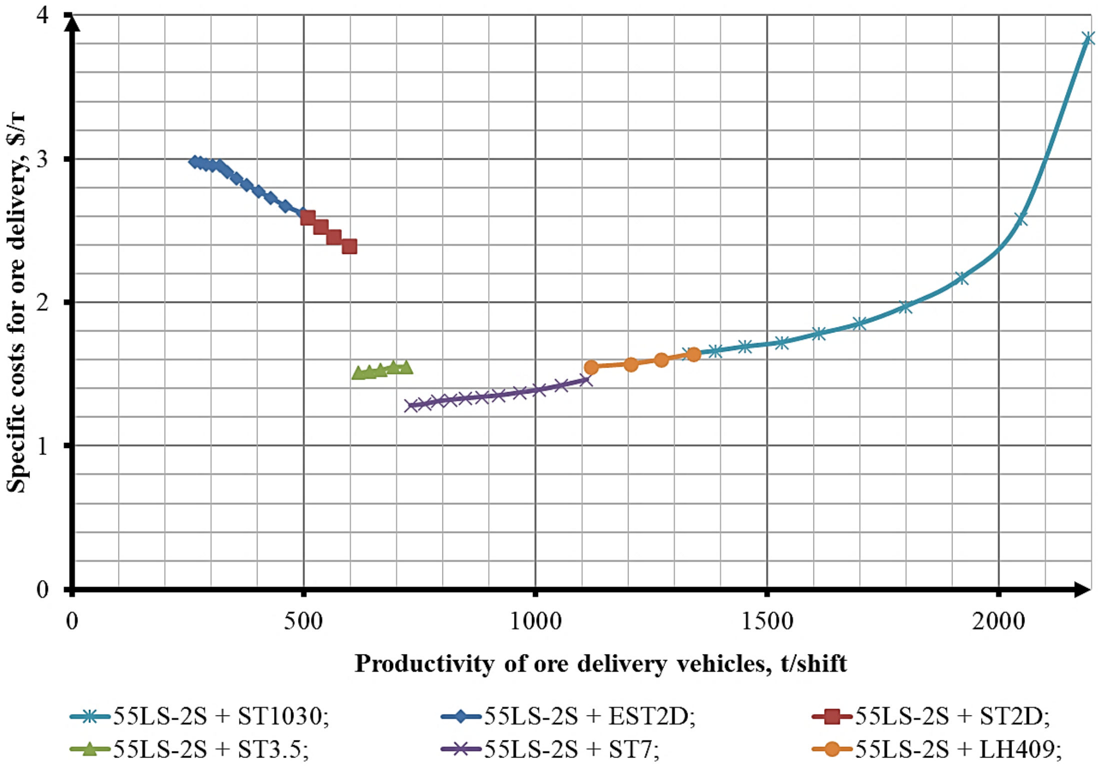

Fig. 4. The dependency of optimal application limits for various types of self-propelled LHDs in secondary ore transport [own study]

As shown in Fig. 4, when employing the combined scraper-self-propelled method for ore transport, scraper winches of the type 55LS-2S are consistently used for primary transport in all cases. To maintain a productivity range of 260–500 tons per shift in the stope, the EST2D self-propelled LHD is necessary for secondary transport, with specific transport costs decreasing from $2.98/ton to $2.62/ton as productivity increases. For productivity between 500–620 tons per shift, the ST2D self-propelled LHD should be used, resulting in a decrease in specific transport costs from $2.59/ton to $2.23/ton as productivity rises.

In the productivity range of 620–720 tons per shift, the ST3.5 self-propelled LHD becomes necessary for secondary transport, though specific transport costs slightly increase from $1.51/ton to $1.55/ton with higher productivity. When productivity ranges from 720–1110 tons per shift, the ST7 LHD is optimal, with costs gradually increasing from $1.28/ton to $1.46/ton. For higher productivity requirements of 1110–1330 tons per shift, the LH409E LHD is recommended, as specific costs rise from $1.59/ton to $1.64/ton.

In cases of extremely high productivity, such as 1330–2200 tons per shift, the ST1030 LHD is necessary, with transport costs increasing significantly from $1.64/ton to $3.84/ton as productivity rises. However, the optimal productivity range for the ST1030 LHD is between 1300–1700 tons per shift, which keeps ore transport costs within a manageable range of $1.64–$1.78 per ton, ensuring efficient and cost-effective ore transportation.

5. Discussion of the results

The research findings offer insights into the cost-effectiveness and operational efficiency of the combined scraper-self-propelled ore transport method. Using an economic-mathematical model tailored to the mining conditions of the Kryvbas region, the study identifies optimal configurations for primary and secondary ore transport. Specifically, scraper winches, such as the 55LS-2SMA model,

Publisher: **KOMAG Institute of Mining Technology, Poland**
© 2024 Author(s). This is an open access article licensed under the Creative Commons BY-NC 4.0 (https://creativecommons.org/licenses/by-nc/4.0/)

are consistently effective for primary ore transport, while various types of self-propelled Load-Haul-Dump (LHD) machines, like the ST7, EST2D, and ST1030, demonstrate specific productivity and cost advantages in secondary transport. This approach reveals that a combined transport system can significantly reduce delivery costs and increase productivity, especially when transport distances range between 120 and 270 meters.

The results indicate that the combined transport method is particularly efficient within specific productivity thresholds. For instance, the ST7 LHD yields optimal results at productivity levels of 720–1110 tons per shift, while the ST1030 LHD is more effective at the higher end of the productivity spectrum, between 1300–1700 tons per shift. Additionally, the study identifies a notable cost reduction when transport distances extend to 270 meters, where capital expenses for ore pass construction decline from $1.24 per ton to $0.21 per ton. However, as transport distances increase, there is a corresponding decline in the productivity of certain LHD models. This interplay between transport distance, equipment type, and operational cost forms a critical component of the optimization process.

The empirical dependency identified through approximation provides a framework for understanding how ore reserves correlate with the cost of constructing primary ore passes. By analyzing this relationship, the study offers a practical approach to managing costs associated with ore pass development. This model also facilitates sensitivity analyses, allowing for adjustments based on reserve balances and varying operational conditions. Through pilot trials and validation, the model proved to be adaptable to the real-world challenges faced by mining operations in the Kryvbas region, underscoring its utility in guiding decisions on resource allocation, equipment choice, and cost management.

6. Conclusions

The study concludes that the use of self-propelled equipment for ore delivery in sublevel caving systems, as applied in the Kryvbas mines, is both feasible and economically justified when employing a combined scraper-self-propelled transport approach. For secondary ore delivery, specific self-propelled Load-Haul-Dump (LHD) machines, such as the EST2D, ST2D, ST3.5, ST7, ST1030, LH409E, and TORO400D, were found to be particularly suitable and cost-effective.

The combined approach, utilizing multi-bucket scraper winches (55LS-2SMA type) for primary delivery and self-propelled ST7 machines for secondary delivery, achieves the lowest specific delivery costs, ranging from $1.28 to $1.46 per ton. This cost advantage is realized when the average transport distance is between 120 and 270 meters, enabling productivity levels between 720 and 1110 tons per shift. Such productivity represents an improvement of 1.4 to 3.3 times compared to a transport scheme that uses dual 55LS-2SMA scraper winches alone.

The research establishes optimal productivity ranges for each type of LHD used in secondary ore delivery under the combined transport system. The identified productivity thresholds include EST2D for 260–500 tons per shift, ST2D for 500–620 tons per shift, ST3.5 for 620–720 tons per shift, ST7 for 720–1110 tons per shift, LH409E for 1110–1330 tons per shift, and ST1030 for 1330–1700 tons per shift. These findings provide a valuable framework for optimizing ore transport operations within similar mining environments, ensuring cost efficiency and increased productivity.

In our further research cwe’ll the integration of automated control systems and advanced monitoring technologies within the combined scraper-self-propelled ore delivery system to improve efficiency and safety. These studies would focus on real-time data collection and predictive maintenance for Load-Haul-Dump (LHD) machinery to reduce downtime and extend equipment lifespan. The analysis would evaluate the environmental impacts of ore transport methods, identifying ways to minimize energy consumption and emissions. Research into optimizing LHD types for varying geological conditions and assessing alternative energy sources, such as electric or hybrid-powered LHDs, could also contribute to more sustainable mining practices.

Publisher: **KOMAG Institute of Mining Technology, Poland**
© 2024 Author(s). This is an open access article licensed under the Creative Commons BY-NC 4.0 (https://creativecommons.org/licenses/by-nc/4.0/)

References

[1] Martynov, V.K., Simforov, G.E., Drochilov, L.G., Koval'skaya, A.A.: Losses and dilution of iron ore in mass-caving systems in Krivoi Rog mines. Soviet Mining Science 1969, 5(2): 166–171. DOI: 10.1007/bf02501895

[2] Dyadechkin, N.I., Malakhov, I.N.: State and prospects of development of methods of booty of iron-stones in Kryvbass. Metallurgicheskaya i Gornorudnaya Promyshlennost 2004, (4): 66-69.

[3] Azaryan, A.A., Batareyev, O.S., Karamanits, F.I., Kolosov, V.O., Morkun, V.S. Ways to Reduce Ore Losses and Dilution in Iron Ore Underground Mining in Kryvbass. Science and Innovation 2018, 14(4): 17–24. DOI: 10.15407/scine14.03.017

[4] Zhang, Z.-X.: Lost-ore mining–A supplementary mining method to sublevel caving. International Journal of Rock Mechanics and Mining Sciences 2023, 168: 105420. DOI: 10.1016/j.ijrmms.2023.105420

[5] Kosenko, A.V.: Improvement of sub-level caving mining methods during high-grade iron ore mining. Naukovyi Visnyk Natsionalnoho Hirnychoho Universytetu 2021, 1: 19–25. DOI: 10.33271/nvngu/2021-1/019

[6] Stupnik, M., Kalinichenko, V., Kalinichenko, O., Shepel, O., Hryshchenko, M.: Scientific and technical problems of transition from open pit to combined technologies for raw materials mining. IOP Conference Series: Earth and Environmental Science 2023, 1254(1): 012070. DOI: 10.1088/1755-1315/1254/1/012070

[7] Stupnik, M., Kalinichenko, V., Kalinichenko, O., Shepel, O., Pochtarev, A.: Improvement of the transitional technology from open pit to underground mining of magnetite quartzite. E3S Web of Conferences 2024, 526: 01026. DOI:10.1051/e3sconf/202452601026

[8] Pysmennyi, S., Fedko, M., Chukharev, S., Sakhno, I., Moraru, R., Panayotov, V.: Enhancement of the rock mass quality in underground iron ore mining through application of resource-saving technologies. IOP Conference Series: Earth and Environmental Science 2023, 1156(1): 012029. DOI: 10.1088/1755-1315/1156/1/012029

[9] Rymarchuk, B.I., Shepel, O.L., Khudyk, M.V.: Expediency of application of the vertical concentrated charges to decrease losses of ore on a lying wall of deposits. Naukovyi Visnyk Natsionalnoho Hirnychoho Universytetu 2017, 3: 32-37.

[10] Kononenko, M., Khomenko, O., Kosenko, A., Myronova, I., Bash, V., Pazynich, Y.: Raises advance using emulsion explosives. E3S Web of Conferences 2024, 526: 01010. DOI: 10.1051/e3sconf/202452601010

[11] Ming, J., Pan, Y., Xie, J., Li, Z., Guo, R.: Study on the law of ore dilution and loss and control strategies under brow line failure in sublevel caving mining 2024. DOI: 10.21203/rs.3.rs-4599767/v1

[12] Pysmennyi, S., Brovko, D., Shwager, N., Kasatkina, I., Paraniuk, D., Serdiuk, O.: Development of complex-structure ore deposits by means of chamber systems under conditions of the Kryvyi Rih iron ore field. Eastern-European Journal of Enterprise Technologies 2018, 5(1-95): 33–45. DOI: 10.15587/1729-4061.2018.142483

[13] Serdaliyev, Y., Iskakov, Y., Bakhramov, B., Amanzholov, D.: Research into the influence of the thin ore body occurrence elements and stope parameters on loss and dilution values. Mining of Mineral Deposits 2022, 16(4): 56–64. DOI: 10.33271/mining16.04.056

[14] Stupnik, M., Kalinichenko, V., Kolosov, V., Pysmennyi, S., Shepel, A.: Modeling of stopes in soft ores during ore mining. Metallurgical and Mining Industry 2014, 3: 32–36.

[15] Kononenko, M., Khomenko, O., Kovalenko, I., Kosenko, A., Zahorodnii, R., Dychkovskyi, R.: Determining the performance of explosives for blasting management. Rudarsko-Geološko-Naftni Zbornik 2023, 38(3): 19–28. DOI:10.17794/rgn.2023.3.2

[16] Khorolskyi, A, Kosenko, A., Chobotko, I.: Application of graphs and network models for designing processes for control the stress-strain state of a rock mass. ARPN Journal of Engineering and Applied Sciences 2024, 19(3): 164–171. DOI: 10.59018/022429

[17] Stupnik, M., Kalinichenko, O., Shepel, O., Bleikher, O.: Study of rock massif strains when creating an internal dump in the zone of transition from open pit to underground mining. E3S Web of Conferences

Publisher: **KOMAG Institute of Mining Technology, Poland**
© 2024 Author(s). This is an open access article licensed under the Creative Commons BY-NC 4.0 (https://creativecommons.org/licenses/by-nc/4.0/)

2024, 567: 01006. DOI: 10.1051/e3sconf/202456701006

[18] Kalinichenko, V., Pysmennyi, S., Peremetchyk, A., Yazhynskyi, I.: Reduction of ore losses on the footwall by improving ore breaking. E3S Web of Conferences 2024, 567: 01022. DOI: 10.1051/e3sconf/202456701022

[19] Kosenko, A.: Development of an Efficient Process Scheme for Breaking High-Grade Iron Ores of Low Strength and Stability During Sublevel Caving. Science and Innovation 2023, 19(3): 38–47. DOI: 10.15407/scine19.03.038

[20] Pysmennyi, S., Chukharev, S., Peremetchy, A., Fedorenko S., Matsui, A.: Study of Stress Concentration on the Contour of Underground Mine Workings. Inzynieria Mineralna 2023, 1: 69–78. DOI: 10.29227/IM-2023-01-08

[21] Kosenko, A., Khomenko, O., Kononenko, M., Myronova, I., Pazynich, Y.: Raises advance using borehole hydraulic technology. E3S Web of Conferences 2024, 567: 01008. DOI: 10.1051/e3sconf/202456701008

[22] Pysmenniy, S., Shvager, N., Shepel, O., Kovbyk, K., Dolgikh, O.: Development of resource-saving technology when mining ore bodies by blocks under rock pressure. E3S Web of Conferences 2020, 166: 02006. DOI: 10.1051/e3sconf/202016602006

[23] Kononenko, M.M., Khomenko, O.Y., Kovalenko, I.L., Savchenko, M.V.: Control of density and velocity of emulsion explosives detonation for ore breaking. Naukovyi Visnyk Natsionalnoho Hirnychoho Universytetu 2021, 2: 69–75. DOI: 10.33271/nvngu/2021-2/069

[24] Zubkov, V.P., Petrov, D.N.: Impact of the distance between the draw holes on the ore loss due to congealing during ore drawing. Mining Industry Journal 2024, 2/2024: 104–110. DOI: 10.30686/1609-9192-2024-2-104-110

[25] Deng, Z., Ma, C., Xia, Z., Ma, Q., Lu, Z.: Influence of ore-drawing port position on ore-rock flow characteristics in ore pass and lateral pressure on ore pass wall. Scientific Reports 2024, 14(1). DOI: 10.1038/s41598-024-72032-8

[26] Niu, X., Zhe, Y., Sun, H., Hou, K., Jiang, J.: Study on the Effect of Ore-Drawing Shear Factor on Underground Debris Flow in the Block Caving Method. Water 2023, 15(20): 3563. DOI: 10.3390/w15203563

[27] Dychkovskyi, R., Dyczko, A., & Borojević Šoštarić, S.: Foreword: Physical and Chemical Geotechnologies – Innovations in Mining and Energy. E3S Web of Conferences, 2024, 567, 00001. https://doi.org/10.1051/e3sconf/202456700001

[28] Khomenko, O., Rudakov, D., Lkhagva, T., Sala, D., Buketov, V., & Dychkovskyi, R.: Managing the horizon-oriented in-situ leaching for the uranium deposits of Mongolia. Rudarsko-Geološko-Naftni Zbornik, 2023, 38(5), 49–60. https://doi.org/10.17794/rgn.2023.5.5

[29] Volkov, A.P., Buktukov, N.S., Kuanyshbaiuly, S.: Safe and effective methods for mining thin tilt and steeply dipping deposits with ore drawing via mud flow. Gornyi Zhurnal 2022, 86–91. DOI: 10.17580/gzh.2022.04.13

[30] Pysmennyi, S., Fedko, M., Peremetchyk, A., Chukharev, S., Pilchyk, V., Mutambo, V.: Improvement of the stoping technology in mining magnetite quartzite by underground methods. E3S Web of Conferences 2024, 526: 01023. DOI: 10.1051/e3sconf/202452601023

[31] Pysmennyi, S., Chukharev, S., Peremetchyk, A., Shvaher, N., Fedorenko, S., Tien, V.T.: Enhancement of the technology of caved ore drawing from the ore deposit footwall “triangle.” IOP Conference Series: Earth and Environmental Science 2023, 1254(1): 012065. DOI: 10.1088/1755-1315/1254/1/012065

[32] Pysmennyi, S., Chukharev, S., Kourouma, I. K., Kalinichenko, V., Matsui, A.: Rozwój technologii wydobywania rudy z niestabilnymi wiszącymi skałami. Inżynieria Mineralna 2023, 1(1(51): 103–112. DOI: 10.29227/im-2023-01-13

[33] Stupnik, M., Fedko, M., Hryshchenko, M., Kalinichenko, O., Kalinichenko, V.: Badanie wpływu kompensacji na stabilność górotworu oraz jakość wydobywanej rudy. Inżynieria Mineralna 2023, 1(1(51): 129–135. DOI: 10.29227/im-2023-01-16

[34] Stupnik, M., Kalinichenko, V., Kalinichenko, O., Yakovlieva, S.: Investigation and optimization of main materials consumption when mining iron ores at deep levels of the Underground Mine Group of the PJSC

Publisher: **KOMAG Institute of Mining Technology, Poland**
© 2024 Author(s). This is an open access article licensed under the Creative Commons BY-NC 4.0 (https://creativecommons.org/licenses/by-nc/4.0/)

"ArcelorMittal Kryvyi Rih." E3S Web of Conferences 2020, 201: 01026. DOI: 10.1051/e3sconf/202020101026

[35] Kalinichenko, V., Pysmennyi, S., Shvaher, N., Kalinichenko, O.: Selective underground mining of complex structured ore bodies of Kryvyi Rih Iron Ore Basin. E3S Web of Conferences 2018, 60: 00041. DOI: 10.1051/e3sconf/20186000041

[36] Stupnik, M., Kalinichenko, V., Bah, I. Pozdnyakov, V., Keita, D.: Service of self-propelled mining equipment in underground conditions. Progressive Technologies of Coal, Coalbed Methane, and Ores Mining 2014, 171–174. DOI: 10.1201/b17547-29

[37] Castro, R., Cid, P., Gómez, R., Weatherley, D.: The influence of drawbell geometry on hang-ups during ore extraction. Mining, Metallurgy & Exploration 2023, 40(3): 787–792. DOI: 10.1007/s42461-023-00756-8

Publisher: **KOMAG Institute of Mining Technology, Poland**
© 2024 Author(s). This is an open access article licensed under the Creative Commons BY-NC 4.0 (https://creativecommons.org/licenses/by-nc/4.0/)

https://doi.org/10.32056/KOMAG2024.4.5.

Automated longwall in Polish hard coal mines – conditions and limitations

Received: 02.12.2024

Accepted: 13.12.2024

Published online: 17.12.2024

Jacek KORSKI [1], **Wojciech KORSKI** [2*],

Author's affiliations and addresses:

[1] KOMAG Institute of Mining Technology, Pszczyńska 37
44-101 Gliwice, Poland

[2*] Lukasiewicz Research Network – Institute for Innovative Technologies EMAG
Leopolda 31
40-189 Katowice, Poland

*** Correspondence:**

e-mail: wojciech.korski@emag.lukasiewicz.gov.pl

Abstract:

The article presents the determinants and limitations of the possibility of implementing longwalls with a high degree of automation in the Polish underground coal mining against the background of similar solutions in the global mining industry. Significant differences in the conditions for mining with longwall systems in Polish conditions and the differences in the planned objectives of longwall automation in Poland were indicated.

Keywords: Longwall mining, automated longwall, automation in mining, mechanized longwall

Publisher: **KOMAG Institute of Mining Technology, Poland**
© 2024 Author(s). This is an open access article licensed under the Creative Commons BY-NC 4.0 (https://creativecommons.org/licenses/by-nc/4.0/)

1. Introduction

Automation is a significant reduction or replacement (the process of replacing) human physical and mental work by the work of machines operating on the basis of self-regulation and performing specific activities without human participation (i.e. automatic) [1, 2, 3, 4]. Automation is also the use of machines for work that is impossible to do otherwise. Automation is the next stage after mechanization. For several years, the topic of automatic or even autonomous longwall has been returning in the Polish hard coal mining industry, but such a solution has not been used so far. The article attempts to analyse the possibility of implementing an automatic longwall in the conditions of Polish hard coal mines based on the analysis of known solutions of automated longwall systems and the conditions of their use.

2. Development of automation of powered walls in Poland and in the world

The development of coal mining automation in Poland has a long history [5]. In the 60s of the twentieth century, automation in the area of shaft hoists and belt conveyors was strongly developed. Work has also begun on full automation of longwall faces. Around 1964, the Polish hard coal mining industry (PGWK) started work on two types of automated longwalls (ASI-1 and BESTA), which were implemented in the Zabrze and Bielszowice mines (BESTA) (Fig.1), then in the mine. Lenin – Wesoła). The ASI system was based on the principle of controlling the machines via a central computer, and in the BESTA system, the shearer started the operation of the support section. In 1968, the Jan Automated Coal Mine was launched on a part of the Wieczorek mine, where an "automatic" ASI-2 longwall controlled by a computer was launched. In 1973, work on the automated longwall was abandoned, at the same time the development of automation of individual devices included in the mechanized longwall system was continued (and continues to this day).

The reasons for abandoning work on the development of automatic longwalls in Poland were:

- Significant capital expenditure and operating costs with no noticeable increase in wall performance/productivity.
- A prerequisite for the introduction of automation of a process or operation is the full (complete) mechanization of this process or operation – however, many activities and operations performed in the longwall at that time were performed manually (especially at the longwall-roadway intersection), and initially single-drum shearers worked in one direction and did not have mining height adjustment. The peeling process was therefore a manual and machine process.
- Availability of qualified specialist staff - a side effect of the launch of automatic longwalls in the Zabrze (ASI 1) and Bielszowice (BESTA) mines, and then the Automated Hard Coal Mine Jan, was the drainage of other mines of automation specialists. Another aspect of this problem was the resignations of project leader.
- State of the art and its imperfections - One of the biggest problems of ASI and BESTA automated walls was the high failure rate caused by sensor errors causing frequent stoppages.

In Table 1 are presented important events in area of LW automation in Poland and worldwide.

Publisher: **KOMAG Institute of Mining Technology, Poland**
© 2024 Author(s). This is an open access article licensed under the Creative Commons BY-NC 4.0 (https://creativecommons.org/licenses/by-nc/4.0/)

Table 1. Selected events in the development of automation in the Polish and global hard coal mining industry – a chronological outline – own study based on [5, 6, 7, 8]

Year	Country	Development of longwall automation
1964	Poland	commencement of work on two types of automated longwalls (ASI-1 and BESTA)
1968	Poland	Commissioning of the Jan Automated Coal Mine with ASI-2 automatic longwall
1973	Poland	Interruption of work on an automatic longwall in the Polish mining industry
2000	Australia	Launch of the Longwall Automated Shearer Control (LASC) program
2007	Australia	Implementation of highly automated longwalls in Australian mining conditions
2009	Poland	Implementation of an automated ploughing system (LW Bogdanka)
2016	Germany	Automated/integrated longwall at Prosper-Haniel (RAG Mining Solutions)
2018	Poland	Announcement of the implementation of an autonomous longwall (JSW S.A.)
2020	Poland/China	MIKRUS complex with remote control and a master control system (FAMUR S.A.)
2022/2023	Poland	Procedure for an automatic longwall (KWK Piast - Ziemowit/PGG S.A.)

Work on the automated longwall was resumed in the 21st century. Around 2000, work began on a remote-controlled longwall at Śląsk Colliery. In 2009, a ploughing system with a high level of automation was implemented in the LW Bogdanka mine. It differed ideologically from the old solutions (ASI/BBESTA), but it allowed the movement of the powered support and conveyor sections following the progress of ploughing and the adjustment of the take-off.

In 2018, Jastrzębska Spółka Węglowa S.A. intended to implement an autonomous longwall in one of its mines without specifying the scope of automation and autonomy – the project was abandoned. In 2020, the Polish company FAMUR S.A. launched a thoroughly modernised MIKRUS complex for the exploitation of low seams in one of the Chinese mines, with a telecontrol system supported by a master control system. In 2022-2023, a tender for an automatic longwall system was announced and opened at the KWK Piast-Ziemowit coal mine, owned by Polska Grupa Górnicza S.A. The tender for the automated longwall announced at the Janina Mine (PKW S.A.) assumes the automation of mining and moving the support behind the shearer without the presence of the crew to complete the longwall mining cycle.

© 2024 Author(s). This is an open access article licensed under the Creative Commons BY-NC 4.0 (https://creativecommons.org/licenses/by-nc/4.0/)

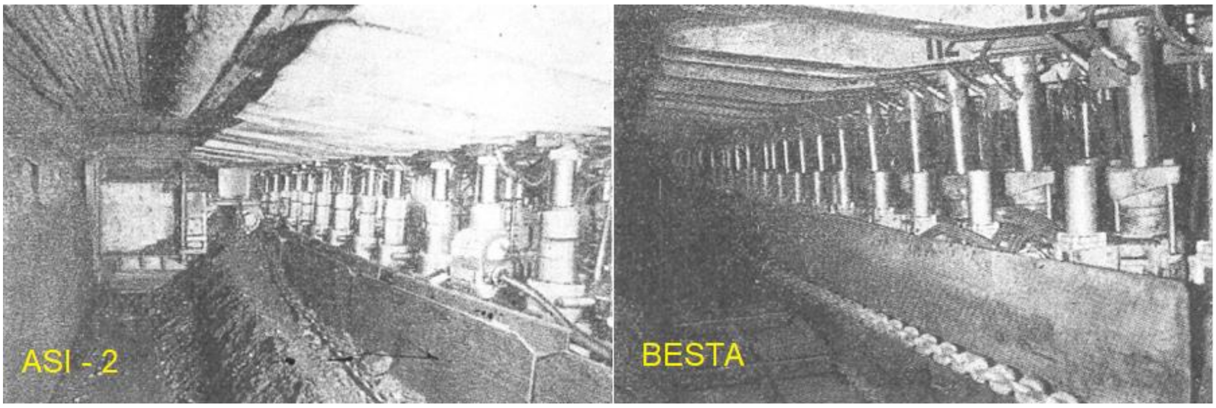

Fig. 1. Automated longwall system ASI-2 in JAN Automated Colliery and automated longwall BESTA in Bielszowice Colliery [5]

It should be noted that in the European hard coal mining industry, there has been practically no longwall with a high degree of automation or fully autonomous in operation to date. In the German coal mining industry, which has already ceased its mining operations, in 2016 RAG Mining Solutions and RAG Deutsche Steinkohle developed a computer system for the Prosper-Haniel mine in Bottrop, which integrates the automation systems of the individual devices included in the longwall excavation complex in the Zollwerein field. One of the key functions of this system is to ensure the interaction between the individual automation systems (modules): the Eickhoff SL750 shearer loader (Eickhoff EiControlSB module) and the longwall support and scraper section of the face conveyor. The most important tasks of the individual modules were to ensure a high degree of reliability and improve the efficiency of the use of longwall equipment. The ability to visualize the data necessary to supervise the operation of devices is also of great importance. The implementation of the new integrated automation system was to effectively improve the supervision of the entire longwall excavation process and the safety of the crew's working environment. The system was connected to the mine's control room and provided a 3D model of the infrastructure of the entire mining area [7]. In the coal mining industry of the Czech Republic, available automation elements of individual longwall system devices supplied by their manufacturers were implemented [7].

In view of the growing expectations for longwall productivity in Australia, in 2000, the LASC Technology (Longwall Automated Shearer Control) program was launched on the initiative of the Australian Coal Association, the aim of which was to implement highly automated longwall systems in Australian conditions. In the conditions of Australian mines, longwalls are laid in regularly almost horizontally lying seam plots without geological disturbances (faults, undulations, significant changes in seam thickness) with longwall galleries in independent bolt support. There is no need to use a shearer loader to remove steel arching elements. It should be emphasized that a high degree of automation of many longwalls has been achieved in Australian mining [9, 10, 11, 12, 13, 14, 15, 16].

Ideologically, the concept of an automatic wall is evolving, which can be traced on the example of Joy Global, which has recently moved from defining detailed solutions in the automation process to defining automation levels from the warning level (manual control of the machine) to the level of full autonomy, where the system is aware of the position and implements the assumed plan, and the necessary changes to this plan are carried out remotely.

In the coal mining industry of China and the USA, advanced research and applications of longwall automation are carried out [16, 17], at the same time pointing to the problems and conditions for the use of such solutions [18].

Publisher: **KOMAG Institute of Mining Technology, Poland**
© 2024 Author(s). This is an open access article licensed under the Creative Commons BY-NC 4.0 (https://creativecommons.org/licenses/by-nc/4.0/)

3. Longwall system in the process system in an underground coal mine

The longwall coal mining system offers the possibility of obtaining the highest efficiency among all those used in underground hard coal mining. A longwall is an underground excavation bounded by two, basically parallel to each other, horizontal workings (galleries) (longwall and longwall) or sloping (ramp). In the longwall, coal is mined (less often potassium salt, stripped soda - tron or phosphate rock) along its entire length. The longwall method of coal mining has been known since the 17th century, initially as traditional mining with all activities and operations performed manually. From the mid-nineteenth century, the first machines (notching machines) and then conveyors were used. Already at that time, the basic distinguishing features of the longwall system were defined:

- Wide (long) front of the selective face.
- Liquidation of the selected space immediately behind the face by a collapse of ceiling rocks (later also by filling the selected space partially or completely with the material provided, i.e. backfill).
- One-way movement of means of transporting excavated material in the longwall (first excavated boxes, then carts and finally conveyors).
- One-way airflow eliminating the need to use ventilation devices in the face (dams, partitions) causing difficulties and conflicts with the activities and operations carried out.

Regardless of the degree of mechanization, the longwall is used to perform the basic operations of the extraction process, i.e.:

- Mining of coal (less often other minerals),
- Loading excavated material onto the means of transport,
- Transport of excavated material along the wall to the outside of the face.

Other operations related to securing the excavation, liquidation of goafs or elimination of mining and technical hazards are also carried out in the longwall. Due to the movement of the equipment of the mechanized longwall system, it may be necessary to correct the mutual position of these devices and to correct the position in the excavation space.

The development of longwall system mechanization is shown in Fig. 2.

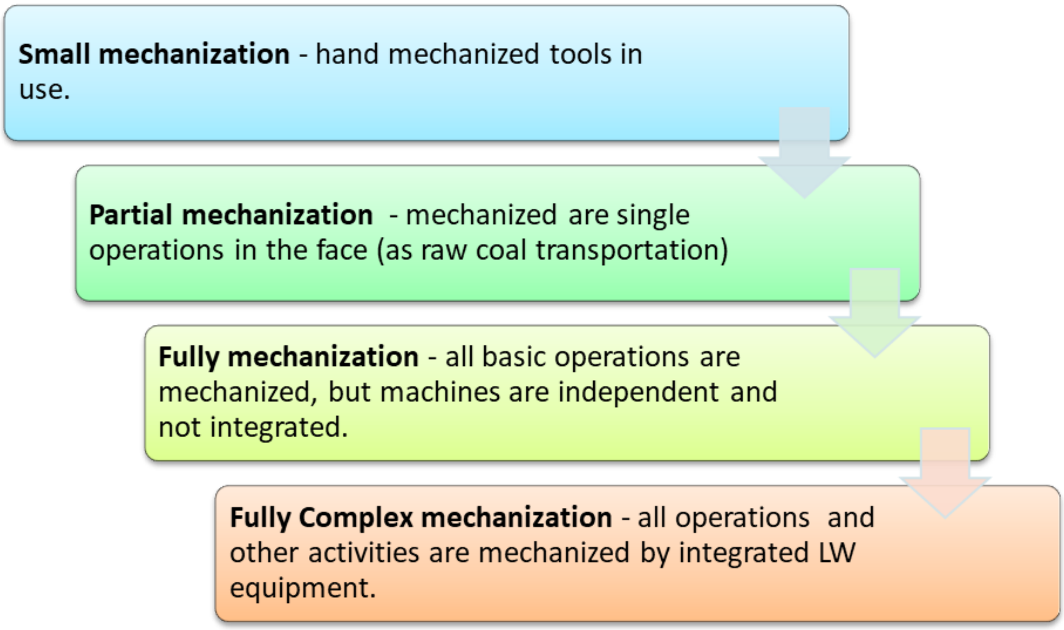

Fig. 2. Longwall mechanization development steps

Publisher: **KOMAG Institute of Mining Technology, Poland**
© 2024 Author(s). This is an open access article licensed under the Creative Commons BY-NC 4.0 (https://creativecommons.org/licenses/by-nc/4.0/)

In the 1960s, the first solutions of comprehensively mechanized longwall systems appeared, the technical development of which continues to this day [19, 20], but traditional mining systems with a low degree of mechanization of works are still used.

A modern comprehensively mechanized longwall system consists of the following basic elements (Fig. 3):

1. Cutting machine (shearer or planer).
2. Scraper face conveyor, the so-called armored one.
3. Powered roof support.
4. Scraper beam stage loader with crusher.
5. Hydraulic pump unit feeding powered casing.
6. A hydraulic pump unit that supplies a combine with water or an air-water mixture.
7. A set of electrical devices supplying power to the wall equipment (apparatus train).

The basic elements of the mechanized longwall system perform various functions for the good operation of the above-mentioned elements and their-mutual correct cooperation.

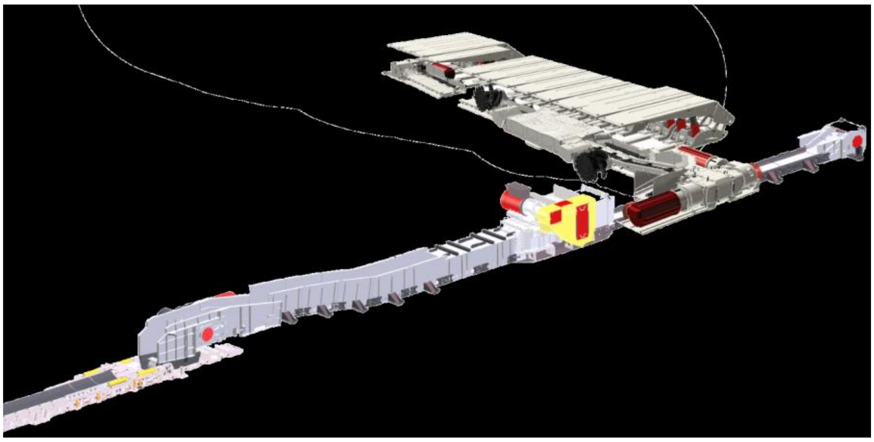

Fig. 3. Fully mechanized longwall complex with coal shearer – general view [own source]

The basic functions performed by the main devices of a comprehensively mechanized longwall are [20, 21]:

- **Coal mining:** A mining machine (shearer or plow) is basically used to mine coal (separate it from the coal pile) and load it onto a longwall scraper conveyor. An additional function of the cutting machine is to prepare (cut) space for other longwall equipment for their proper operation. Therefore, it is sometimes necessary to additionally trim the rocks in the vicinity of the coal seam (in the floor or in the ceiling) or to leave the coal in the floor or ceiling of the wall. In the case of high walls, crushers are sometimes used on the shearer loader (from the side of the reverse drive of the face conveyor) in order to crush large lumps of coal when mined with a shearer in the direction of the reverse drive (in the direction opposite to the direction of movement of the face conveyor chain).
- **Transport of excavated material:** An armoured longwall conveyor is mainly used to transport minerals mined by a mining machine (shearer or plow) in the longwall. A scraper face conveyor also has additional important functions: The longwall conveyor is also a kind of keystone (backbone) of the longwall – it is on it that the mining machine (plow or shearer) moves and the powered roof support is attached to it. In cable guides (penstocks) a movable – trailing part of the cables supplying the combine harvester moves. It is a mechanical connection of the longwall section of the powered roof support with each other (enabling their

Publisher: **KOMAG Institute of Mining Technology, Poland**
© 2024 Author(s). This is an open access article licensed under the Creative Commons BY-NC 4.0 (https://creativecommons.org/licenses/by-nc/4.0/)

movement – movement). The longwall conveyor route also serves as a structure for routing electrical cables and hydraulic hoses through the longwall, and in the plow walls of the pull chain and the plow return chain (as in the Mikrus longwall complex). The design of the scraper conveyor causes the stream of the transported material to be partially leveled during transport.

- **Protection:** Powered roof support – its primary function is to protect the working space of the longwall. This is done by supporting the ceiling and/or protecting against rolling into the working space of the caving debris wall. In addition, powered support: It is the basic strut for moving the face conveyor forward. The sliding system actuator is used to move the powered roof support section forward, its structural elements are the basis for attaching additional actuators – actuators (for correcting or stabilizing wall equipment elements). Stabilizes the conveyor with the cutting shearer. It is the basis for the installation of other wall equipment, including hydraulic hoses, electrical cables, control system elements (including housing), communication and signalling, lighting, etc.
- **Pre-processing of excavated material:** A scraper beam stage loader with a crusher is used to unload the excavated material from the scraper face conveyor, the stream of which is uneven and contains quite large lumps of excavated material. The design of the beam stage loader equalizes the stream of excavated material, and the crusher built on it breaks up large lumps of excavated material before loading it onto the next conveyor – a belt conveyor, which is highly sensitive to overloading and/or the presence of oversized lumps of material. In addition, beam stage loaders are equipped with sandwich devices that enable the movement of this conveyor in the roadway, sometimes together with the belt conveyor turning station.

The other previously mentioned elements are used to supply the above-mentioned utilities and support their operation.

However, the potential high productivity of a mechanized longwall system is currently associated with high capital expenditures (CAPEX) and operating costs (OPEX) of acquiring and using comprehensively mechanized longwall systems and other technical systems adapted to their capabilities in order to implement a complex system of processes related to coal mining in an underground mine [22, 23]. Due to the expectations regarding the high efficiency of mechanized longwall systems, the aim is to fully use their technical potential and eliminate time losses [24, 25, 26]. One of the directions for improving the efficiency of longwall systems has become automation, the prerequisite for which is full mechanization of work.

4. Objectives of longwall system automation

Since the 1960s, the main goal of wall automation has been to eliminate the presence of people in the faces, where there are a number of natural and technical threats to humans. The experience of the Australian mining industry gained with the rapid development of technical longwall equipment indicated the need to automate activities and operations in the longwall due to the psycho-physical limitations of people limiting the possibility of using the technical potential of longwall equipment and favourable mining and geological conditions. Main goals of longwall automation are presented on the Fig.4

Publisher: KOMAG Institute of Mining Technology, Poland
© 2024 Author(s). This is an open access article licensed under the Creative Commons BY-NC 4.0 (https://creativecommons.org/licenses/by-nc/4.0/)

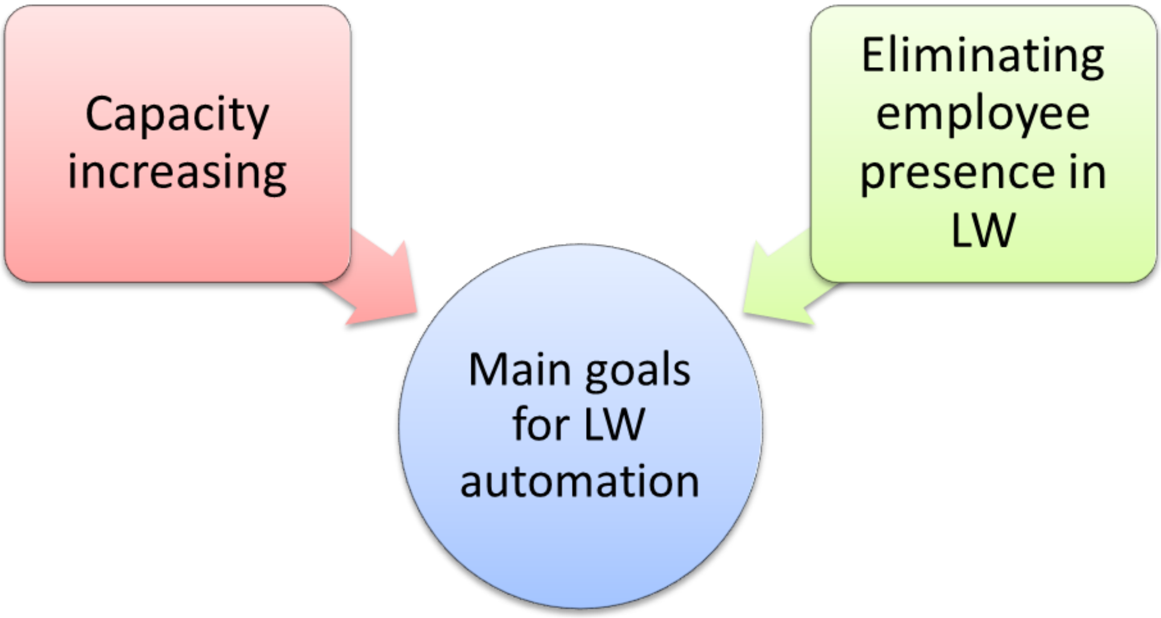

Fig. 4. Basic objectives of longwall automation

In one of conferences in 2021 CAT indicates the basic goals of automation as a:

- Improving health and safety.
- Protecting employees from dust and hazardous and harmful areas.
- Increase in efficiency.
- Transition from control by the employee to control over the process management.
- Reduce downtime and costs – improve equipment reliability.
- Repeatability and accuracy of operation.
- Consistent and predictable performance.

The discussion on the automation of longwalls in the conditions of Polish underground hard coal mines, which has been undertaken in recent years, has also pointed to goals that are not aimed at increasing the efficiency of the extraction process. Justifying the purposefulness of purchasing an automatic longwall, two objectives were indicated:

- Maintaining the daily production volume from one longwall and
- Creating conditions that suit the young generation of employees, accustomed to using smartphones, tablets, etc.

It should be noted that in the conditions of Upper Silesian hard coal mines, the average daily production from one longwall remains at a constant, very low level and in 2022 amounted to 2679 tons per day for the Upper Silesian Basin mines.

5. Conditions and limitations of longwall automation in the conditions of Polish hard coal mines

Due to the lack of experience of the Polish mining industry in the automation of modern longwalls, the conditions in Polish and Australian mines, where longwalls with the highest level of automation are currently mined, were compared (Table 2).

Publisher: **KOMAG Institute of Mining Technology, Poland**
© 2024 Author(s). This is an open access article licensed under the Creative Commons BY-NC 4.0 (https://creativecommons.org/licenses/by-nc/4.0/)

Table 2. Conditions for laying comprehensively mechanized longwalls in Polish and Australian coal mining – comparison [own study]

Poland	Australia
Walls with a slope of up to 35°	Horizontal or nearly horizontal walls
Walls with variable slope in length and wall run-out	Flat walls or walls with little variation in slope
Longwall galleries in support – arch support	Wallwalks anchored with a rectangular cross-section with a height equal to the thickness/height of the exploitation gate
A large share of manual work at the longwall-pavement intersection.	Fully mechanized intersection zones
Low efficiency of methane drainage of the seam before operation	Effective pre-emptive methane drainage of the seam prior to operation
Mining in zones of significant geological disturbances.	Avoiding exploitation in zones of significant geological disturbance
Exploited seams from thin to thick.	Medium and coarse seams mined
Acceptable operation with high levels of natural hazards	Avoid high-risk mining that limits mining efficiency
Single longwall galleries	Longwall galleries in multiple systems (at least double)

In Polish, supposedly mechanized, shearer walls, work at the ends of the longwall – in the area of longwall galleries – is still associated with a large share of manual work, so these are manual and machine operations or processes. Among the manually performed activities in the area of the intersection of the wall and the pavement, the following should be mentioned:

- Unfastening the arches of the roadway support.
- Relocation (or disassembly) of pavement reinforcements in the vicinity of the wall window.
- Cleaning of the forfeit material to spacers.
- Removal (robbing) of the pavement behind the front of the wall.

Significant differences result from the longwall mining conditions between Australian (including American or Chinese) and Polish mines. In the conditions of Australian and American mines, where the slopes of the seams are small, there is no need to correct the position of the section – therefore the support section has much fewer executive devices – actuators (two stands, roof support and shifter), which also significantly simplifies the control system and possible automation. The relatively large take-off and stroke of the shifter cause the section to automatically correct its position in relation to the conveyor. In walls with a slight longitudinal slope, thanks to the section pitch of at least 1.75 m or more, there are fewer problems with maintaining the lateral stability of the support. In the case of full automation, too many sensors will not be required and the system software will be simpler. The risk of section automation malfunctions will also be lower.

Even if software for automatic control of powered roof supports was available in the conditions of Polish mines (large and variable inclinations, faults, etc.), each section would have to be equipped with a system of numerous sensors (inclinometers, pressure gauges, length measurements) with a much greater degree of complexity than in Australia, the maintenance of which would be a great challenge (see the paradox of additional protections). Failure of a single sensor can halt the movement of the wall.

Another limitation is the type of longwall support used, which affects the operational length of the longwall system and the labour intensity of the intersection of the longwall excavation with the

© 2024 Author(s). This is an open access article licensed under the Creative Commons BY-NC 4.0 (https://creativecommons.org/licenses/by-nc/4.0/)

longwall excavation during the progress of mining, as well as the possibility of mechanisation of work in this place.

A distinguishing feature of Polish conditions is also the fact that mining is allowed in difficult geological conditions and with a high level of natural hazards. Limiting this level, e.g. by using methane drainage of the seam before mining, is not very effective – the efficiency increases after the commencement of mining (after the seam is relaxed), while at the same time the effect is increased methane release during mining [27].

6. Classification and requirements for the automation of mining processes

Table 3 presents a proposal for the classification of mining systems and possible scopes of automation depending on the degree of mechanization. Most of the mechanized longwall systems used in Poland carry out mining processes corresponding to manual and machine processes (group 2) with limited automation capabilities.

The use of a fully automated longwall system in much more complex mining and geological conditions than in Australia will require the creation of a very complex technical longwall system.

It should be remembered that the requirement for automation of a given process is its repeatability at every step. In the case of hard coal mining, especially in changing mining and geological conditions, this poses a challenge for human operators. The more complicated the process, the more difficult it is to automate – and the longwall operation in this context is definitely complicated.

Among the requirements related to even partial longwall automation, it is indicated that it is not possible to introduce longwall automation until many other necessary elements, apart from full mechanization, are ready, such as:

- Qualifications and skills of the team supported by appropriate training.
- Reliable equipment with automation capabilities.
- OEM hardware and software to support automation.
- Maintenance systems.
- Operating system – organizing the mine.
- Collection and processing of information (databases).
- Utility supply, including water management.

© 2024 Author(s). This is an open access article licensed under the Creative Commons BY-NC 4.0 (https://creativecommons.org/licenses/by-nc/4.0/)

Table 3. Types of Extraction Processes in Relation to the Degree of Their Mechanization and Possibility of Automation – A Proposal for Classification [own study]

<table>
<tr><th>Level of automation</th><th>Process Type</th><th>Process description</th><th>Degree of process automation</th></tr>
<tr><td>1.</td><td>Manual operations</td><td>Operations occurring in mining processes in which no machinery is used to obtain a mineral</td><td>Manual processes</td></tr>
<tr><td>2.</td><td>Manual and machine (mixed) operations</td><td>Operations in which some of the extraction cycle operations are performed by the machine, and the operator decides to start and stop the machine and controls the operation of the equipment.</td><td rowspan="2">Manual and machine processes (mixed)</td></tr>
<tr><td>3.</td><td>Manual and machine (mixed) operations with automatic cycle</td><td>Operations in which the machine automatically starts and ends the production cycle, and the operator is responsible for supervising and making interventional corrections (locally or remotely).</td></tr>
<tr><td>4.</td><td>Automated mining processes</td><td>The operator's job comes down to supervising automated machines.</td><td rowspan="2">Automated processes</td></tr>
<tr><td>5.</td><td>Autonomous mining processes</td><td>The operator's work comes down only to remote supervision of the process.</td></tr>
</table>

7. Summary and Conclusion

On the basis of a comparison of Polish conditions with Australian conditions (where the automation of the longwall mining process is the most developed), an analysis of longwall mining processes in Polish mines and general requirements for the automation of any process, it is possible to draw the following conclusions.

1. The principles of longwall construction and mining and geological conditions in practice exclude the possibility of implementing fully automated longwalls in the Polish mining industry. The repeatability of the entire longwall coal mining process in such conditions is severely limited, unlike in Australian mining.
2. Without improving longwall productivity, over-development of longwall automation systems will result in a drastic increase in capital expenditure.

Publisher: **KOMAG Institute of Mining Technology, Poland**
© 2024 Author(s). This is an open access article licensed under the Creative Commons BY-NC 4.0 (https://creativecommons.org/licenses/by-nc/4.0/)

3. It is justified to implement elements of targeted automation to be implemented in the conditions of Polish hard coal mines, such as those that serve to improve the safety and increase the reliability of the extraction process.
4. It is advisable to implement a system limiting the shearer feed speed with an increase in the amount of methane emitted, as a system increasing the predictability/continuity of the longwall mining process.
5. Without improving the productivity of walls, excessive development of wall automation systems will result in a drastic increase in expenditures - automation of inefficient processes is ineffective in itself (an effective process should be automated).

Before commencing activities related to a fully automated (or even autonomous) longwall, the following question should also be asked:

Have all the opportunities to increase longwall productivity in the Polish coal mining industry been used? And will the automation of longwalls bring the expected results?

References

[1] Kowal J.: Fundamentals of Automation vol. I. AGH Publishing House, Kraków 2018.

[2] Dudek W., Machowski J., Grzebiela Cz., Machowski A.: Machines, electrical devices and automation in mining. "Śląsk" Publishing House, Katowice 1978.

[3] Grzbiela Cz.: Electrical engineering, automation and electrical equipment in mining. "Śląsk", Katowice 2016.

[4] Nastaliński M., Siwek W.: Electrical engineering, electronics and automation in mining part I. II. Silesian Technical Publishing House, Katowice 1993.

[5] Mitręga J. [Edit.]: Coal mining in People's Poland 1945-1969. Association of Mining Engineers and Technicians, Katowice 1972.

[6] Korski J.: Development of the MIKRUS longwall system for the exploitation of thin coal seams. In: International Conference Proceedings: "Energy, environment, mineral exploitation – management and sustainable development". Energy - Environment, Intelligent Use of Minerals: Management and Sustainable Development". Rybnik, 06/2022. p.131-140.

[7] Mining Report. Gluckauf 4/2018 p.337-341.

[8] Gondek H., Marasova A.: New trends in mechanization and automatization in the OKD (Ostrava-Karvina Mines Kompany). In: Scientific Papers of the Silesian University of Technology Series: Mining z. 246/1480. Gliwice 2000.

[9] https://www.csiro.au/en/work-with-us/industries/mining-resources/Mining/Longwall-automation (accessed 9-10-2024).

[10] Ralston J. C., Reid D. C., Dunn M., T., Hainsworth D.W.: Longwall automation: Delivering enabling technology to achieve safer and more productive underground mining. International Journal of Mining, Science and Technology 25 (2015) pp. 865-876

[11] Kelly M., Hainsworth D., Reid D., Level P., Gurgenci H.: Longwall automation – a new approach. In: 3rd International symposium. Aachen; 2003.

[12] Beitler S., Holm M., Arndt T., Mozar A., Junker M., Bohn C.: State of the art in underground coal mining automation and introduction of a new shield-data-based horizon control approach. In: 13th SGEM geoconference on science and technologies in geology, exploration and mining, vol. 1. Singapore; 2013. p. 715–30.

Publisher: **KOMAG Institute of Mining Technology, Poland**
© 2024 Author(s). This is an open access article licensed under the Creative Commons BY-NC 4.0 (https://creativecommons.org/licenses/by-nc/4.0/)

[13] Ralston J.C.: Automated longwall shearer horizon control using thermal infrared-based seam tracking. In: IEEE International conference on automation science and engineering (CASE). Seoul; 2012.

[14] Owens G.: Longwall automation in practice at Broadmeadow mine (BMA). In: 7th Annual longwall conference. Australia; 2008.

[15] Kelly M., Hainsworth, D., Reid D.: State of the art in longwall automation. In Proceedings of the 2005 Australian Mining Technology Conference "New Technologies", Fremantle, Australia, 27–28 September 2005; The Australasian Institute of Mining and Metallurgy: Victoria, Australia, 2005.

[16] Guan Z, Wang S, Wang J, Ge S.: Longwall Face Automation: Coal Seam Floor Cutting Path Planning based on multiple hierarchical clustering. Applied Sciences. 2023; 13(18).

[17] Peng S.S., Du F., Cheng J., Li Y.: Automation in U.S. longwall coal mining: A state-of-the-art review. International Journal of Mining, Science and Technology 29 (2019) p.p. 151-159

[18] Wang G.: New development of longwall mining equipment based on automation and intelligent technology for thin seam coal. Journal of Coal Science and Engineering (China), volume 19 2013, pp. 97–103.

[19] https://en.wikipedia.org/wiki/Longwall_mining [15-10-2024]

[20] Korski J.: Comprehensively mechanized longwall systems – elements, their cooperation and limitations. https://gwarkowie.pl/images/aktualnosci/Kompleksowo_zmechanizowane_.pdf [15-10-2024]

[21] Korski J.: Capacity losses factors of fully mechanized longwall complexes. Mining Machines No. 3/2020 (163).

[22] Peng S.S.: Longwall Mining 3rd Edition. CRC Press/Balkema 2020.

[23] Korski J., Korski W.: Underground mine as a system of processes. Mining – Informatics, Automation and Electrical Engineering 2(522)/2015.

[24] Korski J., Tobór-Osadnik K., Wyganowska M.: Mining machines effectiveness and OEE Indicator. In: The role of Polish coal in the national and European energy sector, Bristol: Institute of Physics, 2017. pp. 1-12.

[25] Korski J.: Longwall complex efficient time and reasons of its decreasing. Inżynieria Mineralna 2/2019.

[26] Korski J., Korski W.: Safety and efficiency of longwalls in methane hazard conditions. Mining News 05/2016 (R. LXVII) pp. 332-335.

[27] Dylong A.: Monitoring and prediction of methane emission in the longwall and possibilities to control the longwall system, Mining–Informatics, Automation and Electrical Engineering 54 (1), 5-14, 2016

Publisher: **KOMAG Institute of Mining Technology, Poland**
© 2024 Author(s). This is an open access article licensed under the Creative Commons BY-NC 4.0 (https://creativecommons.org/licenses/by-nc/4.0/)

https://doi.org/10.32056/KOMAG2024.4.6

Efficiency coefficient of wind installations

Received: 18.10.2024

Accepted: 25.10.2024

Published online: 17.12.2024

Volodymyr ANTONCHIK[1*], **Valentin HANKEVICH**[2], **Oleksandr PASCHENKO**[2], **Artem PAZYNICH**[1], **Olena VARON**[1], **Nataliia PEREDERII**[2], **Stanislav SCHUBNIKOV**[1]

Author's affiliations and addresses:

[1*] The M.S. Poliakov Institute of Geotechnical Mechanics NAS of Ukraine, 15 Simferopolska Street, Dnipro, Ukraine, 49000

[2] Dnipro University of Technology, 19 Yavornytskoho Ave., 49005, Dnipro, Ukraine

*** Correspondence:**

e-mail: vladimir.antonchik1958@gmail.com

Abstract:

This study examines the main trends in the modern development of wind energy, addressing the critical tasks and proposing solutions for advancing wind energy technology. It includes theoretical calculations of the efficiency factor of wind turbines, particularly focusing on the Betz limit, which traditionally sets an upper bound on their efficiency. The research highlights the fallibility of Betz's limit calculations in both physics and mathematics, challenging its long-held assumptions. A novel formula for the true dependence of wind turbine efficiency on the utilized energy of the wind flow is derived, providing a more accurate representation of their performance. This new formula is supported by a graph illustrating the relationship between wind energy input and turbine efficiency. Additionally, the study explores various strategies and innovative approaches to enhance the efficiency of wind turbines, aiming to maximize their potential in harnessing wind energy. These findings contribute to the ongoing efforts to improve renewable energy technologies and increase the viability of wind power as a sustainable energy source.

Keywords: vertical-axial wind turbine; horizontal-axial wind turbine; wind flow; coefficient of wind flow energy utilization; blades

Publisher: **KOMAG Institute of Mining Technology, Poland**
© 2024 Author(s). This is an open access article licensed under the Creative Commons BY-NC 4.0 (https://creativecommons.org/licenses/by-nc/4.0/)

1. Introduction

The use of wind energy has undergone a significant and lengthy evolutionary process, transitioning from simple mechanical windmills used for basic agricultural tasks to sophisticated, large-scale industrial wind turbines. These modern turbines are designed to harness the power of wind more efficiently and are now capable of generating substantial amounts of energy [1]. Over the years, technological advancements have led to the development of wind turbines with impressive capacities ranging from 6 to 8 megawatts (MW) per unit. These turbines are massive structures, with mast heights typically reaching between 120 and 140 meters, and the lengths of their blades extending up to 60 to 80 meters [2]. Such dimensions allow the turbines to capture greater wind energy over a larger swept area, significantly improving their energy output [3].

However, these advancements come with substantial material and structural demands. The total weight of modern wind turbines can reach up to 6,000 tons, including the heavy components of the tower, rotor blades, nacelle, and various other mechanical and electrical systems [4]. This immense weight and size are necessary to withstand varying wind speeds and environmental conditions while maintaining operational stability and efficiency [5]. The scale of these installations also reflects the level of investment in research and development to optimize the design and performance of wind turbines, making them not only more powerful but also more resilient to wear and tear over time [1, 6].

Despite these impressive achievements, the main challenge facing the wind energy sector today is not merely about maximizing energy output from each turbine [7]. A critical focus is on producing renewable energy at a cost that can compete with traditional energy sources, such as those derived from burning hydrocarbon fuels [8]. This involves enhancing the efficiency of wind turbines, improving energy conversion technologies, and reducing the costs associated with manufacturing, installation, and maintenance [9]. The ultimate goal is to make wind energy an economically viable alternative that can contribute substantially to global energy needs while helping to reduce carbon emissions and combat climate change [10].

The purpose of this article is to demonstrate methods to increase the efficiency of wind energy and to reduce the costs associated with the creation and operation of wind turbines [11, 12]. At present, large-capacity horizontal-axis wind turbines, which produce up to 70% of all wind energy, have become the most widespread [11, 13, 14]. However, these turbines come with several significant disadvantages:

- Their large size and weight result in high material consumption and extended manufacturing times. This, in turn, increases the cost of the wind turbines themselves and the energy they produce [15].
- The logistics of delivery, installation, and operation of these large structures are complex and costly, further driving up the cost of the electricity generated [16].
- These turbines have a relatively low coefficient of wind flow energy utilization (EU) on the swept area of the windmill [17]. Typically equipped with three blades, they can only harness a small portion of the available wind flow.

To address these issues, it is essential to explore innovative designs and technologies that can enhance the efficiency of wind turbines [18]. This includes investigating new materials that are lighter and stronger, improving aerodynamic designs to capture more wind energy, and developing more efficient manufacturing processes to reduce costs [19]. Additionally, optimizing the placement and maintenance of wind turbines can help maximize their energy output and operational lifespan [20]. By addressing these challenges, the goal is to make wind energy a more viable and cost-effective alternative to traditional fossil fuels, contributing to a more sustainable and renewable energy future.

Publisher: **KOMAG Institute of Mining Technology, Poland**
© 2024 Author(s). This is an open access article licensed under the Creative Commons BY-NC 4.0 (https://creativecommons.org/licenses/by-nc/4.0/)

2. Literature and patterns background

The task of this article is to determine the physical processes of converting the energy of the wind flow into mechanical energy and to find mathematical formulas for the dependence of the efficiency coefficient on the mode of operation of wind turbines. The efficiency coefficient, often termed as the "power coefficient", measures the effectiveness of a wind turbine in converting wind energy into usable electrical power. It is defined as the ratio of the turbine's actual power output to the total wind energy passing through the swept area of the turbine blades. It should be noted that even if the entire swept area of the windmill was covered by blades, according to the theory of today's wind energy, the coefficient of wind energy use could not exceed 0.593 according to the Betz limit [11, 21]. However, the authors of this article believe that the analytically obtained maximum theoretical efficiency of all types of wind turbines obtained by Betz does not correspond to reality and prove it based on the reasons given below. There are discrepancies in the equations obtained by Betz and other authors both in the field of physics and in the field of mathematics [11, 12].

Several factors influence the efficiency coefficient of a wind turbine, including blade design, aerodynamic efficiency, wind speed variations, and turbine orientation. Blade shape, material, and length significantly impact the conversion efficiency since they determine how much energy is captured and transferred to the turbine rotor [13, 14]. Additionally, wind speed plays a crucial role in determining efficiency, as power output is proportional to the cube of wind speed. Thus, even small variations in wind speed can cause substantial changes in the turbine's power output. Technologies like pitch control and yaw mechanisms help optimize turbine orientation and blade angle to maintain higher efficiency.

Over the years, advancements in materials and design have led to improvements in the efficiency coefficient of wind turbines [22]. Modern wind installations often use composite materials that offer high strength-to-weight ratios, reducing energy losses due to structural inefficiencies. Additionally, advanced aerodynamic modeling and simulations help optimize blade design, leading to reduced drag and increased lift forces. Control systems, such as smart sensors and real-time feedback loops, help monitor wind speed, direction, and blade position, enabling continuous optimization of turbine performance, thereby improving efficiency.

Despite advancements, challenges remain in achieving higher efficiency coefficients. Wind turbines face issues like turbulence, mechanical losses, and energy conversion inefficiencies. Turbulence near ground level or due to nearby structures can lead to irregular wind flows, affecting the turbine's efficiency. Additionally, mechanical and electrical losses in components like gearboxes and generators reduce the overall efficiency. Ongoing research focuses on enhancing turbine reliability and durability through better materials, control algorithms, and maintenance strategies to minimize downtime and energy losses. Furthermore, integrating wind installations with smart grids and storage solutions can help in maintaining energy output consistency and better utilization of the harvested wind energy.

The same efficiency limit of wind turbines was independently derived by three distinguished authors from different backgrounds, showcasing the universal nature of their findings. The German physicist Albert Betz first presented this limit in 1919, significantly influencing the field of aerodynamics and wind energy [23]. Prior to Betz, the British scientist Frederick Lanchester explored similar concepts in 1915, contributing to the understanding of fluid dynamics in relation to wind turbines. Meanwhile, the Ukrainian scientist Mykola Zhukovskyi also arrived at this efficiency limit in 1920, further enriching the discourse on wind energy [19, 24]. The concurrence of these three scientists from various nations underscores the fundamental principles governing wind turbine efficiency, highlighting its significance in both historical and contemporary contexts.

© 2024 Author(s). This is an open access article licensed under the Creative Commons BY-NC 4.0 (https://creativecommons.org/licenses/by-nc/4.0/)

However, the general error of energy selection by the device-wind turbine is uniquely determined by the equation of the flow power at the input and output of the device and, accordingly, the efficiency of the device (wind turbine), fully determines the amount of initial energy given to the device and the energy remaining in the flow [25]. An attempt to add here additional equations of this process during a detailed examination shows the inability of additional equations, their further addition to the equation of state and obtaining an incorrect result.

3. Methods

The Fig. 1 shows the mathematical scheme of the theoretical transformation of part of the energy of the wind flow into mechanical energy with simultaneous transmission of it outside the given wind flow by any device and shows: V_0 – the EU speed at the input to the device, S_0 – cross-sectional area of the flow at the input to the device, S – cross-sectional area of the flow at the output of the device, V – the EU speed at the output to the device.

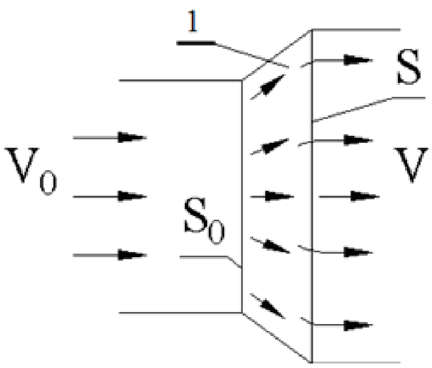

Fig. 1. Scheme of theoretical conversion of part of the wind energy flow: V_0 – the EU speed at the input to the device, S_0 – cross-sectional area of the flow at the input to the device, S – cross-sectional area of the flow at the output of the device, V – the EU speed at the output to the device

For the theoretical determination of the efficiency of using energy units (EU), the design of the EU energy conversion device itself is not of primary importance. The focus is solely on the input and output parameters of the energy unit, disregarding the specific internal mechanisms or structural characteristics of the conversion device. In this context, only the energy entering and exiting the system is considered relevant for calculating efficiency. The internal design elements, such as material composition or mechanical configurations, do not directly impact the theoretical efficiency analysis. This approach allows for a more generalized assessment, independent of variations in device architecture. Therefore, the efficiency can be evaluated by comparing the input energy to the output energy, regardless of how the conversion process is carried out within the device.

According to the law of conservation of mass, the amount of air entering and leaving device 1 (Fig. 1) per unit of time is the same. Based on this, the power of the wind flow used in the device will be the difference in the energies of this wind flow at the entrance and exit of the device per unit of time.

$$P_y = P_0 - P_B \quad (1)$$

where P_0 – EU power at the input to the device 1, P_B – EU power at the output of the device 1, P_y – wind energy power that is converted into mechanical energy and used in the device 1.

Based on this, it is possible to obtain the dependence of the amount of wind energy used by device 1 on its parameters at the input and output of the device.

Publisher: **KOMAG Institute of Mining Technology, Poland**
© 2024 Author(s). This is an open access article licensed under the Creative Commons BY-NC 4.0 (https://creativecommons.org/licenses/by-nc/4.0/)

As you know, the second mass flow of air is equal to:

$$\dot{m} = p \cdot v \cdot s,$$

where $\dot{m}$ – mass second flow of air passing through the transverse wind flow cross section, p - air density, s – cross-sectional area of the wind flow, v – wind flow speed.

For the scheme of Figure 1.

$$\dot{m} = p \cdot v_0 \cdot s_0 = p \cdot v \cdot s \qquad (2)$$

Where $\dot{m}$– the EU mass per second flow through the device, s_0 – cross-sectional area EU at the input to the device, v_0 – the EU speed at the input to the device, p - air density, s - cross-sectional area of the flow at the output to the device, v - the EU speed at the output to the device. Formula (2) shows us that:

$$\frac{v_0}{v} = \frac{S}{S_0} = n \qquad (3)$$

where n a dimensionless quantity.

It is determined that the power is taken from the wind flow in the device, taking the value of the second mass flow from (2), expressing v and S from (3).

Through $\frac{v_0}{n} = v, S = S_0 n$ and also considering that $P = \frac{\dot{m} \cdot v^2}{2}$, and by substituting these values (1) we get:

$$P_y = \frac{\dot{m} \cdot v_0^2}{2} - \frac{\dot{m}}{2}$$

$$P_y = \frac{p \cdot v_0 \cdot S_0 \cdot v_0^2}{2} - \frac{p \cdot \frac{v_0}{n} \cdot S_0 \cdot n \cdot \left(\frac{v_0}{n}\right)^2}{2}$$

Or after transformations we will get:

$$P_y = 0{,}5 \cdot p \cdot v_0^2 \cdot S_0 \cdot \left(1 - \frac{1}{n^2}\right) \qquad (4)$$

the first element of formula (4) $0{,}5 \cdot p \cdot v_0^2 \cdot S_0$ represents the entire power or specific kinetic energy of the wind flow entering the device (1), i.e. it is practically all the energy of the wind flow that can be used in the wind turbine device.

The second element $1-1/n_2$ shows what part of the power of the wind flow is selected in the device (1), i.e.

4. Results of the research

Wind turbines, the same figure is the coefficient of wind flow utilization. Formula (4) presents a graph illustrating the relationship between the power of the wind flow that is harnessed and utilized by the wind turbine (referred to as device 1). This relationship is depicted based on the ratio of the wind flow's energy at the input and output of the turbine.

The graph highlights how the power captured by the wind turbine changes as the difference between the input and output energy levels varies. Essentially, it demonstrates the efficiency of energy conversion within the turbine by visualizing how much of the incoming wind energy is successfully

© 2024 Author(s). This is an open access article licensed under the Creative Commons BY-NC 4.0 (https://creativecommons.org/licenses/by-nc/4.0/)

extracted. The graph thus serves as a crucial tool for understanding the turbine's performance and energy utilization in varying wind conditions.

By dividing P_y by P_0, we get the EU energy utilization factor in device 1, that is, the wind turbine:

$$P_y = 0{,}5 \cdot p \cdot v_0^2 \cdot S_0$$

$$K = \frac{P_y}{P_0} = \frac{0{,}5 \cdot p \cdot v_0^2 \cdot S_0 \cdot (1 - \frac{1}{n^2})}{0{,}5 \cdot p \cdot v_0^2 \cdot S_0} = 1 - \frac{1}{n^2} \tag{5}$$

$$\mathrm{K} = 1 - \frac{1}{n^2}$$

The graph of this dependence obtained by formula (5) is shown in Fig. 2.

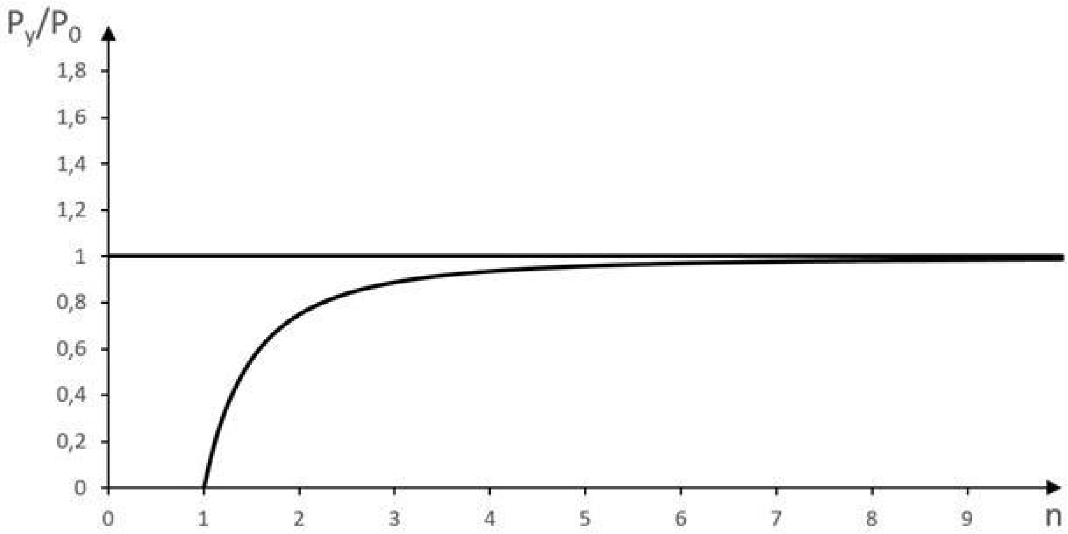

Fig. 2. Wind turbine efficiency dependence graph

For value n = 1, P_y = 0 means that the speed of the wind flow at the entrance and exit of the device is the same and no energy transfer of the EU of the device 1 has occurred. Further, as the difference in the speed of the EU at the input and output of device 1 decreases, the amount of energy extracted from the EU by the device increases and, accordingly, this is the efficiency of the device.

The efficiency function of wind turbines (5) Fig. 2 does not have an extremum, but smoothly approaches "1", like the efficiency of other machines, particularly in thermodynamics, therefore there are no theoretical restrictions on the efficiency of wind turbines up to "1", since physically it would mean that from a certain position, the moving elements of the wind turbine structure (device 1) perceive the pressure of the wind turbine and convert it into mechanical energy, which is output outside the device 1, cease to perceive the impact of the wind turbine, which is impossible. And if the impact of wind turbines on the moving elements of the wind turbine structure is constant, then it is always possible to use a certain geometry of the moving elements of the wind turbine to remove part of the turbine energy, reducing the velocity of the wind turbine, passing it through a larger section of the wind turbine. When considering the effect of EU on the wind turbine blades, it may seem that the optimal angle of attack of the blades gives the maximum amount of energy received, but this can only apply to the specific design of the wind turbine and has nothing to do with the theoretical efficiency of wind turbines.

Publisher: **KOMAG Institute of Mining Technology, Poland**
© 2024 Author(s). This is an open access article licensed under the Creative Commons BY-NC 4.0 (https://creativecommons.org/licenses/by-nc/4.0/)

There are discrepancies in the equations obtained by Betz and other authors both in the field of physics and in the field of mathematics [11, 12].

The same efficiency limit of wind turbines was obtained independently by three different authors: the German physicist Albert Betz in 1919, the British scientist Frederick Lanchester in 1915, and the Russian scientist Mykola Zhukovsky in 1920. However, the general error of energy selection by the device-wind turbine is uniquely determined by the equation of the flow power at the input and output of the device and, accordingly, the efficiency of the device (wind turbine), fully determines the amount of initial energy given to the device and the energy remaining in the flow. An attempt to add here additional equations of this process during a detailed examination shows the inability of additional equations, their further addition to the equation of state and obtaining an incorrect result.

Thus, in one of the methods of proving the Betz limit [12], the force created by the wind flow (shaded section in the form of an ellipse) and acting on the sensor in Fig. 3.

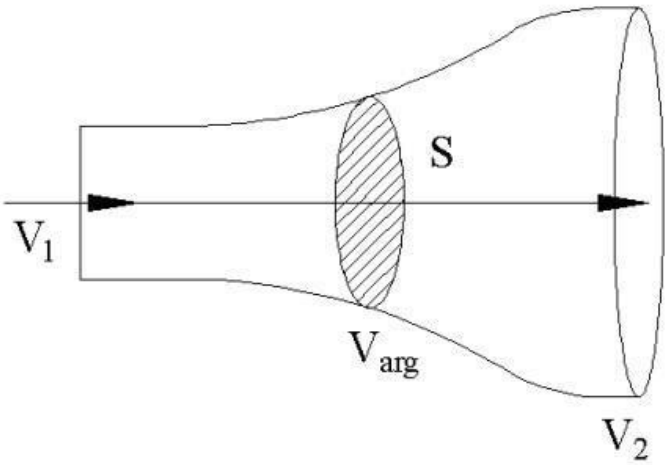

Fig. 3. Scheme of the flow of air through the rotor of the wind generator

A sensor is a device for obtaining wind energy - a wind turbine obtained by applying Bernoulli's theorem twice on one side between a point upstream and a point directly in front of the sensor. On the other hand, a point immediately after the sensor and a point downstream.

$$\frac{P_0}{p} + \frac{v_1^2}{2} = \frac{P_1}{p} + \frac{v^2}{2} \tag{6}$$

$$\frac{P_0}{p} + \frac{v_2^2}{2} = \frac{P_2}{p} + \frac{v^2}{2}. \tag{7}$$

Subtracting (6) from (7) gives:

$$P_1 - P_2 = (v_1^2 - v_2^2)\,. \tag{8}$$

The final equation (3) relates the pressure in the flow on one line at the beginning and at the end of the flow according to this scheme, and the presence of a wind turbine (sensor) is not taken into account here. At the same time, it is assumed that the pressure and flow rate before and after the sensor

Publisher: **KOMAG Institute of Mining Technology, Poland**
© 2024 Author(s). This is an open access article licensed under the Creative Commons BY-NC 4.0 (https://creativecommons.org/licenses/by-nc/4.0/)

are the same, and this will mean that the flow did not transfer energy to the sensor. In fact, the parameters of the flow, that is, the pressure and speed before the sensor and immediately after it, differ significantly, since the flow gives the sensor part of its energy and slows down significantly in the sensor, so the difference (6) - (7) does not give (8).

In addition, Bernoulli's equation is derived with the fundamental assumption that the work done to move a specific mass of fluid in the flow is directly proportional to the change in the total energy of that mass. This relationship is crucial for understanding fluid dynamics, as it helps to explain how energy is conserved within a fluid system. However, if, for instance, a device within the flow extracts an unknown portion of energy, the classical application of Bernoulli's equation becomes problematic. In such a scenario, the equation will not hold true at the extreme points of the flow, specifically at the beginning and end of the energy extraction process. This discrepancy highlights a significant limitation in applying Bernoulli's principle when external forces or devices alter the energy distribution in the flow. Therefore, the presence of energy-extracting devices necessitates a more nuanced approach to analyze the fluid's behavior and the energy dynamics involved.

Thus, other forms of derivation of equations [11] include the use of the equation of Newton's second law: "The force acting on the air flow from the side of the rotor is equal to the air mass multiplied by its acceleration." The work done by a force can be written in differential form as:

$$dE=F\cdot dx.$$

Errors in the derivation and obtaining of the Betz formula for the coefficient of performance of wind turbines are eliminated. In accordance with the physics of the process of wind flow energy transfer and according to the mathematical model of this process, the formula for determining the coefficient of performance for wind turbines of any type and design is obtained, the dependence of which is shown in Fig. 2.

$$K = 1 - \frac{1}{n^2}$$

In the analyzed physical model, there is no way of moving the object under the action of force, that is, there is no work performed by this force. Indeed, the force acts on the rotor blades and the rotor itself. But the rotor remains in place according to the conditions of the model and in fact, and the air flow goes strictly along the axis of the rotor and perpendicular to its blades, therefore the projection of the force of the wind flow on the plane of rotation of the rotor blades is zero, and accordingly in this scheme and the work of this force is equal to "0". It follows that the replacement of force with power [11] and all subsequent transformations are erroneous and lead to an erroneous result.

5. Discussion the research results

The discussion of results focuses on the theoretical framework and practical implications of the wind energy conversion depicted in Fig. 1. The mathematical scheme illustrates the transformation of part of the wind flow's energy into mechanical energy and the transfer of this energy outside the wind flow by a wind turbine (device 1). The theoretical model indicates that the efficiency of wind energy conversion relies solely on the input and output parameters – specifically, the wind flow's speed and cross-sectional area at the input (V_0, S_0) and output (V, S). This approach isolates energy conversion efficiency from internal design specifics, which allows a generalized understanding of the energy exchange process.

Publisher: KOMAG Institute of Mining Technology, Poland
© 2024 Author(s). This is an open access article licensed under the Creative Commons BY-NC 4.0 (https://creativecommons.org/licenses/by-nc/4.0/)

The results confirm that, according to the law of conservation of mass, the volume of air entering and leaving the wind turbine remains constant. Consequently, the power harnessed is expressed as the difference between the incoming power (P_0) and the residual power (P_y) that exists the device. This power relationship is mathematically modeled to demonstrate the efficiency coefficient K. As shown in the discussion, when the speed of the wind flow at the input and output remains the same (n = 1), there is no energy transfer, resulting in zero power extracted. The increase in energy extraction as the difference in wind speed increases highlights the impact of the wind turbine's design and configuration on its overall efficiency.

The comparison with the Betz limit and the derivation of similar equations by Lanchester and Zhukovsky emphasize discrepancies in historical interpretations of wind turbine efficiency. This discussion challenges the theoretical assumptions underlying the Betz limit, particularly the application of Bernoulli's principle and Newton's second law, which suggest that additional complexities in energy transfer are not adequately represented in traditional models. The critique implies that prior methods overestimate the efficiency limits due to incorrect assumptions about energy transfer and flow characteristics within the turbine structure.

Finally, the presented physical model challenges the prevailing assumption that wind turbines achieve maximum efficiency solely at specific blade angles. It argues that optimal energy capture is not necessarily linked to design specifications but is instead governed by the theoretical constraints outlined in the derived formula. This perspective raises significant questions about the traditional limitations imposed on wind turbine efficiency, suggesting that these constraints may be more flexible than previously thought. Moreover, the findings indicate that continuous improvements in turbine design and technology could lead to higher energy utilization rates than currently realized. This opens the door to innovative approaches that go beyond the conventional parameters of wind turbine efficiency. Additionally, the implications of this model encourage further investigation into alternative wind turbine designs, particularly those that explore options beyond existing theoretical limits. Ultimately, embracing this broader understanding of efficiency may lead to more effective strategies for harnessing wind energy in the future.

6. Conclusions

Returning to the problems of wind energy, it is necessary to note that the operation of real wind turbines often differs significantly from theoretical models. A considerable portion of the wind flow that meets the rotor blades can be reflected and lost, delivering only a fraction of its energy to the rotor. Thus, the main challenge in improving wind turbine efficiency lies in utilizing the maximum energy of the wind flow passing through the area of the rotating blades. Although large industrial wind turbines utilize some of this energy, there is potential to achieve similar energy yields with smaller turbines through more complete wind flow utilization.

Wind turbines that rely on the lifting force of the wing to rotate the rotor face certain structural limitations. The lifting force occurs only when the blade interacts correctly with the wind flow, limiting the amount of energy the air can transfer. This results in relatively low efficiency. However, wind turbines designed to use the pressure of the wind flow show greater potential, especially in modern vertical-axis turbines, where a higher degree of energy extraction is possible.

The evolution of wind energy technology has led to substantial advancements, transforming basic windmills into large industrial turbines with capacities ranging from 6 to 8 MW. The masts of these turbines now reach heights of 120 to 140 meters, and blade lengths extend to 60 to 80 meters. By enlarging the swept area of the blades, modern turbines can capture more energy from wind flows, optimizing overall efficiency and output.

Publisher: **KOMAG Institute of Mining Technology, Poland**
© 2024 Author(s). This is an open access article licensed under the Creative Commons BY-NC 4.0 (https://creativecommons.org/licenses/by-nc/4.0/)

Despite these advancements, the considerable size and weight of modern turbines, which can reach up to 6,000 tons, pose challenges. While the increased weight provides structural stability, especially under changing environmental conditions, it also emphasizes the need to improve efficiency. The limitations in current designs mean that a significant portion of wind energy remains unutilized. This calls for a focus on innovations that can harness more energy from the same wind flow.

One of the primary goals of wind energy development is to make wind-generated power economically competitive with conventional energy sources. The objective is to produce renewable energy at a cost per kilowatt-hour comparable to that of burning hydrocarbon fuels. Achieving this requires improving not just the capacity of wind turbines, but also their efficiency in extracting wind flow energy, potentially through more refined designs.

Future strategies to enhance wind energy production involve improving energy conversion technologies, enhancing component durability, and refining manufacturing processes. Vertical-axis wind turbines, which rely on wind flow pressure rather than lift forces, present a promising opportunity for better energy extraction. This could lead to smaller, more efficient turbines capable of delivering higher energy yields.

In conclusion, while the evolution of wind energy technology continues to drive advancements in turbine size, efficiency, and cost-effectiveness, further development is essential. By addressing current limitations and focusing on maximizing wind flow utilization, the industry can move closer to achieving its sustainability goals. Such efforts, combined with careful consideration of environmental and social impacts, will be crucial for establishing wind energy as a significant and viable component of the global energy mix. It also, be the topicks of our further research investigations.

References

[1] Darvish Falehi A., & Rafiee M.: Maximum efficiency of wind energy using novel Dynamic Voltage Restorer for DFIG based Wind Turbine. Energy Reports, 2018, 4, 308–322. https://doi.org/10.1016/j.egyr.2018.01.006

[2] Pereira S., Ferreira P., & Vaz A. I. F.: Short-term electricity planning with increase wind capacity. Energy, 2014, 69, 12–22. https://doi.org/10.1016/j.energy.2014.01.037

[3] Mahfouz M. Y., & Cheng P.: A passively self-adjusting floating wind farm layout to increase the annual energy production. Wind Energy, 2022,26(3), 251–265. Portico. https://doi.org/10.1002/we.2797

[4] Leahy R.: Proposed circuit design could increase switching efficiency in wind energy grids. Scilight, 2018, 34, 23-41. https://doi.org/10.1063/1.5053101

[5] Khomenko O., Rudakov D., Lkhagva T., Sala D., Buketov V., & Dychkovskyi R.: Managing the horizon-oriented in-situ leaching for the uranium deposits of Mongolia. Rudarsko-Geološko-Naftni Zbornik, 2023, 38(5), 49–60. https://doi.org/10.17794/rgn.2023.5.5

[6] Somoano M., & Huera-Huarte F. J.: Bio-inspired blades with local trailing edge flexibility increase the efficiency of vertical axis wind turbines. Energy Reports, 2022, 8, 3244–3250. https://doi.org/10.1016/j.egyr.2022.02.151

[7] Berg E.: Wind Energy Conversion. Energy Efficiency and Renewable Energy Handbook, 2015, 1371–1416. https://doi.org/10.1201/b18947-52

[8] Kondoh J.: Autonomous frequency regulation by controllable loads to increase acceptable wind power generation. Wind Energy, 2009, 13(6), 529–541. Portico. https://doi.org/10.1002/we.375

[9] Dychkovskyi R., Dyczko A., & Borojević Šoštarić S.: Foreword: Physical and Chemical Geotechnologies – Innovations in Mining and Energy. E3S Web of Conferences, 2024, 567, 00001. https://doi.org/10.1051/e3sconf/202456700001

[10] Dychkovskyi R., Saik P., Sala D., & Cabana E. C.: The current state of the non-ore mineral deposits mining in the concept of the Ukraine reconstruction in the post-war period. Mineral Economics, 2024, 37(3), 589–599. https://doi.org/10.1007/s13563-024-00436-z

Publisher: **KOMAG Institute of Mining Technology, Poland**
© 2024 Author(s). This is an open access article licensed under the Creative Commons BY-NC 4.0 (https://creativecommons.org/licenses/by-nc/4.0/)

[11] Betz A.: Introduction to the Theory of Flow Machines. D. G. Randall, Trans., Oxford. Pergamon Press, 1966, 165 p.

[12] Bulat A.F., Mineev S.P., Antonchyk V.E., Maltseva V.E., Demchenko S.V.: Patent UA 124749 F03D 3/04 publ. 11/10/2021 Bul. No. 45 Vertical-axial wind turbine

[13] Bulat A.F., Mineev S.P., Antonchyk V.E., Chelkan V.V.: Patent UA 153208 F03D 3/04 publ. 06/07/2023 Bul. No. 23 Biaxial wind turbine

[14] Mineev S.P., Antonchyk V.E., Maltseva V.E.: Patent UA 154098 F03D 3/06 publ. 11.10.2023 Bul. No. 41 Vertical-axial wind turbine.

[15] Lam G. C. K.: Wind Energy Conversion Efficiency Limit. Wind Engineering, 2006, 30(5), 431–437. https://doi.org/10.1260/030952406779502687

[16] Kazemzadeh E., Fuinhas J. A., Shirazi M., Koengkan M., & Silva N.: Does economic complexity increase energy intensity? Energy Efficiency, 2023, 16(4). https://doi.org/10.1007/s12053-023-10104-w

[17] Barthelmie R. J., & Jensen L. E.: Evaluation of wind farm efficiency and wind turbine wakes at the Nysted offshore wind farm. Wind Energy, 2010, 13(6), 573–586. Portico. https://doi.org/10.1002/we.408

[18] Max L., & Lundberg S.: System efficiency of a DC/DC converter-based wind farm. Wind Energy, 2007, 11(1), 109–120. Portico. https://doi.org/10.1002/we.25

[19] Xydis G., & Mihet-Popa L.: Wind energy integration via residential appliances. Energy Efficiency, 2016, 10(2), 319–329. https://doi.org/10.1007/s12053-016-9459-2

[20] Wiser R., & Bolinger M.: Wind Technologies Market Report. Office of Scientific and Technical Information (OSTI), 2011. https://doi.org/10.2172/1219205

[21] Smith R. B.: Gravity wave effects on wind farm efficiency. Wind Energy, 2010, 13(5), 449–458. Portico. https://doi.org/10.1002/we.366

[22] Saik P., Dychkovskyi R., Lozynskyi V., Falshtynskyi V., Cabana E. C., & Hrytsenko L.: Chemistry of the Gasification of Carbonaceous Raw Material. Materials Science Forum, 2021, 1045, 67–78. https://doi.org/10.4028/www.scientific.net/msf.1045.67

[23] Riegels F., & Backhaus H.: ALBERT BETZ 65 Jahre/ERNST LÜBCKE 60 Jahre. Physikalische Blätter, 1951, 7(1), 32–33. Portico. https://doi.org/10.1002/phbl.19510070107

[24] Dolgopolov A. V., Kazancev D. A., Markin I. V., Orlova O. A., & Shalaev S. V.: The Modern Method of Creating Dynamically Scaled Models to Study Aircraft Flutter Characteristics. Uchenye Zapiski Kazanskogo Universiteta. Seriya Fiziko-Matematicheskie Nauki, 2020, 162(4), 441–454. https://doi.org/10.26907/2541-7746.2020.4.441-454

[25] Krishna M., Fraser E. J., Wills R. G. A., & Walsh F. C.: Developments in soluble lead flow batteries and remaining challenges: An illustrated review. Journal of Energy Storage, 2018, 15, 69–90. https://doi.org/10.1016/j.est.2017.10.020

Publisher: **KOMAG Institute of Mining Technology, Poland**
© 2024 Author(s). This is an open access article licensed under the Creative Commons BY-NC 4.0 (https://creativecommons.org/licenses/by-nc/4.0/)